12-2017

Modeling Post Stroke Respiratory Dysfunction, Apneas and Cognitive Decline

Anthony Patrizz

Modeling Post Stroke Respiratory Dysfunction, Apneas and Cognitive Decline

by

Anthony Patrizz, B.A.

Approved:

_____
Dr. Louise McCullough, M.D., Ph.D.
Advisory Professor

_____
Dr. Jarek Aronowski, M.D., Ph.D.

_____
Dr. Shane Cunha, Ph.D.

_____
Dr. Andrew J. Bean, Ph.D.

_____
Dr. Robert M. Bryan, Ph.D.

_____
Dr. Daniel Mulkey, Ph.D.

Approved:

_____
Dean, The University of Texas
MD Anderson Cancer Center UTHealth Graduate School of Biomedical Sciences

Modeling Post Stroke Respiratory Dysfunction, Apneas and Cognitive Decline

A

DISSERTATION

Presented to the Faculty of

The University of Texas MD Anderson Cancer Center UTHealth

Graduate School of Biomedical Science

in Partial Fulfillment

of the Requirements

for the Degree of

DOCTOR OF PHILOSOPHY

by

Anthony Nicholas Patrizz III, B.A.

Houston, Texas

December 2017

Modeling Post Stroke Respiratory Dysfunction, Apneas and Cognitive Decline

Anthony Patrizz, B.A.

Advisory Professor: Louise McCullough M.D., Ph.D.

Stroke is a major cause of mortality and the leading cause of long-term disability in the US. More than 60% of individuals suffering a first time stroke develop respiratory dysfunction, prolonging recovery and increasing mortality. Post-stroke cognitive decline is a major contributor to disability and nursing home placement, therefore the cognitive consequences of Stroke Induced Respiratory Dysfunction (SIRD) need to be explored if we hope to enhance functional recovery. The first step towards treatment of the negative consequences of SIRD is the development of appropriate animal models that will allow us to explore the pathophysiology of SIRD and provide the opportunity to test potential pharmacological agents.

We developed and characterized an animal model of stroke induced respiratory dysfunction recapitulating the respiratory phenotype witnessed in the clinical population, characterized by incidences of apnea and hypoventilation. Interestingly, mice with high incidence of apneas display signs of progressive cognitive decline compared to those with low/no incidence of apneas. Histological analysis of vital brainstem respiratory control sites unveiled reactive astrocytosis, an important cell type in the neurovascular unit and an essential component of chemoreception. Respiratory dysfunction and brainstem astrocytosis was reproduced in mice that underwent intracerebroventricular injections of TGF-β. Suggesting the TGF-β signaling pathway contributes to the onset of astrogliosis and respiratory dysfunction.

Our data suggests that stroke disrupts basal breathing rather than increasing chemoreceptor gain. Therefore, we predict treatments designed to stimulate breathing independent of chemoreceptor gain will improve respiratory instability, behavior, cognition and mortality. Systemic application of acetazolamide eliminated apneas while preventing further cognitive decline.

This work not only developed a model of stroke induced respiratory dysfunction that recapitulates the respiratory phenotype witnessed in the clinical population, but also providing translational relevance to the field of stroke, aging, and cognitive decline. Successful treatment of SIRD may lead to significant improvements in post-stroke recovery and cognition.

Table of Contents:

List of Illustrations:

List of Tables

Chapter 1. Introduction.

1.1. Stroke is a leading cause of adult disability:

Stroke continues to be the leading cause of serious long-term disability in the United States. (1) In 2012, stroke care cost an astounding 77.1 billion dollars, and due to the aging of the US population, this number is expected to triple by 2030 to 183 billion. Over 4% of the US population has suffered a stroke. (2) This public health issue is not just faced by the United States; globally stroke is the second leading cause of death behind ischemic heart disease. (3) Stroke results from the lack of blood supply (ischemia) to the brain due to a thrombus, embolus or hemorrhage. Thrombotic and embolic strokes are both classified as ischemic strokes and account for 87% of all strokes. (4) Periods of ischemia quickly kill brain cells, disrupting brain function and resulting in disability or death. Currently, there is only one pharmacological treatment for stroke, tissue plasminogen activator (tPA), which has a short therapeutic window and carries a significant risk of hemorrhage in the periphery and in the brain. (5) Although acute mortality from stroke has declined due to improvements in medical care, this has led to a growing number of stroke survivors in our communities. Therefore, enhancing functional recovery and preventing further disability in stroke patients is critical.

Advanced chronological age is the most important non-modifiable risk factor for stroke. (6) Since >80% of strokes occur in individuals over the age of 65(2), the aging population bears the major brunt of stroke related mortality and disability. Age is an independent predictor of poor outcome after stroke, and older patients have

both higher in-hospital mortality and poorer functional outcomes after an ischemic event(2, 7), leading to high rates of nursing home placement, poor quality of life and skyrocketing public health costs.(8)

1.2. Stroke and Respiratory Dysfunction

It is well documented that respiratory dysfunction, particularly during sleep, is common following stroke and is associated with a worse prognosis. (9-13) More than 60% of individuals suffering a first stroke develop respiratory dysfunction characterized by apneas and hypoventilation. (9) Over 80% of stroke survivors initially diagnosed with stroke disordered breathing had continued deficits even three years after their initial stroke. (14) Despite the high prevalence of stroke induced respiratory dysfunction (SIRD), little is known about the mechanism by which stroke affects breathing in part due to the lack of animal models of this disorder. Direct lesions to brainstem respiratory centers can severely disrupt breathing. (15, 16) However, patients with hemispheric strokes (the most common type of stroke) also develop disordered breathing, and damage from these strokes do not directly affect the brainstem. Additionally, there is a lack of correlation between respiratory dysfunction and stroke location and/or severity.[8] Disordered breathing that accompanies stroke is associated with higher one-year mortality and worse functional outcome at 3 months and 12 months following stroke. (17, 18) Importantly, a decrease in cognitive performance was closely associated with the severity of respiratory disturbance, and an increase in daytime sleepiness after stroke was a strong predictor of cognitive decline.(19)

A common type of stroke-induced periodic breathing is known as Cheyne-Stokes respiration, which results from hyper-activation of the mechanism by which the brain controls breathing in response to changes in tissue CO_2/H^+ (i.e., respiratory chemoreceptors). Currently the only treatments available for stroke induced respiratory disorders are physical interventions designed to maintain airway patency i.e. continuous positive airway pressure (CPAP). Unfortunately, this type of intervention is only marginally successful. Studies have shown that CPAP therapy has proven beneficial in improving outcomes for stroke patients with obstructive sleep apnea but not those with central sleep apnea. (20) Another study reported no benefit from CPAP treatment during the sub-acute phase of stroke. (21) Further, CPAP treatment is not well tolerated in recent stroke victims so patient adherence is poor. (22) Therefore, an effective treatment of stroke-induced respiratory dysfunction, particularly central apnea, is needed.

1.3. Respiratory dysfunction and cognitive decline

The majority of the evidence linking disordered breathing to cognitive decline has come from studies of obstructive sleep apnea (OSA). OSA increases the risk of cardiac and cerebrovascular events. It is has been shown that periods of intermittent hypoxia can affect cerebral circulation and result in brain hypoperfusion(23, 24), leading to decreased cerebral auto-regulation. (25, 26) In animal models of OSA, cellular stress promotes white matter loss and axonal injury in brain regions such as the hippocampus. (27, 28) Consistent with this finding, hypomyelination and

impairments in long and short-term working memory have been seen in intermittent hypoxia (IH) models such as sleep apnea(29).

Possibly due to this shared neuro-circuitry, sleep disturbances are common among Alzheimer's patients. Over 40% of patients with Alzheimer's have evidence of sleep-disordered breathing compared to only 5% of healthy controls. (30) Evidence suggests that sleep disturbances can lead to a decline in cognitive function and exacerbate memory impairment. Fragmented sleep and hypoxia induce a neuroinflammaory state, disrupting neuronal plasticity and impairing hippocampal dependent learning and memory. (31) Several studies have shown a link between sleep apnea and executive function, working memory, episodic memory and attention. (32, 33) In elderly women, those with sleep apnea are at a significantly higher risk of developing cognitive impairment than controls. Females with sleep apnea also exhibit increased white matter loss and changes in structural integrity in several brain regions compared to age-matched males. (34) Although it did not account for severity of sleep apnea and type or size of stroke, the REGARDS study found a strong correlation between stroke and sleep apnea with poorer memory and executive function compared to individuals with stroke or sleep apnea alone. Beyond the cognitive damage that is sustained with the stroke itself, stroke patients have accelerated cognitive decline in the years following the injury compared to controls, which may be more pronounced in females. (35, 36) Poor cognitive function is a strong predictor of nursing home placement and increases the length of hospitalization. (37) The mechanism underlying "post-stroke cognitive decline" are

unknown. This thesis work specifically aims to answer the question: *does disordered breathing following stroke result in cognitive decline?*

1.4. Respiratory physiology

Breathing is maintained by a negative feedback regulator designed to maintain blood gas homeostasis (i.e., obtain O_2 and eliminate CO_2). Central and peripheral chemoreceptors form the feedback portion of the control loop by adjusting the rate and depth of breathing in response to changes in tissue CO_2/H^+ and O_2. The forward component of the respiratory control loop reflects effects of ventilation on blood gases, and so determines the relationship between ventilation and arterial CO_2 (Fig.1.1). The stability of breathing depends on the sensitivity of the feedback and forward components, which are referred to as controller (chemoreceptor) and plant gain, respectively. Chemoreceptor gain is a linear relationship between ventilation and arterial CO_2, where the x-axis intercept represents the level of CO_2 required to stimulate breathing (i.e., apneic threshold). Plant gain is reflected as an isometabolic line, and where it intersects with chemoreceptor gain represents the predicted equilibrium point (eupneic CO_2). The difference between eupneic and apneic CO_2 (i.e., the CO_2 reserve) is considered a key determinant of respiratory stability; the larger the CO_2 reserve the more breathing must increase to reduce arterial CO_2 to apneic threshold (Fig. 1.2). The CO_2 reserve and consequently respiratory stability varies inversely with both plant and chemoreceptor gain. Therefore, an increase in either plant or chemoreceptor gain is predicted to destabilize breathing. As long as the $PaCO_2$ remains above apneic threshold there

will be a constant stimulus to the respiratory network inducing rhythmic breathing.(38, 39)

Respiration is mainly an autonomous activity determined by the metabolic demands of the body. The pons and medulla have been identified as the anatomical structures responsible for the autonomic control of respiration. (40) The medulla contains a diverse set of respiratory neurons, divided into the ventral respiratory group (VRG) and dorsal respiratory group (DRG), each with a distinct function involved in respiratory control. This central site of respiratory activity is a point of convergence of peripheral and central chemoreceptors, and is critical in maintaining normal respiratory function. Central chemoreceptors communicate directly with the central pattern generator (CPG), known as the Botzinger Complex. In coordination with key respiratory neuronal populations such as the nucleus tract solitarius (NTS) and the retrotrapezoid nucleus (RTN), the pacemaker and non-pacemaker cells of the Botzinger complex controls rhythmic respiratory activity.

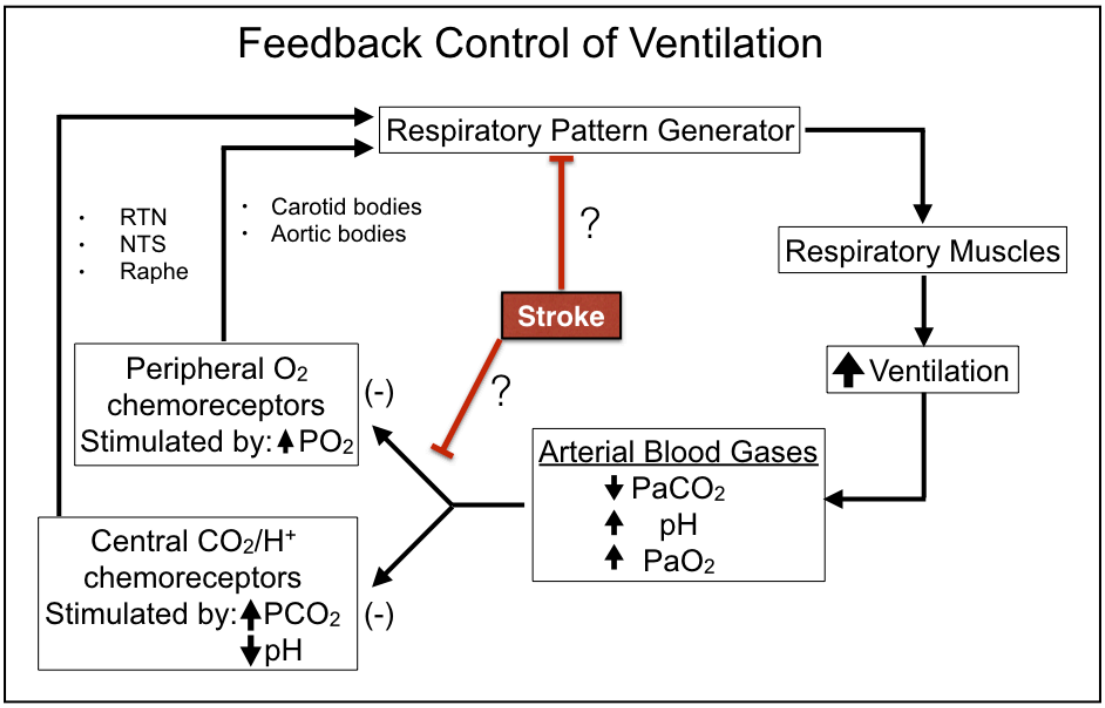

Figure 1.1. Schematic of the feed back control of ventilation. Respiratory activity is controlled by a combination of peripheral/central chemoreceptors and the central pattern generator (CPG). Peripheral and central chemoreceptors receive stimulus input in the form of PO_2 and PCO_2, respectively, communicating directly with the central pattern generator. In response to changes in levels of PO_2 and PCO_2, the CPG coordinates ventilation to maintain narrow parameters of ABGs. Stroke may disrupt the breathing loop by altering the chemosensitivity of peripheral and central receptors or by fluctuating the ventilatory response to levels of O_2/CO_2.

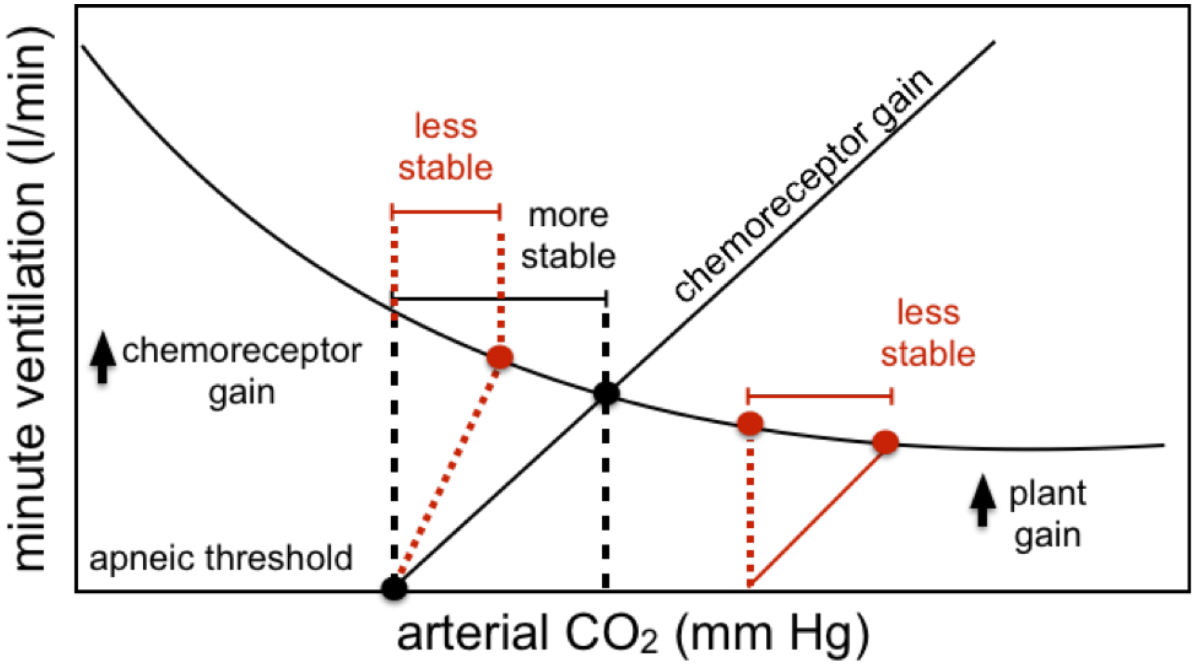

Figure 1.2. Relationship between minute ventilation and arterial CO_2. The linear relationship between minute ventilation and arterial CO_2 dictates that an increase in minute ventilation produces a larger reduction in arterial CO_2. Apneic threshold is a measurable level of CO_2 at which the drive to breath exists. Once the detectable level of CO_2 drops below threshold the drive to breath ceases. Increases in plant gain (increase the effect of ventilation of ABGs) are predicated to destabilize breathing by decreasing the CO_2 reserve. Similarly, increases in chemoreceptor gain (increase in ventilatory response to CO_2) by eliciting a larger ventilatory response to a misperception of ABGs are predicted to destabilize breathing.

1.5. Central chemoreception

1.5.1. Retrotrapezoid Nucleus

Located in the rostroventrolateral medulla and part of the VRG, a population of neurons referred to as the retrotrapezoid nucleus (RTN), functions as an important site of central chemoreception. (41, 42) These neurons are intrinsically pH sensitive, glutamatergic and project directly to the respiratory pattern generator. Chemosensitive RTN neurons also express the transcription factor Phox2b, which is considered a molecular signature of chemosensitive RTN neurons (Fig. 1.3). (43) Mutations in this gene have been shown to cause severe respiratory deficits known as congenital central hypoventilation syndrome (CCHS), also known as Ondine's Curse, the principal symptom of which is hypoventilation during sleep and reduced or absent chemical drive to breath. Activation of RTN neurons expressing channel rhodopsin increases both inspiratory and expiratory activity in conscious animals. (44, 45) It has recently been shown that GPR4 channels in the RTN serve as the H^+ sensing mechanism and disruption of these channels produces frequent apneas and an altered CO_2 evoked breathing response. (46) A common type of disordered breathing, Cheyne-Stokes respiration, is thought to result from hyper-activation of the chemo sensing mechanism by which the brain controls breathing in response to changes in tissue CO_2/H^+, a form of breathing reproduced in our stroke model.

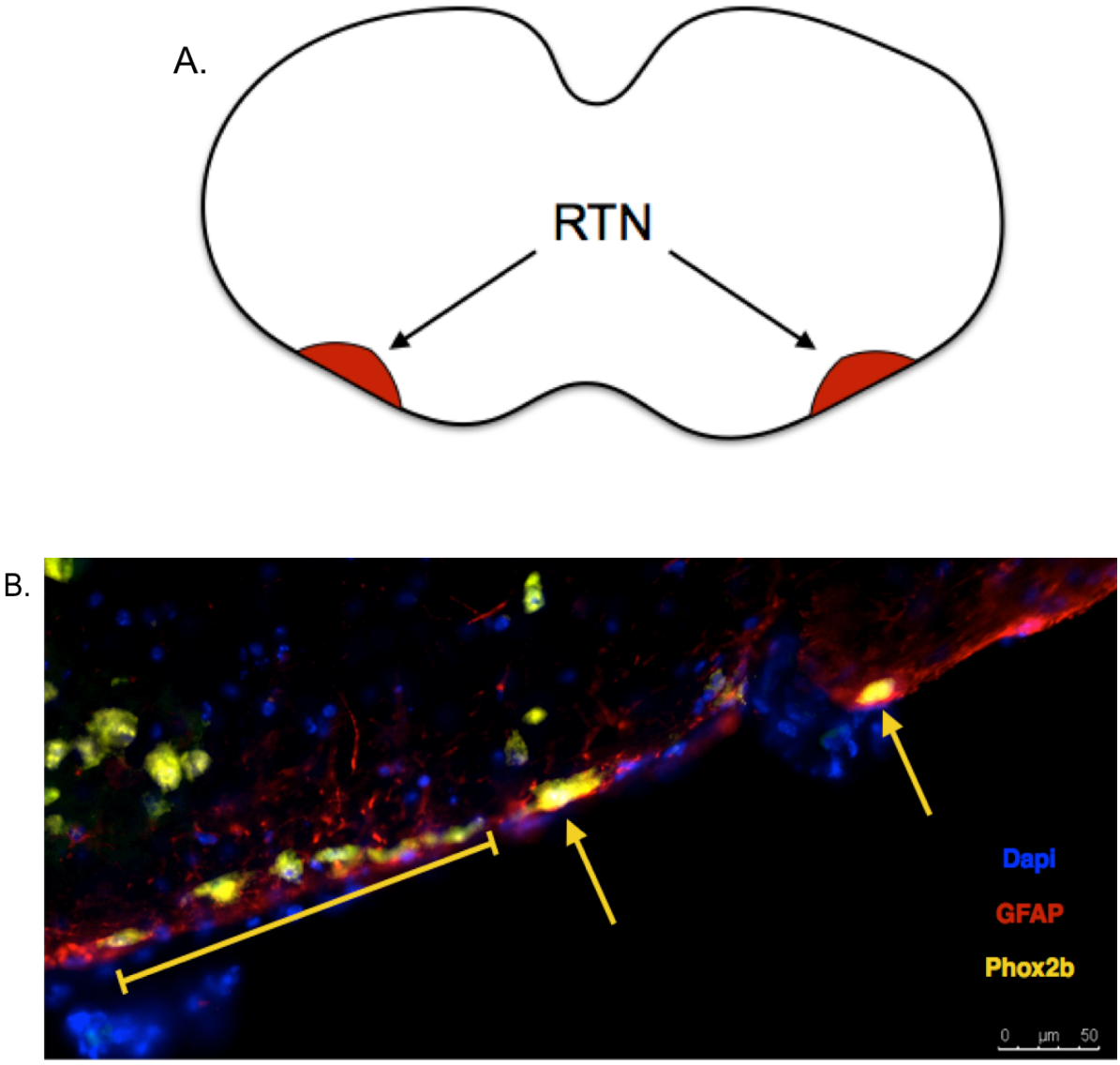

Figure 1.3. Phox2b immunoreactivity of RTN neurons. 20x fluorescence image of a 30-micron coronal brainstem slice. RTN neurons in the ventral medulla surface characterized by transcription factor Phox2b immunoreactivity (yellow). Glial fibrillary acidic protein GFAP (red), dapi (blue).

1.5.1.1. KCNQ channels

The KCNQ family of K^+ channels, namely KCNQ 2 and 3, found in the RTN, are essential regulators of neuronal excitability and a K^+ conductance known as M-current. M-currents first activate at sub threshold potentials and increase outward K^+ conductance as neurons approach action potential threshold. This outward K^+ efflux counteracts Na^+ influx, preventing full action potential. (47, 48) These channels are regulators of RTN excitability and can be pharmacologically manipulated to alter responsiveness to carbon dioxide. Loss of function of either KCNQ channel 2 or 3 results in certain types of epilepsy and is proposed to contribute to apnea related deaths in Sudden Unexplained Death in Epilepsy (SUDEP). (49-51) Specifically, patients with KCNQ2 encephalopathy exhibit apnea with some reported cases of SUDEP. (52) Furthermore, genetically engineered KCNQ2 knockout mice succumb to respiratory failure within 24 hours of birth. (53) Pharmacological inhibition of RTN KCNQ channels with XE991 increases both basal activity and responsiveness to CO_2 of RTN neurons both *in vivo* and *in vitro*. (54) In contrast, activation of KCNQ channels with Retigabine decreases neuronal action potentials and silences RTN activity. (54)

1.5.2. Nucleus Tract Solitarius

The Nucleus Tract Solitarius (NTS) is located in the dorsal medial aspect of the medulla and is a point of central entry of cardiovascular and respiratory afferents namely peripheral chemoreceptors, baroreceptors and pulmonary stretch receptors relaying information on pH, O2, CO2 and blood pressure. (55, 56) Neurons of the

NTS not only receive excitatory input from these afferent fibers in response to low levels of PaO_2, but are also capable of detecting changes in PaO_2. (57) In response to hypoxic conditions the NTS coordinates sympathetic and respiratory output to the ventral lateral medulla and the CPG by increasing blood pressure and enhancing ventilation. (58, 59) The NTS contains both glutamatergic and P2-purinergic receptors, which influence the sympathetic response of the NTS. (60, 61) The NTS projects axons to numerous areas including the ventral medullary surface, respiratory pattern generator, as well as bulbospinal neurons that project to the spinal cord to innervate respiratory associated muscles (Fig. 1.4).

In addition to contributing to the hypoxic ventilatory response, the neurons of the NTS have been demonstrated to supplement the hypercapnic ventilatory response (HCVR). Lesioning or pharmacological inhibition of these neurons attenuates the HCVR. Many neurons of the NTS also express Phox2b, similar to RTN neurons. The Phox2b transcription factor is required for normal development and migration of reflex circuitry pathways of the autonomic system that persist through adulthood. (62), Ablation of Phox2b NTS neurons with substance P-saporin impairs HCVR but had no effect on basal activity under normocapnia(63) extending the evidence that Phox2b expressing neurons are essential central chemoreceptors.

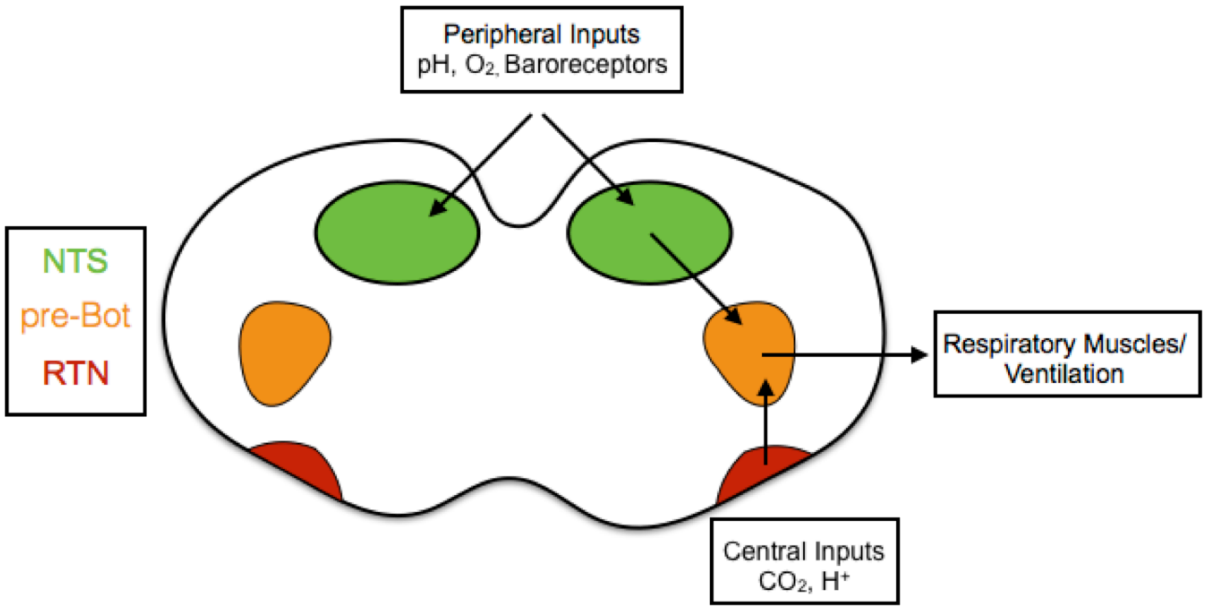

Figure 1.4. Schematic of brainstem respiratory circuitry. NTS receives peripheral input from the carotid bodies, aortic arch and baroreceptors detecting pH, O_2 and blood pressure, relaying information to the pre-Botzinger's complex. RTN central chemoreceptors monitor levels of CO_2/H^+ in the brain, also sending projections to the pre-Botzinger's complex.

1.5.3. Astrocyte, purinergic signaling and central chemoreception

The traditional view of astrocytes is that they provide structural and metabolic support to neurons, regulate blood flow and maintain blood brain barrier integrity. (64) Under pathological conditions such as stroke, astrocytes become reactive, markedly increasing the expression of glial fibrillary acidic protein (GFAP), the hallmark signature of reactive gliosis, in response to intercellular signaling molecules including but not limited to IL6, TNFα, TGFβ, INFγ and IL10 released from neurons, microglia, monocytes and endothelial cells. (64) Reactive astrocytes have the potential to alter their function and this can be both beneficial and detrimental to the brain. (65) In response to cortical stroke, reactive astrocyte processes overlap forming a persistent scar acting as a neuroprotective barrier to the ischemic site but also increases infarct size while limiting neurological recovery. (66)

Research over the past decade has begun to elucidate additional dynamic astrocytic functions. One is to modulate respiratory chemoreceptor activity in response to hypercapnia through purinergic signaling, P2X and P2Y receptors. (67) Injections of ATP in the region of the chemosensitive RTN increase respiratory activity that can be reversed by application of the P2X antagonist, PPADS. (63, 67) Ventral surface brainstem astrocytes sense extracellular pH changes and respond to acidification through elevations of intracellular Ca^{2+} evoking ATP release, uniquely different from cortical astrocytes. (68, 69)

This finding is not unique to RTN astrocytes, ATP injections into the region of the NTS stimulate cardiorespiratory activity although P2 receptor blockade did not alter the ventilator response to CO_2/H^+, suggesting an alternative mechanism by

which astrocytes contribute to respiratory activity. It is proposed that astrocytes in this region decrease glutamate uptake in response to acidification subsequently increasing output of the NTS. (70) Besides the hypercapnic ventilatory response, astrocytic purinergic signaling contributes to the hypoxic ventilatory response in the pre-Botzinger complex, in which blockade of vesicular release of ATP reduces the hypoxic ventilatory response. (71) Blockade of ATP release enhanced the secondary response to hypoxia, respiratory depression, a product of normoxia combined with hypocapnia. In response to hypoxia the respiratory system will increase minute ventilation to improve oxygenation. In doing so levels of end tidal CO_2 increase while $PaCO_2$ decreases. As PaO_2 returns to normal, $PaCO_2$ has plummeted below apneic threshold producing a system with no chemical inputs resulting in apnea. By controlling the ventilatory response to hypoxia, large fluctuations in arterial blood gases can be avoided, stabilizing respiratory patterns, a major goal in treating the clinical conditions of apnea and sleep disordered breathing.

Astrocytic end feet are closely associated with cerebrovasculature and provide a vital role in regulating vascular tone in response to neuronal metabolic demands(72) (Fig. 1.5). Recently, purinergic signaling has been shown to modulate arterial tone in the region of the RTN. Disruption of this mechanism increases vessel diameter and more importantly decreases the ventilatory response to CO_2. (73) Astrocytes play a seemingly vital role in contributing to respiratory chemoreception while disrupting cellular functions alters the ventilator response to CO_2. *We hypothesize that ischemic stroke induces brainstem reactive gliosis contributing to respiratory dysfunction.*

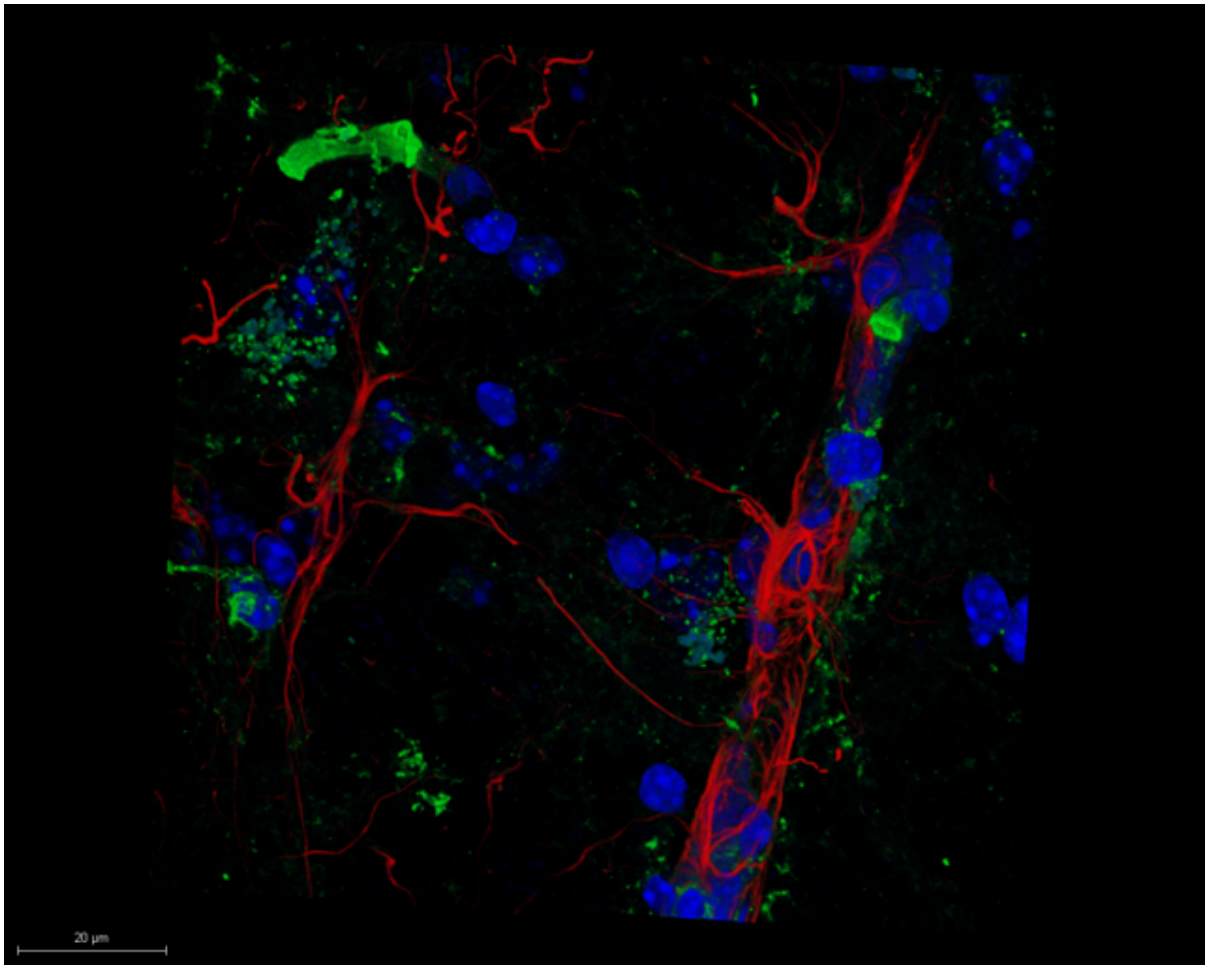

Figure 1.5 Astrocyte end feet closely associate with vasculature. 40x confocal image of GFAP staining of astrocytic (red) end feet “wrapping” around lectin stained (green) cerebral brainstem vasculature. Dapi – blue.

1.6. Disordered breathing

Sleep disordered breathing (SDB) refers to periods of reductions in breathing amplitude or complete cessation of airflow which results in hypoxia, hypercapnia, arousals and fragmented sleep. SDB is associated with increased morbidity and mortality, and increases the risk of development of hypertension, stroke, cardiac failure and diabetes. (74) Regardless of the subtype of disordered breathing, patients suffer numerous episodes of hyponea or apnea per hour as defined by the apnea-hyponea index. Five or more episodes an hour is classified as minor while 15 or more is severe. (75) During episodes of hypoventilation oxygen levels plummet with concurrent increase in CO_2 levels. Decreases in P_aO_2 levels stimulate the O_2 sensing carotid body while rises in $PaCO_2$ activate central chemoreceptors, resulting in sympathetic excitation of brainstem neurons stimulating breathing, arousals and producing fragmented and decreased quality of sleep.

Although Cheyne-Stokes respiration is proposed to be a result of alterations in chemoreception, the underlying mechanism and circuitry remains to be elucidated. There are many alterations that can produce disordered breathing including chemosensitivity, plant gain or transport time delays of arterial blood flow between the lungs and respiratory chemoreceptors. (76) All can result in periodic breathing characterized by $PaCO_2$ levels that drop below apneic threshold and subsequently lead to apneas. (77) Following periods of apnea, $PaCO_2$ levels rapidly rise stimulating a large ventilatory overshoot, which lowers $PaCO_2$ levels below apneic threshold. Concurrently, during periods of apnea PaO_2 levels plummet resulting in hypoxia.

Disordered breathing with recurrent apneas is associated with intermittent hypoxia, defined as an apneic period of sufficient duration to cause a >3% drop in oxygen saturation of hemoglobin. (78) Hypoxemia activates peripheral chemoreceptors in the aortic arch and carotid bodies potentiated by catecholamines. Peripheral afferent fibers integrate with the brainstem respiratory network innervating the respiratory pattern generator. In response to hypoxia alone, respiratory frequency and tidal volume increase, raising levels of PaO_2 while decreasing levels of $PaCO_2$. An unfortunate byproduct of this response is O_2 levels above threshold and CO_2 levels below apneic threshold resulting in apnea. Hypercapnia and hypoxia following apnea can synergistically stimulate the sympathetic response further complicating this matter.

*1.7. TGF*β *increases in the ipsilateral hemisphere following stroke*

Transforming Growth Factor Beta (TGFβ) is a multifunctional cytokine belonging to the large transforming growth factor family. It has many cellular functions in both development/embryogenesis and adulthood, including cell growth, differentiation, apoptosis and a context dependent activation/inhibition of inflammation. (79) TGFβ can be secreted as four different latent isoforms, named TGFβ1-4, that become active following proteolytic cleavage and binding to the type II TFGβ receptor. (80) Binding with the TGFβ receptor initiates the SMAD signaling pathway, resulting in phosphorylation of SMAD proteins, with the RSMAD/coSmad complex translocating to the nucleus, binding various transcriptional promoter sites, and altering expression of a variety of genes. TGFβ activity can be evaluated by

measuring the downstream effects on the SMAD signaling pathway, specifically phosphorylated SMAD2 (Fig. 1.6).(81)

The TFGβ receptor is expressed on all major cell types of the brain, including neurons, microglia and astrocytes. (82) After brain injury TGFβ has powerful effects on the immune system, being both pro and anti-inflammatory depending on the cell type and context. In the setting of experimental stroke TFGβ expression remains elevated for a week and is thought to be neuroprotective, as blocking TGFβ1 signaling exacerbates injury. (83, 84) Activated microglia and macrophages appear to be the source of TGFβ following ischemic stroke and signal in an autocrine manner promoting an anti-inflammatory phenotype resulting in a wound healing response. Activated astrocytes also upregulate TGFβ signaling during ischemic stroke as evidenced by increased pSmad2 promoting reactive gliosis and scar formation (Fig. 1.6).(85)Inhibition of TGFβ signaling via the Smad3 pathway improves wound healing and decreases scar formation, as evidenced by decreased GFAP immunoreactivity and fibronectin expression in a brain stab wound model. (86) Glial scar formation is proposed to be detrimental to post stroke recovery preventing neurogenesis and angiogenesis in the infarct region. (87) The effect of TGFβ on astrocytes outside the infarct region remains to be elucidated. The varying roles of the different TGFβ isoforms further complicate this matter.

The amount of TGF-β in the aged 18-month-old murine brain was elevated compared to that of a 5-month-old brain while following a similar time course of expression; these levels further increase following ischemic stroke. Interestingly, baseline levels of TGF-B do not fluctuate with sex though sex based changes in the

aged brain in response to stroke are still unknown. (85) Corresponding with findings of increased TGFβ expression is evidence of an accelerated glial reactivity in aged brain following cerebral ischemia, resulting in premature scar formation hindering post stroke recovery. (88) Early scar formation is also associated with an untimely accumulation of BRD-U positive astrocytes further indicative of proliferation and reactive gliosis. (89)

In the aged brain activated microglia produce an exaggerated level of cytokines contributing to a prolonged neuroinflammatory condition. Following immune challenge, astrocytes will respond to IL-10 in turn attenuating microglia activation in a TGF-β1/Smad3 dependent manner. (90) Inhibition of this signaling in young mice prolonged sickness behavior while amplifying the pro inflammatory cytokine profile in LPS challenged mice. (91) Following immune challenge, astrocytes from the aged brain show a 3 fold increase in GFAP expression compared to young counterparts as well as decreased expression of IL-10 receptor,(92)suggesting a dysfunctional reactive astrocyte profile contributing to an increase in neuroinflammation. Interestingly, the TGF-B1/Smad3 signaling pathway is also impaired in aged mice promoting further neuronal dysfunction and neurodegenerative disease. Differential astrocyte reactivity in the aged brain could explain, at least partially, why aged animals display worse functional outcomes and may contribute to the development of disordered breathing and further cognitive impairment.

A.

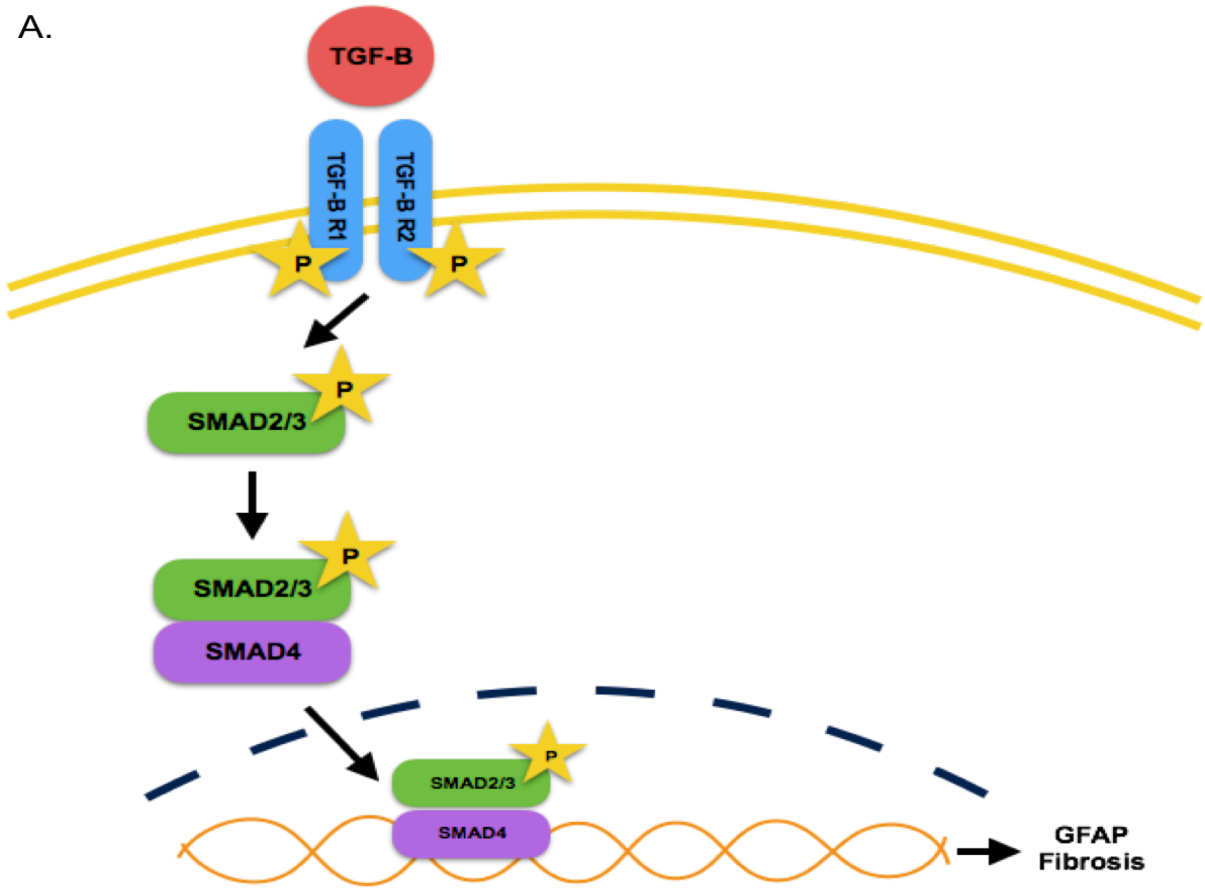
TGF-B
TGF-B R1
TGF-B R2
P
P
P
SMAD2/3
P
SMAD2/3
SMAD4
P
SMAD2/3
SMAD4
GFAP
Fibrosis

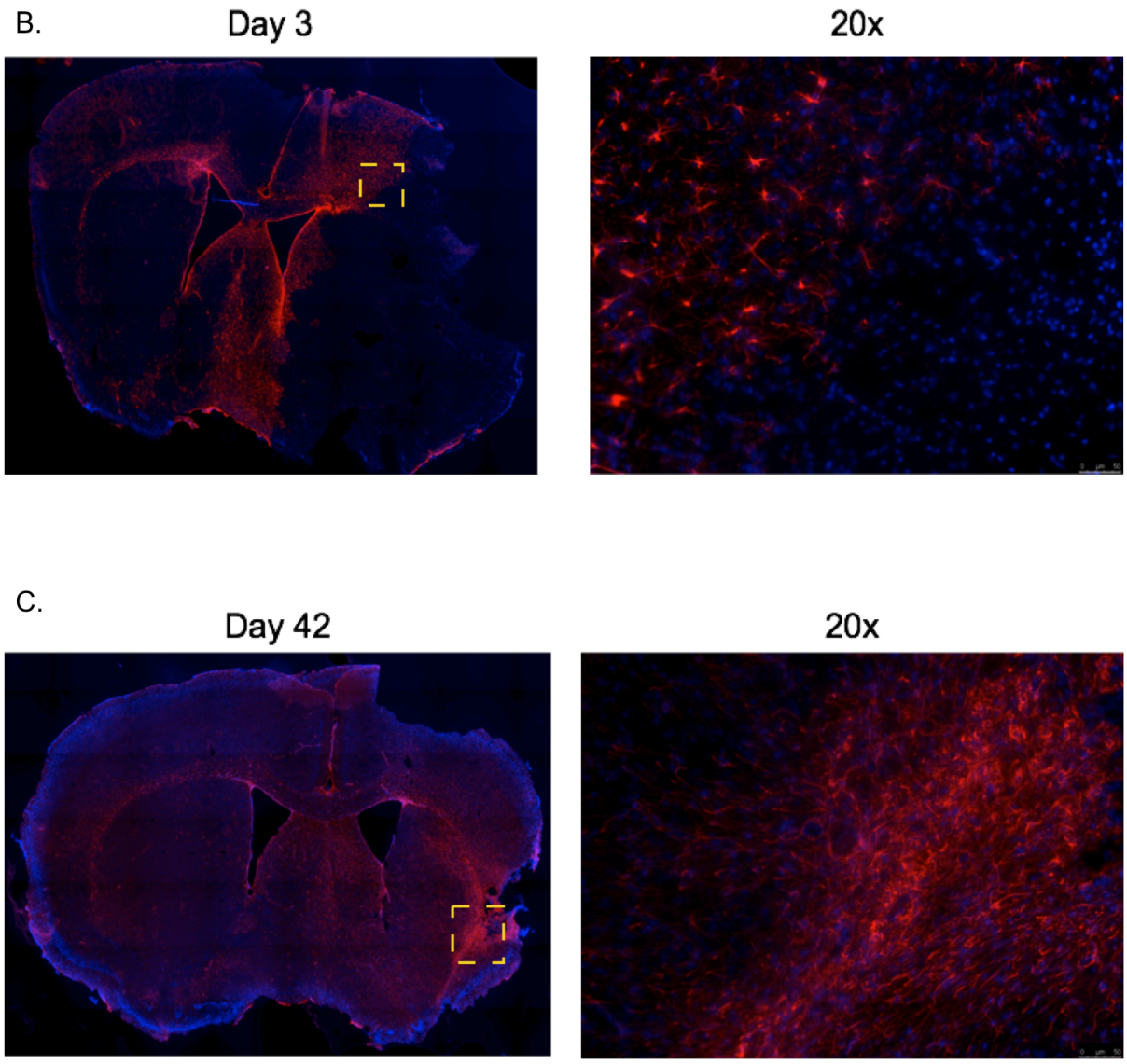

Figure 1.6. TGF-β signaling and MCAO induced astrogliosis. (**A**) Schematic of TGF-β signaling pathway via phosphorylation of SMAD2/3 complex leading to increased GFAP expression and fibrosis. (**B**) Fluorescence image of a day 3 post stroke 10x mosaic coronal slice depicting increased astrocyte expression of GFAP on ipsilateral side. 20x image of yellow reference frame shown. (**C**) Day 42-post

stroke coronal slice of GFAP staining depicting glial scar formation surrounding injury. 20x image of yellow reference frame shown. GFAP-red, dapi – blue.

1.8. Acetazolamide and cerebral blood flow

Carbonic anhydrase is an enzyme that catalyzes the removal of a water molecule from carbonic acid predominantly expressed in blood cells and exerting its effects on the kidney allowing for the reabsorption of bicarbonate and other electrolytes. (93) Acetazolamide, also known as Diamox, is a carbonic anhydrous inhibitor that prevents the reabsorption of bicarbonate in the kidneys and increases its excretion. According to Le Chatelier's principle the carbonic acid equation shifts towards an increase in bicarbonate and hydrogen ions, lowering blood pH, which can modulate respiratory neuronal excitability. Acetazolamide has shown promise in the treatment of intracranial hypertension, altitude sickness and obstructive sleep apnea. (94-96) In the treatment of obstructive sleep apnea, Acetazolamide is proposed to improve breathing by either decreasing the efficacy of CO_2 removal, i.e. decreasing plant gain, or by increasing neuronal excitability by increasing H^+ concentration.

It has been well established that acetazolamide's increases cerebral blood flow. A balance between intraluminal pressure and interstitial pressure regulates regional blood flow. The water-shed channel, aquaporin 4 (AQP4), has been shown to regulate this balance. As interstitial water flow increases vascular diameter decreases and subsequent blood flow decreases. (97, 98) AQP4 channels are inhibited by H^+ under physiological conditions, decreasing interstitial flow while increasing regional blood flow. Recently, MRI has demonstrated that regional neural activity increase H^+ concentration while increasing blood flow. (99) Furthermore,

acetazolamide administration results in accumulation of extracellular H^+, increased capillary dilation and cerebral blood flow (Fig. 1.7).(100)

Cerebral autoregulation maintains constant blood flow irrespective of pressure changes to meet regional metabolic demands. (101) Increase in concentrations of metabolites such as CO_2 and H^+ induce vascular changes that lead to an increase blood flow. (102, 103) This in turn facilitates removal of excess metabolites, matching blood flow to metabolic need. (104) Respiration is one method in which the body regulates the removal of CO_2/H^+, which is initiated by respiratory centers and leads to an increase in minute ventilation. If the vasculature surrounding key respiratory neuronal populations responded to CO_2/H^+ in a similar manner as other vessels in the cerebral vascular bed, this would facilitate the removal of CO_2/H^+ limiting the ability of respiratory chemoreceptor to detect these metabolites. (105) Recently this concept of reversed vascular reactivity has been demonstrated in the arterioles in the RTN. Arterioles in this region and the cortex are differentially regulated during exposure to CO_2/H^+ via purinergic signaling. (73) Whereas the vasculature in the cortex *dilates* in the presence of CO_2/H^+, RTN arterioles *constrict* following identical stimuli.

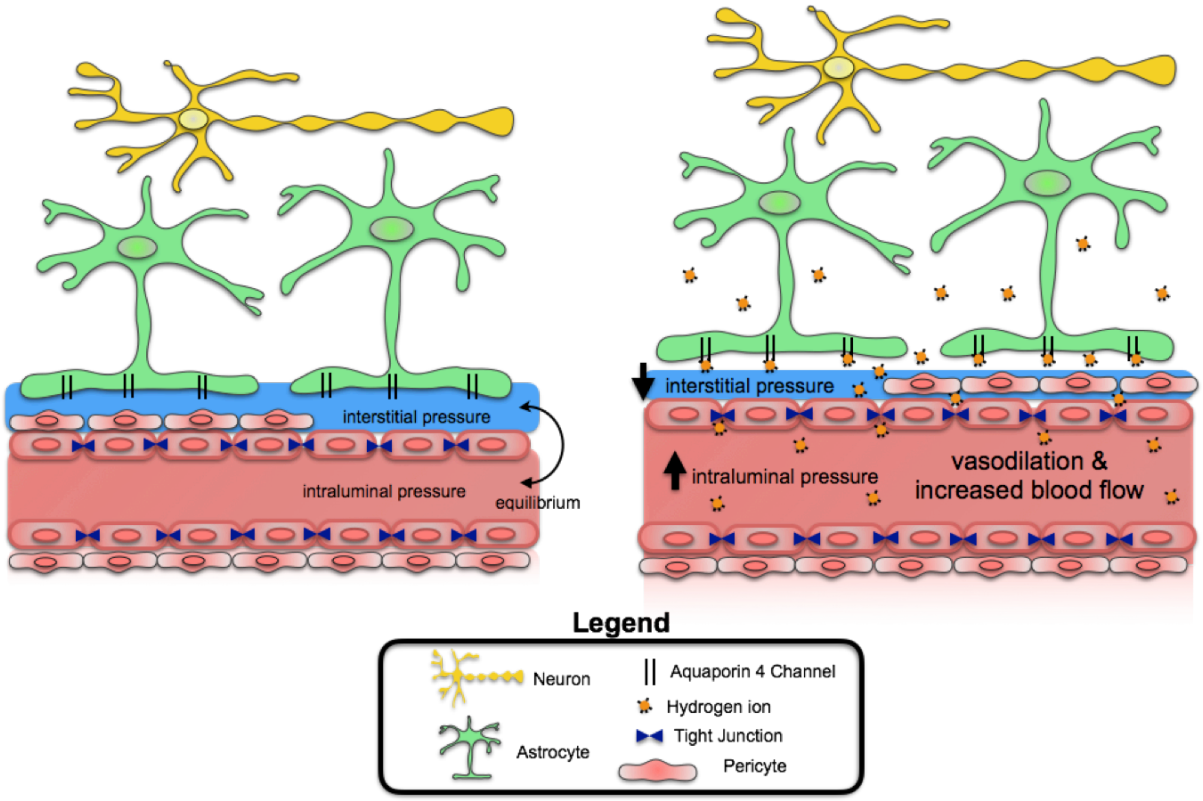

Figure 1.7. Astrocyte aquaporin 4 mediated control of regional cerebral blood flow. Regional cerebral blood flow is regulated by an equilibrium between intraluminal and interstitial pressure. Intraluminal pressure is maintained by cerebral autoregulation, while interstitial pressure is predominantly sustained by bulk water flow through astrocytic aquaporin 4 channels (Aqp4). Aqp4 channels are inhibited by excess H^+, decreasing interstitial pressure, subsequently leading to vasodilation and increase regional blood flow.

1.9. Objectives

The objective of this thesis is to determine if a mouse model of ischemic stroke produces disordered breathing recapitulating the phenotype seen in clinical populations. Numerous studies have reported stroke patients with disordered breathing have worse functional and cognitive outcomes than those with stroke alone. (17-19) The first step towards treatment of the negative consequences of SIRD is the development of appropriate animal models to study the pathophysiology of SIRD and to test potential pharmacological agents. My central hypothesis is that stroke will induce chronic respiratory instability and apnea in mice, and that this is linked to higher mortality and greater post-stroke cognitive deficits. As the aging population suffers the brunt of stroke related morbidity and mortality it is critical to investigate the mechanisms contributing to these factors. Previously, we have found that although aged male mice have similar size infarcts as females they suffer higher mortality and functional deficits compared to aged females. This poor recovery witnessed in aged males may be linked to respiratory dysfunction. I expect aged male animals will have a slower recovery following MCAO compared to young animals and that the severity of disordered breathing will correlate with poorer cognitive outcomes.

The mechanisms that lead to post-stroke respiratory dysfunction are unknown. The contribution of central apnea to progressive cognitive decline that is seen after stroke is also unclear. This work specifically aims to answer the questions: does disordered breathing occur after stroke in animal models? Is this worse in aged animals? Does the severity of post stroke respiratory dysfunction

correlate with post-stroke cognitive decline? We performed longitudinal studies in young and aged mice to evaluate the prevalence and evolution of post-stroke disordered breathing. We then examined how post-stroke respiratory dysfunction contributed to progressive cognitive decline. Next we assessed the role of TGF-β induced astrogliosis and subsequent respiratory dysfunction.

Lastly we determined if targeting specific aspects of respiratory control could improve the breathing phenotype leading to an enhancement in long-term recovery after stroke. We employed various pharmacological techniques to manipulate plant gain in order to suppress hypoxic apneic events. We proposed the following three aims to answer these questions (Fig. 1.8).

Aim 1: Determine the phenotype of stroke disordered breathing across age and sex. The MCAO model of ischemic stroke produces a disordered breathing phenotype characterized by a decrease in respiratory frequency as well as an increase in incidence of spontaneous apneas. Prior work has shown that the response to stroke differs dramatically based on both the age and sex of the animal examined. We have examined young (2-3 month) and aged (18-20 month) male and female mice and discovered that aged males present with a severe form of disordered breathing while aged females display a very mild phenotype.

Aim 2: Assess the severity of stroke induced respiratory dysfunction and its relationship with post-stroke progressive cognitive decline. We will employ the MCAO model of ischemic stroke to replicate the disordered breathing phenotype

seen in the clinical stroke population. Utilizing this pattern of respiratory instability we will explore the severity of disordered breathing, progression of cognitive decline and overall outcomes across both age and sex over a six-week period. Lastly, we will explore if increased TFG-β expression following ischemic stroke contributes to brain stem glial cell reactivity and respiratory dysfunction.

Aim 3: Targeting stroke induced respiratory dysfunction to improve neurological recovery. Apneas are a central trait of disordered breathing and produce numerous physiological changes. Manipulating individual components of the respiratory control system may stabilize respiratory activity, eliminate hypoxic events and promote the maintenance of normal blood levels of O_2 and CO_2. This will reduce progressive insults to neuronal tissue and improve cognitive outcomes after stroke. Preliminary evidence shows that administration of Acetazolamide stabilizes respiratory activity by eliminating apneas. We propose continuous treatment with Acetazolamide will not only stabilize respiratory instability but will also reduce post-stroke cognitive deficits.

This work will not only develop a model of stroke induced respiratory dysfunction that recapitulates the respiratory phenotype seen in the clinical population, but will also provide significant translational relevance to the field of stroke, aging, and cognitive decline. We have integrated studies to examine SIRD in both males and females, as our preliminary studies have shown significant differences in respiratory function after stroke based on the sex of the animal

examined, recapitulating clinical data. Successful treatment of SIRD may lead to significant improvements in post-stroke recovery and cognition, resulting in improved outcomes and prevention of further disability.

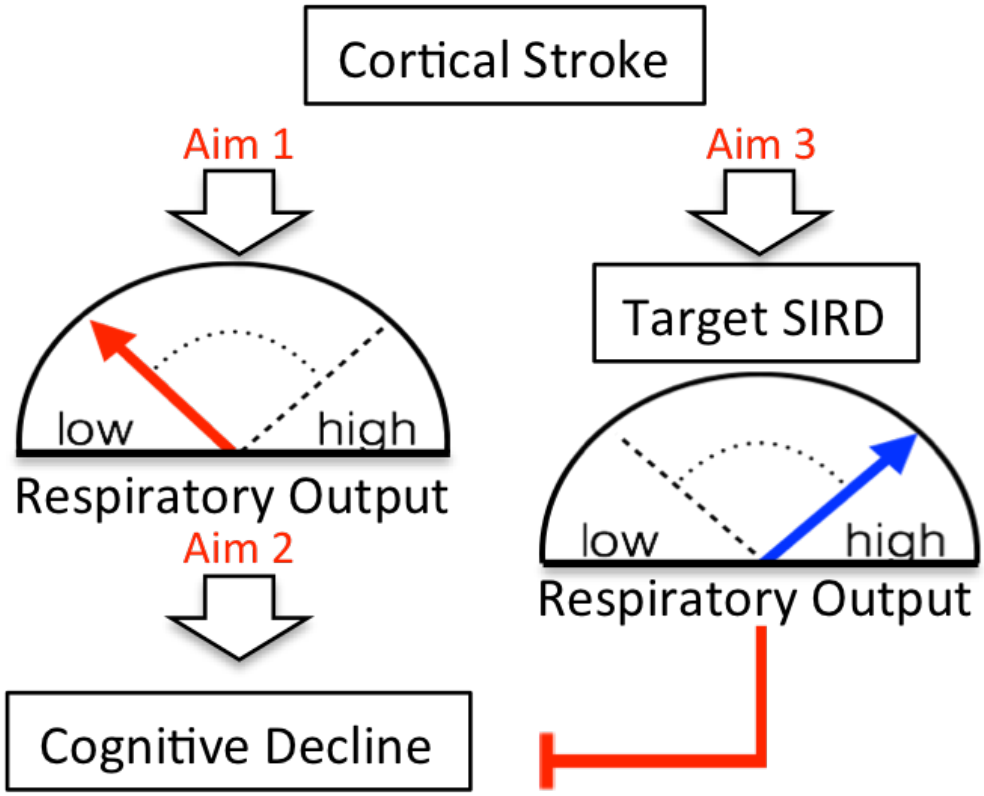

Figure 1.8. Schematic overview of experimental aims.

Chapter 2. Materials and Methods.

2.1. Animals

Young (8-12 weeks, 21-27g) C57/B6 male and female mice were purchased from Jackson Laboratories. Aged C57/B6 mice (18-21 months) of both sexes were obtained from the National Institute on Aging. All mice were housed in a temperature- and humidity-controlled vivarium, 5 per cage (11”L, 6”W, 6”H) with a 12-hour light/dark schedule with *ad libitum* access to food and water for 4 weeks after arrival. All experiments were performed according to NIH guidelines for the care and use of animals in research and under protocols approved by the University of Texas Health Science Center Houston Institutional Animal Care and Use Committee.

Cohort	Sacrifice	
Plethysmography	Day 7	
Brainstem Histology	Day 3	TTC & Fluorojade
Arterial Blood Gases	Day 3	
Pulse Oximetry	Day 3	Perfused
42 day studies of cognitive outcomes	Day 42	IHC/CV/Western
Distal MCAO	Day 42	IHC/CV
Cohorts for each: Acute Retigabine/XE991/ Actazolamide Assessment	Day 7	Perfused
Chronic Acetazolamide	Day 42	IHC/CV/Western
TGF- **β**	Day 7	IHC

Table 1. Cohort Table.

2.2. Middle cerebral artery occlusion

Focal transient ischemia was induced by middle cerebral artery occlusion for 60 minutes under Isoflurane anesthesia followed by reperfusion as described previously. (106, 107) Briefly, mice were placed prone onto a heating pad and a midline incision was made into the skin. The carotid artery was ligated to allow for placement of a silicon filament through the external carotid into the internal carotid, which allowed access to the middle cerebral artery (MCA). An 80% drop in cerebral blood flow confirmed occlusion of the MCA by Laser Doppler (Moore Instruments). After 60 minutes of occlusion the silicone filament was withdrawn, the surgical site was sutured and the animals were returned to home cages and monitored. The same procedure was conducted in sham animals except the silicone filament was not introduced past the internal carotid. Body temperatures were monitored rectally and maintained at approximately 37 °C.

2.3. Neurological-Deficit Score (NDS)

Mice were given a neurological-deficit score as previously described. (108) Neurological deficits were scored using the following rubric on a scale from 0-5: 0 = no deficit, 1 = forelimb weakness and torso turning to ipsilateral side when held by the tail, 2 = circling to affected side; 3 = unable to bear weight on affected side and circling immediately when placed on a bench, 4 = no spontaneous locomotor activity or barrel rolling, and 5 = dead.

2.4. Distal middle cerebral artery occlusion

Mice were subjected to permanent distal middle cerebral artery occlusion (pDMCAO) as previously described. (109) Following this, the right dorsolateral cranium was shaved and a 1cm^2 skin flap was cut over the temporalis muscle, which was then incised with Vannas scissors to expose the temporal bone. The skull was scrubbed with sterile saline and a 2 mm burr hole was drilled over the middle cerebral artery, immediately dorsal to the zygomatic arch. The dura were reflected with sharp forceps and the middle cerebral artery washed with sterile saline. Stroke was then induced by 1-2 seconds of low temperature cauterization of the exposed middle cerebral artery, and ischemia confirmed by laser doppler as a greater than 90% drop in blood flow to the cortex distal to the occlusion. Following successful induction of ischemia, the burr hole was closed with dental cement, the temporalis muscle incision repaired with Vetbond and the skin incision closed with Vicryl 5-0 nylon sutures. Sham surgeries were performed following an identical procedure, except that no cauterization was performed.

2.5. Whole body plethysmography

Respiratory parameters (frequency, tidal volume, minute ventilation, # of apneas) were measured using whole body plethysmography, a well-established technique for respiratory activity. (110, 111) Mice were placed individually into a ventilated (1L/min) plexiglass chamber and allowed 1 hour to acclimate. Inspiration and expiration result in decreases or increases in chamber pressure relative to a reference chamber that are detected using a pressure transducer, which is

calibrated prior to every experiment. Tidal volume (ml, normalized to body weight and corrected for chamber temperature, pressure and humidity) and respiratory frequency (breaths/min) will be recorded on a breath-to-breath basis and analyzed from periods of relative quiescence during the last 2 minutes of each experimental condition; the product of tidal volume and frequency is minute ventilation (ml/min/g). The frequency of apneas (defined as ≥3 or more missed breaths) will be determined for the duration of the recording. We confirmed that the section of data selected for analysis is devoid of behavior artifacts and is most representative of each animal's breathing pattern. All animals received baseline assessment of respiratory activity prior to undergoing surgery. Central chemosensitivity was assessed starting 3 days after surgery by exposing animals to graded hypercapnia (3, 5 and 7% CO_2 balanced O_2; 5 minutes per condition). During a separate period of testing peripheral chemoreflexes were assessed by exposing animals to 5 minutes of hypoxia (10% O_2 balanced N_2) to stimulate carotid chemoreceptors. Control of gases and calculation of respiratory parameters was controlled by Buxico Finepoint software (DSI).

2.6. Arterial blood gas analysis

A small volume of blood (100ul) was collected via a cannula surgically implanted into the carotid artery on day 3-post surgery to measure arterial blood gases (ABG) and analyzed using CG8+ iStat cartridges (Abbott).

2.7. O_2 consumption

To assess differences in metabolic activity animals were placed in individual chambers where they were allowed to move freely and have access to food and water. Under room air conditions O_2 consumption was measured using Oxymax (CLAMS) open flow system as described. (112) Levels of O_2 and CO_2 were measured for 24 hours to capture both wake and rest periods.

2.8. Pulse oximetry

On day 3-post surgery pulse oximetry measurements (SpO_2) were recording using MouseOx neck collar (Starr Life Sciences Corp.). Collars were place around shaved neck of both stroke and sham mice. Mice were returned to their home cages and allowed to acclimate to the collars. Recordings were taken during periods of time when the animals were at rest (calmly sitting in cage without any signs of distress or motor activity).

2.9. Histological assessment

Mice were anesthetized with a 0.1mL/10g body weight dose of Avertin (T48402, Sigma-Aldrich) dissolved in 2-Methyl-2-Butanol. Animals were perfused transcardially with phosphate-buffered saline followed by 4% paraformaldehyde. The brain was removed from the skull, post-fixed for 24 h, and subsequently placed in cyroprotectant (30% sucrose). The brain tissue was cut into 30-μm free-floating coronal sections and was stained using cresyl violet (CV, C5042, Sigma-Aldrich) for evaluation of ischemic cell damage. Images were acquired by a charge-coupled

device camera (Micropublisher 5.0 RTV, QImaging) and analyzed using Sigmascan Pro5 (Systat Software Inc.) as described. (113) Atrophy volumes were expressed as a percentage of the ipsilateral hemisphere. Animals were excluded if they had a posterior cerebral artery occlusion or no intra-ischemic deficits.

2.10. 2,3,5-triphenyltetrazolium chloride (TTC) staining

Brains were extracted after euthanasia and cut into five 2-mm coronal sections, and stained with 1.5% 2,3,5 triphenyltetrazolium chloride (TTC) as performed. (114) This stain is used to distinguish between metabolically active versus inactive tissue, here it is used as a measurement of infarct size.

2.11. Fluorojade staining

Thirty micron sections were slide mounted and stained for degenerating neurons(115) using Fluorojade (EMD Millipore) following manufacturer's recommendations.

2.12. Immunohistochemistry

Thirty micron sections were slide mounted and heat induced antigen retrieval was performed using citrate acid pH 6. Permeabilized in 0.15% TritonX in PBS and blocked in 10% Normal Donkey Serum / 1% Bovine Serum Albumin (Sigma). Sections were incubated overnight with rabbit anti-pSmad2 (1:200, Abcam), CY3 conjugated GFAP (EMD Millipore) and then incubated for 60 min with anti-host antibody conjugated with a fluorophore (1:1000), DAPI nuclear stain solution

(1:1000; Invitrogen), and images were then taken using an inverted light Leica fluorescence microscope. Quantifications performed with Leica LAS X software platform.

2.13. Acetazolamide administration

For acute studies mice received a 40mg/kg subcutaneous (SQ) or vehicle injection day 3 post surgery. For long term studies osmotically driven alzet pumps (Alzet) filled with acetazolamide or saline were surgically placed SQ on day 14 following surgery. Following manufacturer's instructions for pump priming, animals were placed prone under Isoflurane anesthesia and a small SQ incision was made between the shoulder blades. A pair of blunt sterile scissors was introduced into the incision and slowly advanced to create a pocket for pump placement. Following pump placement the wound was sutured closed and a local anesthetic was administered. Animals were monitored daily for wound healing and to make sure the pump stayed in place.

2.14. Retigabine and XE991 administration

As discussed earlier, subthreshold K+ conductance is produced by KCNQ channels which regulate basal activity of chemo sensitive RTN neurons. (54) We employ Retigabine a KCNQ channel agonist and XE991, a KCNQ channel antagonist, to decrease and increase respiratory instability respectively. Retigabine (10mg/kg) or DMSO vehicle was administered SQ day 3 post surgery. XE991 (2mg/kg) or DMSO vehicle was administered SQ on day 3 post surgery.

2.15. Transforming Growth Factor-Beta (TFG- B) administration

TGF-*B* or vehicle (5 uL sterile saline) was administered by intracerebroventricular (ICV) injection into naïve mice under Isoflurane anesthesia under stereotaxic guidance. (116) A burr hole was made with the tip of a 30 gauge needle in the right skull at the coordinates -0.9mm lateral and -0.1mm posterior from Bregma, followed by needle insertion of a 10 uL, 33 gauge syringe (Model 701 SN, Hamilton Company) to a depth of -3.1mm. 5 ul of TFG-*B* or vehicle was injected over 2 minutes. The needle was left in place for 5 minutes to prevent efflux of solution.

2.16. Behavioral tests

2.16.1. Novel Object Recognition Test (NORT)

This test was conducted in a quiet temperature controlled room. Mice are individually place into separate plexiglass rectangular boxes with 2 identical objects, termed familiar objects, equally placed on each side. Mice are allowed to freely explore the chamber and objects for 10 minutes. At the end of the training period mice are returned to their home cage for 5 minutes. During this time the chambers are cleaned and one of the objects in each arena is replaced with a novel object of different shape, size and color. At the conclusion of the 5-minute rest period mice were placed into the same chamber as the training probe and again allowed to freely explore for 10 minutes. Following this test trial mice were returned to their home cage and the test was concluded. Both the training and test trials were recorded using a video tracking system (Noldus EthioVision XT) via an overhead mounted

camera. Familiar and Novel objects were identical for all mice. New novel objects were used during subsequent testing periods.

2.16.2. Barnes Maze

Barnes maze was conducted on an elevated circular platform (92cm diameter) with 20 evenly spaced holes (5cm diameter). (117) A randomly chosen hole was designated as the escape hole, which allowed the animal to escape the platform into a dark rectangular box below. During training trials, mice learn the location of the escape hole by spatial clues positioned around the platform. All training trials and the test trial were performed in a dark room with the platform lit by bright white light. Animals received 3 training trials followed by a test trial 4 hours later on day 21 or 42-post surgery. During the first training trial, the mouse was placed into the center of the arena and then guided to the escape hole by a clear cylindrical chamber, which it was allowed to explore for 1 minute. During the second and third trials the animal was again placed into the center of the platform and allowed to freely explore the arena for 5 minutes. At the end of each trial if the animal did not find the escape hole it was guided to it using the same clear chamber. The arena was cleaned between trials. The testing period consisted of one 3-minute trial. The trial was terminated when the animal entered the escape hole or at the end of the 3 minute period. Any animal that did not find the escape hole once during any training trial was excluded. A camera was mounted above the maze to monitor performance through a video tracking system (Noldus EthoVision XT).

2.16.3. Contextual fear conditioning

Animals were allowed to acclimate to a square plexiglass container with metal grid floor (Harvard Apparatus) for 2 minutes on day 42 post surgery. Two opposing walls of the chamber displayed different patterns, the back wall was white and the front wall was clear. Contextual chambers were inside a larger soundproof box lite by white light and closed during acclimation, training and testing trials. Chambers were cleaned prior to use and between animals with scented wipes. White noise was played inside the box. Following all acclimation trials animals were placed back into the plexiglass container for 2 minutes then received a 0.7mA shock through the metal grid floor lasting 2 seconds. Animals were then returned to their home cage. 24 hours later animals were again placed in the contextual fear chambers and the session was recorded for 3 minutes. (Noluds EthioVision XT) The amount percent of time the animal spent freezing was calculated. (118)

2.16.4. Corner test

This test detects integrated sensory-motor function as it involves stimulation of vibrissae sensory) and rearing (motor). This test was carried out as described. (119) Briefly, a mouse is encouraged to enter a 30-degree corner created by two cardboard pieces. Once in the corner, the boards stimulate both sides of the vibrissae, the mouse then rears forward and up, turning to face the open end. Twenty trials are performed and the percentage of right turns is calculated.

2.17. Statistical analysis

Statistics are presented as means ± SEM for all experiments. Statistics were performed using GraphPad Prism 7. Interval power analysis was performed to determine group size. A student's t-test was used when comparing 2 groups and a 2-way ANOVA was performed when comparing multiple groups. If an interaction was statistically significant, then Sidak's post-hoc analysis was used to assess where the interaction occurred. If there was no significant interaction, main effects were reported when significance. Linear regression analysis was used to assess changes in chemosensitivity. A probability value of $p<0.05$ was considered statistically significant. All investigators were blinded to surgical condition when analyzing data.

Chapter 3. Stroke Induces Respiratory Dysfunction Characterized By Apneas and Hypoxia.

Rationale: Stroke induced respiratory dysfunction is highly prevalent amongst individuals suffering a first time stroke. Patients suffering respiratory dysfunction, characterized by apneas and periods of hypoxia, have worse functional outcomes and demonstrate progressive cognitive decline following ischemic stroke. CPAP, the only approved therapy for respiratory dysfunction, is poorly tolerated by stroke patients and has proven futile in improving respiratory activity. This first step towards treatment of the negative consequences of SIRD is the development of appropriate animal models that will allow us to explore the pathophysiology of SIRD and provide us with the opportunity to test potential pharmacological agents.

3.1. Middle cerebral artery occlusion produces disordered breathing characterized by hypoventilation and increased apneas.

To determine if MCAO produces disordered breathing 6-8 week old male mice were subject to 60 minutes of MCAO or sham surgery. To establish baseline respiratory activity mice underwent plethysmography testing as described in 2.4 1-day prior to surgery. On day 3-post surgery mice underwent plethysmography to identify the phenotype of stroke induced respiratory dysfunction. Respiratory frequency, measured as breaths per minute, decreased compared to sham, (164.4±5.09 stroke vs. 286.7±13.97 sham) respectively, $p<0.0001$ (Fig. 3.1a). Stroke mice displayed an increase in tidal volume (ml/min), although not significant, (0.0079±0.0003 stroke vs. 0.006±0.0004 sham), $p=0.06$, Fig. 3.1b). Under room air

conditions minute ventilation (ml/min/kg) was decreased compared to sham, (1.244±0.24 stroke vs. 2.037±0.24 sham, $p<0.01$, Fig. 3.1c). Strikingly, stroke mice (6.8±1.7) display an increase incidence of apneas of compared to baseline (1.2±0.4) or sham (0.8±0.8), $p<0.01$ (Fig. 3.1d). Representative waveforms of respiratory activity shown of baseline sham, and stroke respectively. (Fig. 3.1e) n=12.

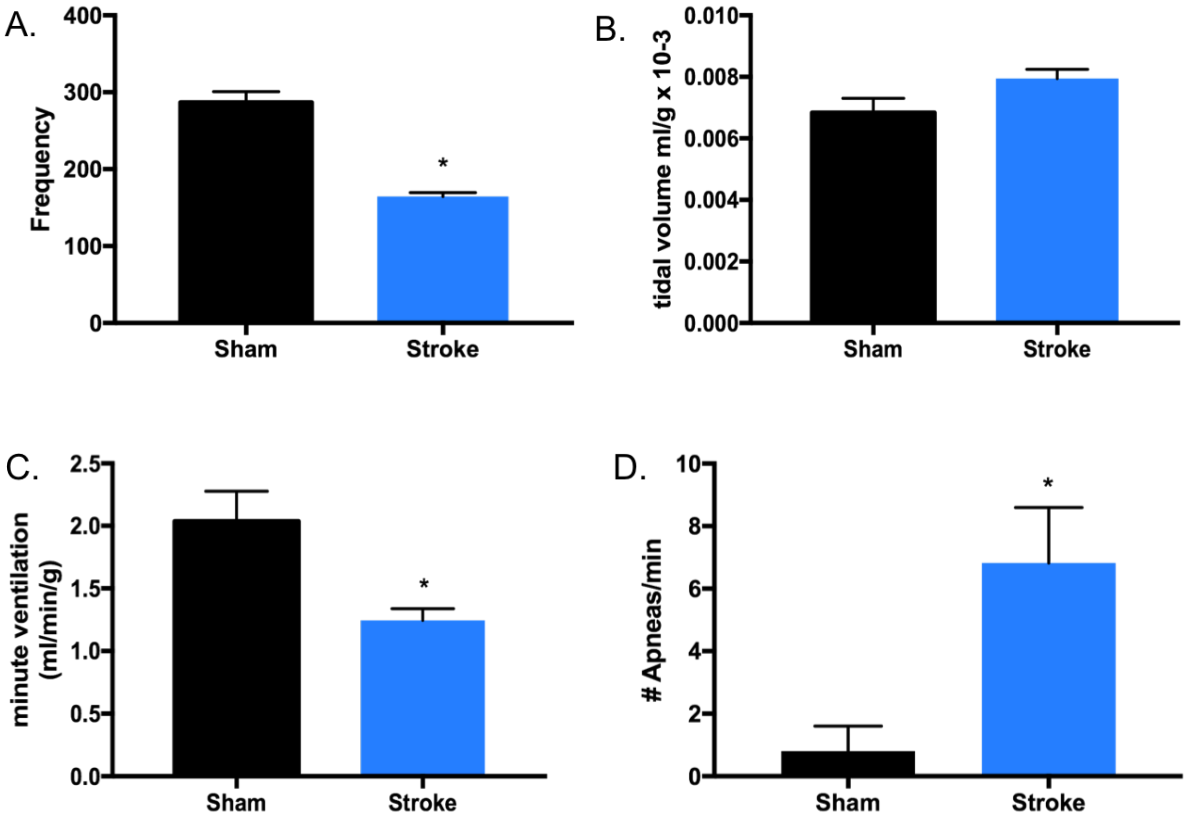
A.
Frequency
400
300
200
100
0
*
Sham
Stroke
B.
tidal volume ml/g x 10-3
0.010
0.008
0.006
0.004
0.002
0.000
Sham
Stroke
C.
minute ventilation (ml/min/g)
2.5
2.0
1.5
1.0
0.5
0.0
*
Sham
Stroke
D.
Apneas/min
10
8
6
4
2
0
*
Sham
Stroke

E.

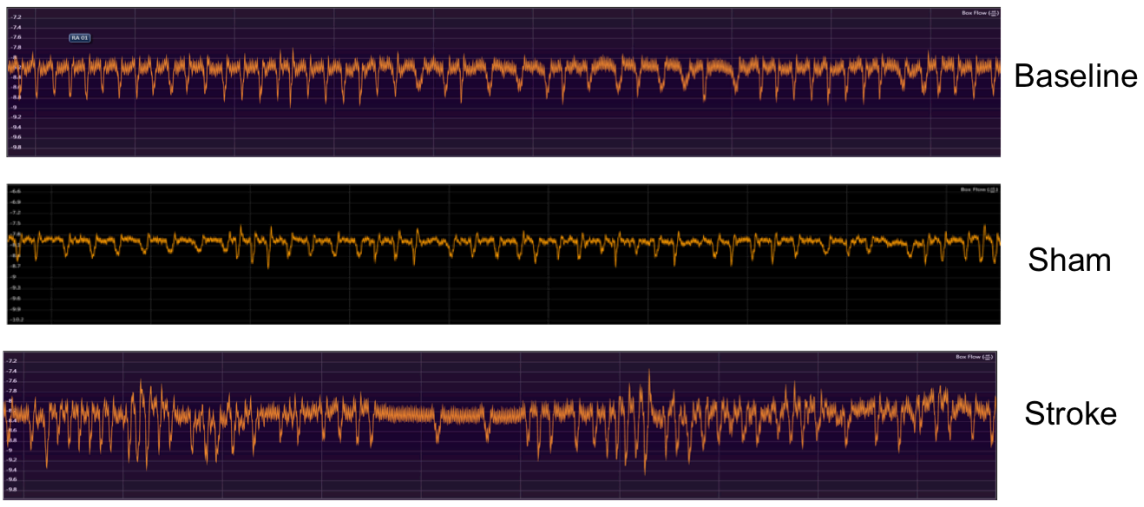
Baseline
Sham
Stroke

Figure 3.1. Phenotype of stroke induced respiratory dysfunction. Whole body plethysmography was performed on stroke and sham mice day 3 post surgery. Under room air conditions respiratory frequency, measured in breaths per minute, decreased, 164.4±5.09 and 286.7±13.97, $p<0.0001$ (**A**) while tidal volume (ml/g) increased although not significantly, 0.006±0.0004 vs. 0.0079±0.0003, $p=0.06$ (**B**). The product of frequency and tidal volume, minute ventilation (ml/min/g), decreased (**C**) following MCAO, suggestion hypoventilation, 1.244±0.24 vs. 2.037±0.24, $p<0.01$. The number of apneas per minute markedly increased following stroke, 6.8±1.7±0.8±0.8, $p<0.01$ (**D**). Representative respiratory waveform tracings of mice at baseline, sham and stroke are shown (**E**). n=14

3.2. Respiratory dysfunction results in hypoxia & hemoglobin desaturation.

To determine if changes in respiratory parameters following MCAO had physiological consequences both stroke and sham mice underwent arterial blood gas analysis and pulse oximetry monitoring on day 3 following surgery. Arterial blood gas analysis found that stroke mice had a decreased level of PaO_2 (104±4.7 vs. 79.3±0.57, $p<0.05$), and an increased $PaCO_2$ level (33.9±5.1 vs. 48.1±0.8, $p=0.5$) while pH remained unchanged (7.35±0.02 vs. 7.37±0.01, n=3). (Table 2.)

Stroke mice undergoing pulse oximetry monitoring displayed oscillations in their hemoglobin saturation levels (SpO_2). Baseline SpO_2 levels fluctuated between 94-96% and would periodically drop between 80-90% based on the duration of the apnea. Sham mice consistently maintained a SpO_2 level between 97-100%. Representative tracings shown (Fig3.2).

	Sham	Stroke
pH	7.35	7.37
CO2	33.9	48.1
O2	104	79.3

Table 2. Arterial blood gases. Obtained day 3 following surgery from stroke and sham mice. Stroke mice have an increase in $PaCO_2$, 33.9±5.1 vs. 48.1±0.8, p=0.5, and a decrease in PaO_2, 104±4.7 vs. 79.3±0.57, $p<0.05$, suggesting a state of hypercapnia and hypoxia. pH remained unchanged 7.35±0.02 vs. 7.37±0.01, n=3.

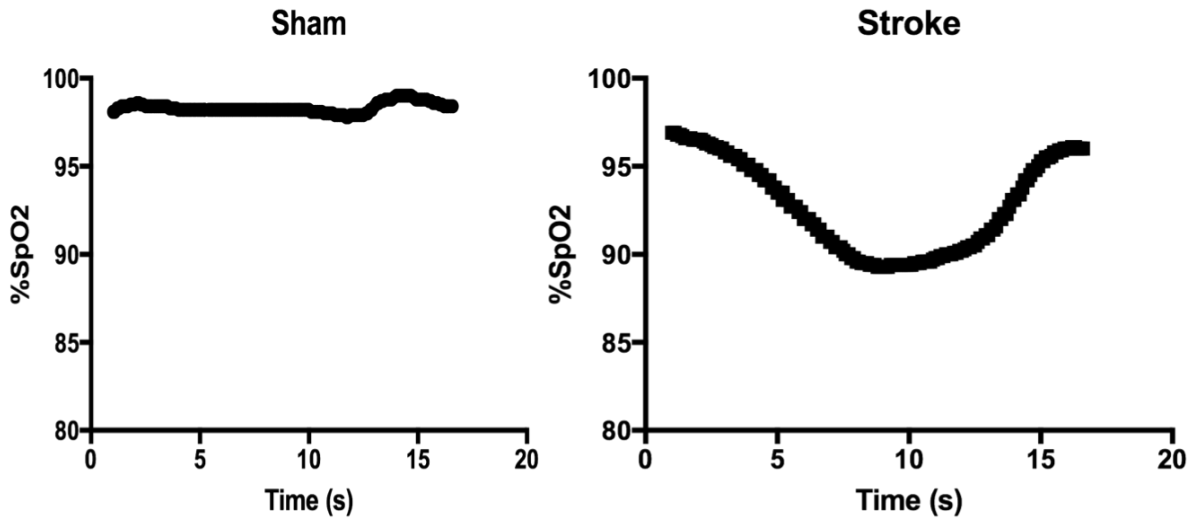

Figure 3.2. Pulse oximetry tracings day 3 post surgery. Oxygen hemoglobin saturation is maintained between 97-100% in sham mice. SpO_2 levels drop in stroke mice representing intermittent hypoxia. A 3-4% drop in SpO_2 is considered an indicator of a hypoxic event, $p<0.05$ n=3

3.3. Ischemic stroke does not alter chemoreceptor gain as measured by whole body plethysmography.

As part of whole body plethysmography testing mice were exposed to 100% O_2 and a graded CO_2 response to assess changes in the central chemoreflex. Under conditions of increased atmospheric O_2 peripheral chemoreceptor input is silent allowing for the assessment of CO_2/H^+ driven central chemoreceptors. (120) Both respiratory frequency and minute ventilation were blunted across all air conditions compared to sham. (Fig. 3.3a) No difference was observed between stroke and sham in the slope of the ventilatory response to CO_2 across the four gas conditions as a measure of chemosensitivity, sham=0.38, stroke=0.34, p=0.77. (Fig. 3.3b)

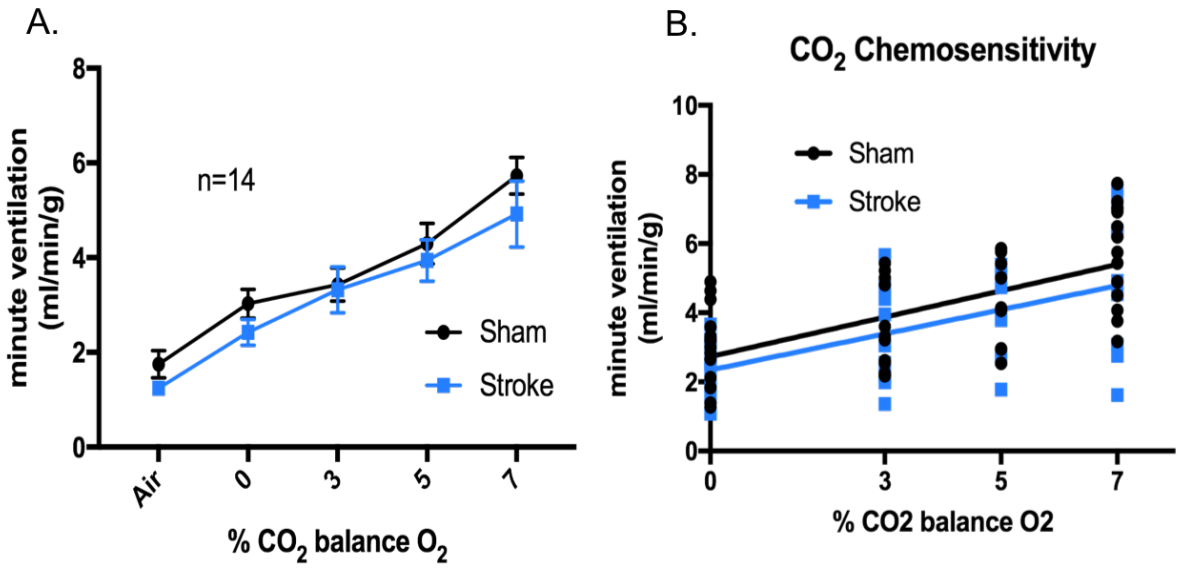

Figure 3.3. MCAO does not alter CO_2/H^+ sensitivity. Minute ventilatory response to CO_2 is slightly blunted, evident by the right shift in minute ventilatory response to CO_2, following 60 minute MCAO in young male mice (**A**). The slope of the minute ventilatory response to CO_2 is unchanged following MCAO (**B**), slope sham=0.38, stroke=0.34, p=0.77. n=14

3.4. Peripheral chemoreflex.

To understand if MCAO disrupts the hypoxic ventilatory response, mice underwent plethysmography recordings with exposure to 21% O_2 (room air) followed by 10% O_2. Day 3 post surgery the minute ventilatory response to hypoxia of stroke mice was blunted (2.02±0.15 vs. 1.51±0.28, $p<0.05$), yet the chemosensitivity to hypoxia remained unchanged. Slope of the chemosensitivity to hypoxia in sham=0.03, stroke=0.04, difference between the slopes was not significant, $p=0.73$. (Fig. 3.4) n=14

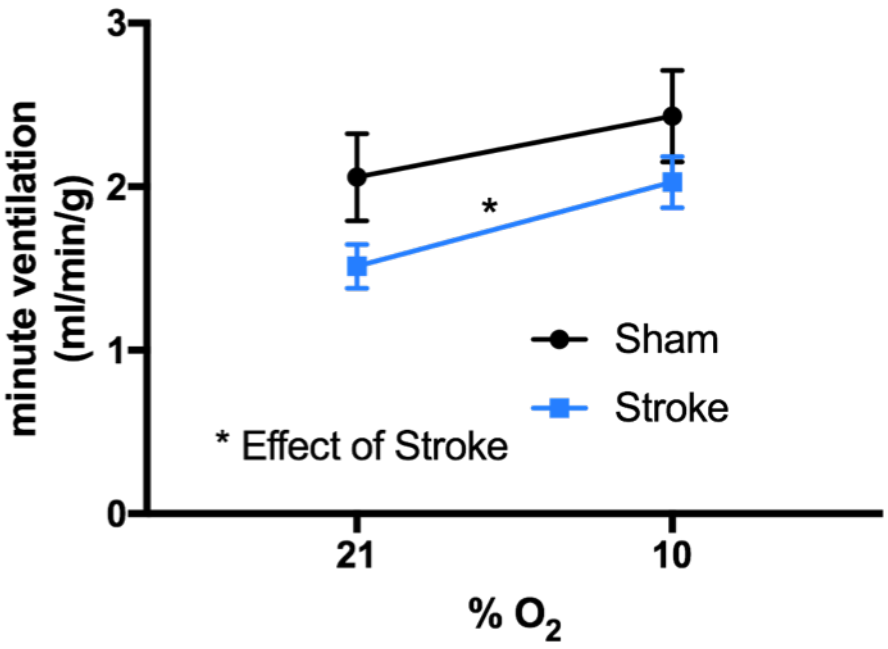

Figure 3.4. Hypoxic ventilatory response. Ventilation and the ventilatory response to hypoxia are blunted following MCAO. Yet, the chemosensitivity to hypoxia remains unaltered. Slope sham=0.03, stroke=0.04, difference between the slopes was not significant, p=0.73.

3.5. MCAO does not result in brainstem cell death.

To rule out brainstem neuronal cell death as a causative factor of disordered breathing, tissue was assessed for histological damage at day 3-post surgery. No cell death or neuronal degeneration was observed in the brainstem as evidenced by either TTC staining or Fluorojade staining. (Fig. 3.5) TTC staining is used as a marker metabolically active tissue and is used to distinguish healthy neuronal tissue from infarcted. It is enzymatically reduced to a red color in living tissue and will remain white in infarcted regions. Fluorojade staining is used as a marker of degenerating neurons.

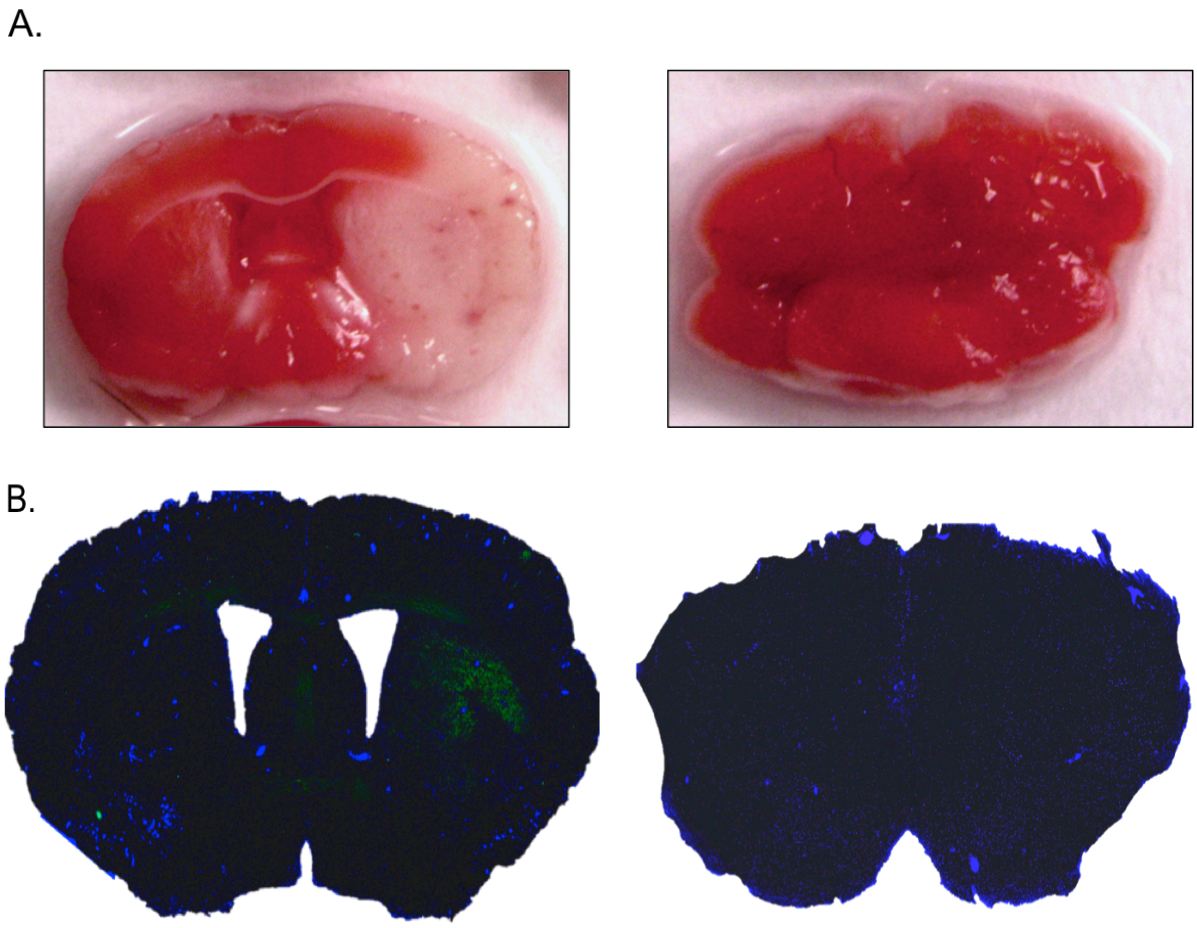

Figure 3.5. MCAO does not result in direct brainstem cell death. Brainstem cell death was assessed by both TTC (A) and fluorojade staining (B) on day 3 following MCAO. MCAO produces a large wedge shaped infarct in the hemisphere indicated by lack of “red” staining by TTC. The brainstem was unaffected (A). Fluorojade, a marker for degenerating neurons, was positive in the striatum of the right

hemisphere in mice that underwent MCAO. The brainstem was negative for any fluorojade positive cells, n=3. Fluorojade green, dapi blue.

3.6. Ischemic stroke does not alter basal metabolic activity.

To determine if factors other than deficits in central respiratory circuitry contribute to stroke disordered breathing, mice underwent metabolic activity assessments. Stroke has the potential to alter other parameters such as body temperature, food intake and overall energy expenditure. Systemic energy metabolism can be evaluated by monitoring the volume of oxygen consumption in individual animals. (121) If stroke were to decrease energy expenditure in mice, metabolic activity would therefore decrease (observed by decrease in O_2 consumption). A decrease in O_2 consumption would present as a decrease in minute ventilation on whole body plethysmography, similar to our observed outcomes. Stroke had a negligible effect on O_2 consumption compared to sham on day 7, 21 or 42-post surgery. Day 7 data shown (Fig. 3.7) (sham 56.75±4.37 vs. 65.35±4.5, p=0.24). This further supports the conclusion that disordered breathing is a consequence of stroke, not a compensatory response to a decrease in activity or alterations in metabolic activity.

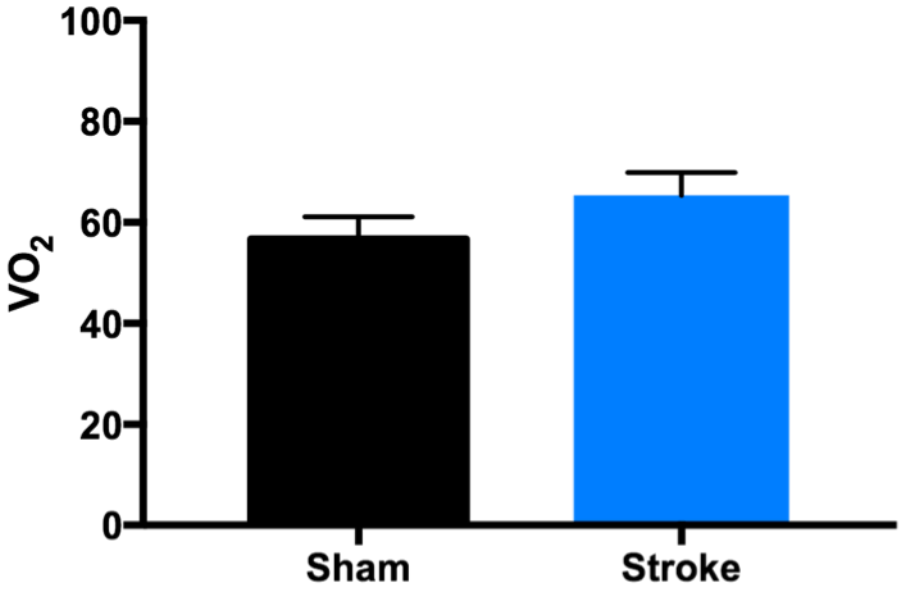

Figure 3.6. Oxygen consumption as a measurement of metabolic activity. Metabolic activity was assessed on day 3-post surgery. The volume of oxygen consumed was recorded every 10 minutes and averaged per mouse over a 4-hour period during resting hours. MCAO did not alter basal metabolic activity, minimizing the possibility that alterations in metabolic activity contributions to SIRD. Sham 56.75±4.37 vs. 65.35±4.5, p=0.24, n=5.

3.7. Effect of age on post-stroke respiratory activity

Age is an independent predictor of poor outcomes as older individuals have both higher in hospital mortality and worse functional and cognitive outcomes following an ischemic event. (122) Age may also affect the SIRD phenotype we observed in young mice. Therefore, we performed a comprehensive assessment of the effects of age on respiratory physiology in stroke and sham mice. On day 3-post surgery aged male mice that underwent MCAO display decreases in both respiratory frequency (243.5±29.6 vs. 185.3±12.4bpm, $p<0.05$, Fig. 3.7a) and minute ventilation (2.5±0.3 vs. 1.1± 0.15 ml/g/min $p=0.001$, Fig. 3.7b&c), indicators of hypoventilation. Although blunted, the ventilatory response to CO_2 was unchanged, $p=0.21$, data not shown. The incidence of apneas did increase following stroke (2.8±0.8 vs. 9.25±1.37, $p<0.01$, Fig. 3.7d). There was an effect of stroke on the ventilatory response to hypoxia ($p=0.05$, Fig. 3.7e), although the chemosensitivity to hypoxia remained unchanged, $p=0.68$, data not shown.

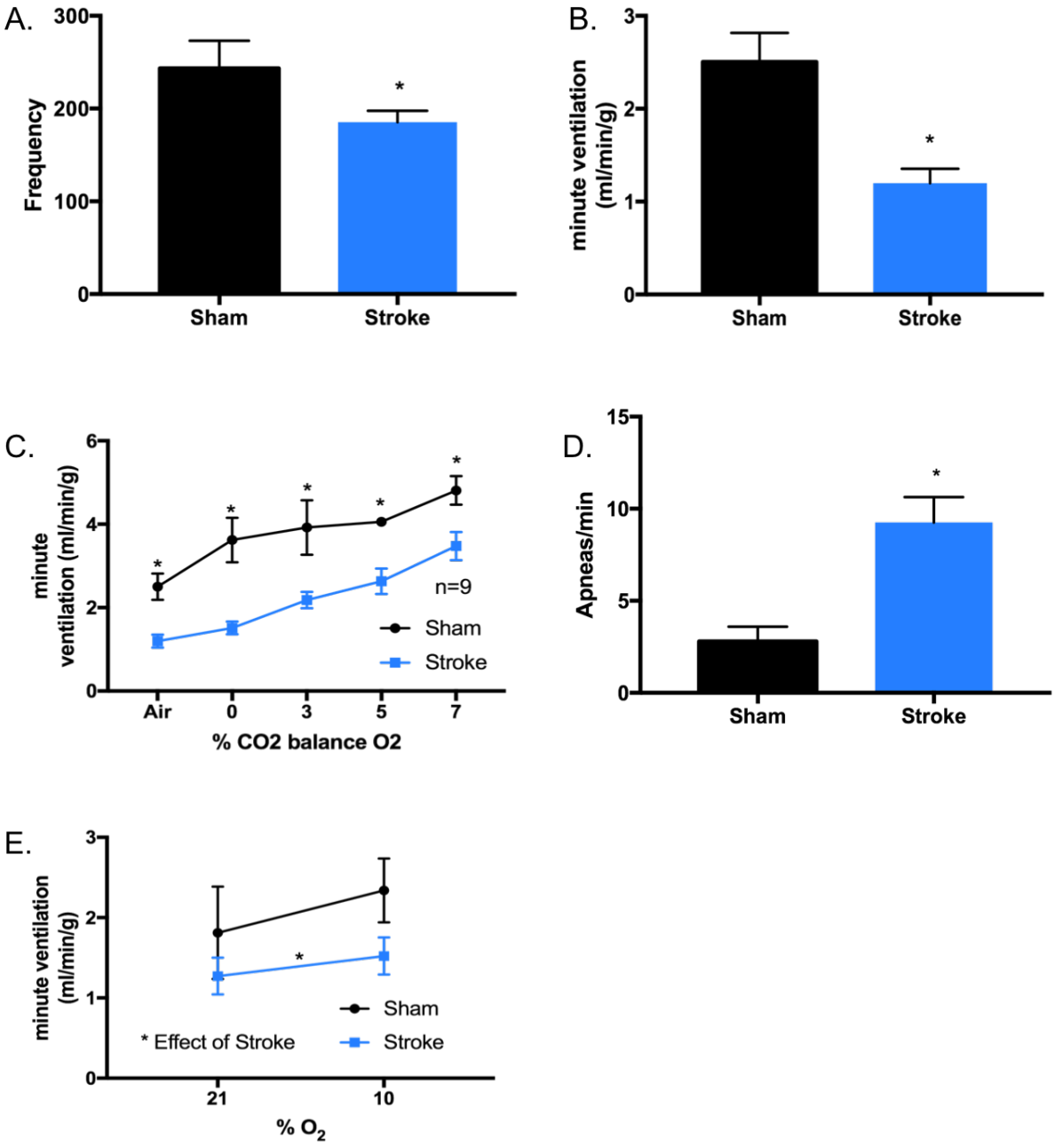
A.
Frequency
300
200
100
0
*
Sham
Stroke
B.
minute ventilation (ml/min/g)
3
2
1
0
*
Sham
Stroke
C.
minute ventilation (ml/min/g)
6
4
2
0
*
n=9
Sham
Stroke
Air
0
3
5
7
% CO2 balance O2
D.
Apneas/min
15
10
5
0
*
Sham
Stroke
E.
minute ventilation (ml/min/g)
3
2
1
0
*
Sham
Stroke
* Effect of Stroke
21
10
% O2

Figure 3.7. Respiratory parameters of post-MCAO in aged males. The respiratory phenotype of aged males (18-20 months) at day 3 that underwent MCAO is similar to young males. Respiratory frequency is decreased, 243.5±29.6 vs. 185.3±12.4, $p<0.05$ (**A**) resulting in diminished minute ventilation under room air conditions, 2.5±0.3 vs. 1.1± 0.15 ml/g/min $p=0.001$ (**B**). The ventilatory response to CO_2 is significantly blunted across all tested conditions, suggesting that aging is a contributing factor limiting the system's ability to respond to changes in ABG. Interestingly, at day 3 the incidence of apneas increased significantly, 2.8±0.8 vs. 9.25±1.37, $p<0.01$ (**D**). Stroke also had a strong effect on the ventilatory response to hypoxia, $p=0.05$ (**E**).

3.8. Effect of sex on stroke induced respiratory dysfunction.

Stroke is a sexually dimorphic disease, with women having a lower incidence of stroke in the age group of 55-75, until the age of 85 when women have a higher incidence. (123, 124) Elderly women are disproportionally affected by stroke, having higher age specific mortality and worse post stroke outcomes. (125) The majority of human studies report an age dependent blunting of hypoxic and hypercapnic ventilatory responses. (126, 127) However, there is conflicting evidence regarding sex-associated change in the control of breathing. (128, 129) Sleep apnea has a higher prevalence among men at all ages especially in elderly men who have a higher incidence of all forms of sleep apnea: central, mixed and obstructive. (130) Interestingly, elderly females with sleep apnea exhibit increased white matter loss and changes in structural integrity in several brain regions compared to age-matched males. (131) The incidence of SIRD as well as morbidity and mortality has never been evaluated on the basis of sex.

To investigate sex differences in respiratory dysfunction following stroke we subjected age 18-20 month old female mice to MCAO and assessed respiratory parameters on day 3 post stroke. Minute ventilation was decreased in stroke mice on day 3, sham 2.481±0.2179 vs. 1.849±0.1602 ml/min/g, $p=0.03$(**A**). Yet, there was no increase in the incidence of apneas, sham 0.6±0.6 vs. 1.778±0.49 apneas/min, $p=0.16$ (**B**). Aged female mice had higher baseline minute ventilation across all air conditions compared to age males, room air females 2.729±0.18 vs. 2.22±0.07 ml/min/g, $p<0.05$ (**C**). Aged males displayed a greater percent change in minute ventilation from baseline following stroke, males 52.66±3.25% vs. 30.22±3.1%

$p<0.001$ (**D**). Metabolic demand, as measured by consumption of O_2, was higher in females accounting for increased levels of minute ventilation in comparison to age-matched males, females 72.79±13.28 vs. 55.19±4.68 males, effect of sex p=0.01, 2-way ANOVA. (**E**). Stroke did not affect metabolic activity in neither males nor females. This does not explain the greater change in minute ventilation experienced by males post stroke than females. Variations in infarct did not account for the discrepancies in minute ventilation observed between the sexes, day 7 % cerebral atrophy male 17.07±8.91% vs. 24.22±4.65%, p=0.44 (**F**).

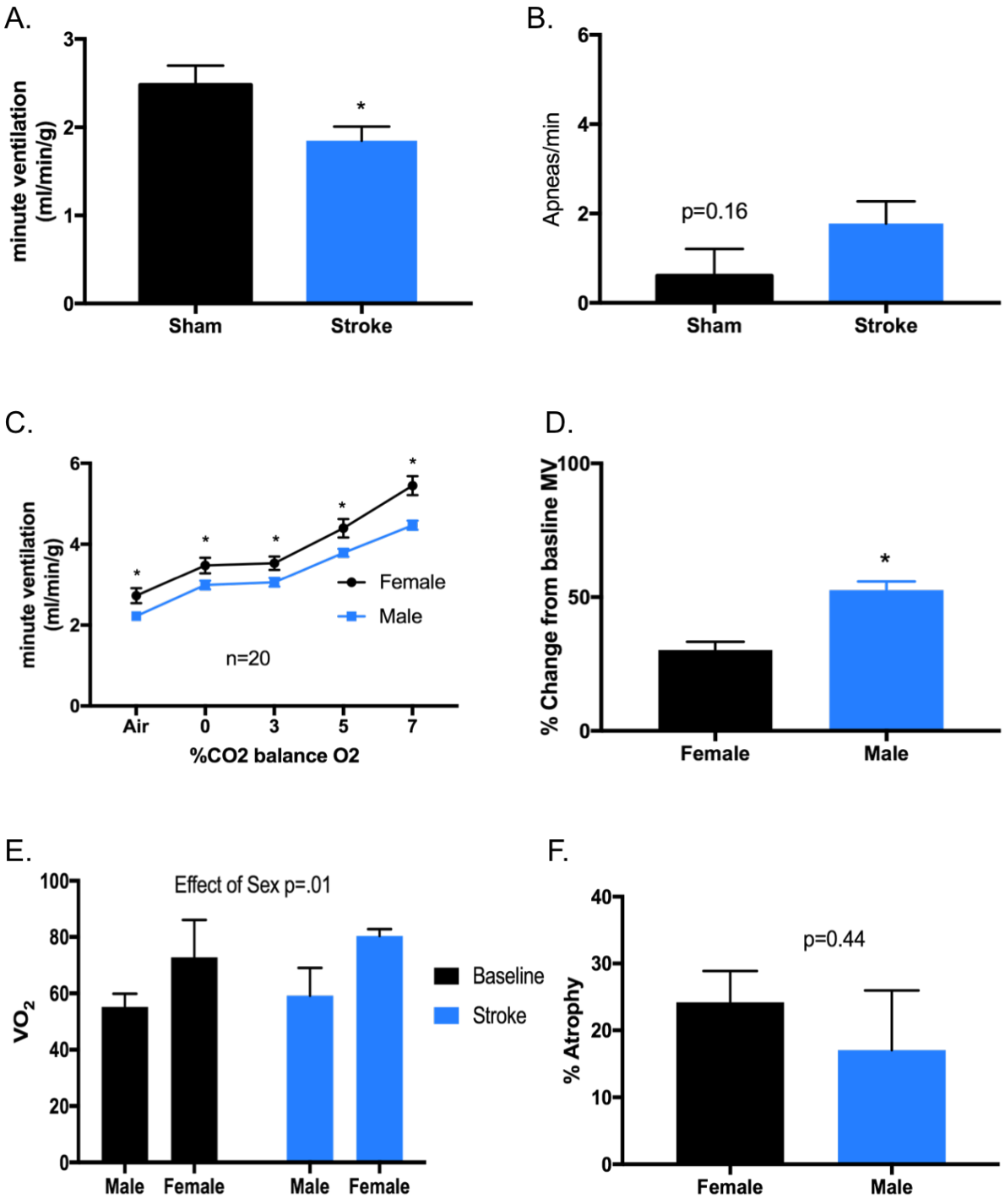
A.
minute ventilation (ml/min/g)
3
2
1
0
*
Sham
Stroke
B.
Apneas/min
6
4
2
0
p=0.16
Sham
Stroke
C.
minute ventilation (ml/min/g)
6
4
2
0
*
Female
Male
n=20
Air
0
3
5
7
%CO2 balance O2
D.
% Change from basline MV
100
50
0
*
Female
Male
E.
Effect of Sex p=.01
VO2
100
80
60
40
20
0
Baseline
Stroke
Male
Female
Male
Female
F.
% Atrophy
40
30
20
10
0
p=0.44
Female
Male

3.8. Effect of sex on stroke induced respiratory dysfunction. Aged female mice undergoing MCAO display a decrease in minute ventilation on day 3 following surgery, sham 2.481±0.2179 vs. 1.849±0.1602 ml/min/g, p=0.03 (**A**). Despite having no increase in the incidence of apnea, sham 0.6±0.6 vs. 1.778±0.49 apneas/min, p=0.16 (**B**). At baseline aged females display an higher minute ventilation under room air conditions and in response to hypercapnia, room air females 2.729±0.18 vs. 2.22±0.07 ml/min/g, $p<0.05$ (**C**). Aged males displayed a greater percent change in minute ventilation from baseline following stroke, males 52.66±3.25% vs. 30.22±3.1% $p<0.001$ (**D**). Metabolic activity was increased in females compared to males at baseline, females 72.79±13.28 vs. 55.19±4.68, 2-way ANOVA effect of sex p=0.01, whereas stroke had no effect on metabolic activity in either sex (**E**). Variations in infarcts did not account for the discrepancies in minute ventilation observed between the sexes, male 17.07±8.91% vs. 24.22±4.65% atrophy, p=0.44 (**F**).

3.9. Discussion.

We found that ischemic stroke induced by a transient 60 minute MCAO produced respiratory dysfunction characterized by apneas and hypoventilation in both young and aged male mice. This recapitulates the respiratory phenotype observed in human stroke patients. Stroke mice displayed a decrease in respiratory frequency as well as an increase in the incidence of apneas resulting in a blunted minute ventilatory response. This state of hypoventilation results in systemic hypoxia and hypercapnia as measured by ABG, reconfirmed by periodic desaturations in SpO_2. ABG and SpO_2 measurements were performed on day 3-post surgery during the acute phase of post stroke recovery. Our long-term studies, (see Chapter 4), found that apneas persist in mice up to 6 weeks following surgery. Weekly ABG measurements following mice over this time period would further the understanding of the magnitude of chronic apneas. Apneas and systemic hypoxia can have far reaching consequences. In models of OSA, apneas produce arousals and fragmented sleep. Experimental evidence utilizing chronic intermittent hypoxia found amplified sympathetic response contributing to a hypertensive state. (132, 133) With further consequences resulting in cellular stress promoting white matter loss and axonal injury in brain regions such as the hippocampus.

Taken together, this suggests that the respiratory phenotype following stroke is not a physiological compensatory response to changes in metabolic activity. Tidal volumes in stroke mice do not decrease, but actually increase slightly compared to sham, possibly as a compensatory mechanism in an attempt to maintain minute ventilation. Implying that stroke induced hypoventilation is not a result of paralysis or

paresis. Understandably, as direct brainstem lesions result in respiratory dysfunction we wanted to rule out neuronal brainstem cell death as a contributing factor to disordered breathing. MCAO does not result in any observable brainstem cell death or degenerating neurons as assessed by TTC or Fluorojade staining. Unfortunately, this does not rule out withdrawal of excitatory input from higher-level neuronal circuitry disrupting respiratory neuron function.

Respiratory constancy relies on a delicate balance of chemoreceptor gain, plant gain and temporal control of brain/heart blood flow. The Cheyne-Stokes respiratory pattern observed in humans is proposed to be a result of the gaining up of the chemoreflex. In this model of SIRD the slope of the ventilatory response to CO_2 remains unchanged, suggesting that chemoreceptor gain is not perturbed following MCAO in an in-vivo whole body respiratory assessment. To further confirm this electrophysiology techniques must be employed to assess the chemosensitivity of varying neuronal respiratory control sites. Electrophysiology studies will also allow for the interrogation of respiratory rate control neuron populations,.

The ventilatory response to hypoxia was explored by exposing mice to 10% O_2 environment. MCAO blunts the ventilatory response to hypoxia, yet the chemosensitivity of this system was not affected. Suggesting that the intrinsic ability of the neuronal populations responsible for detecting hypoxia remain intact, yet the output of these groups is altered. Time delays in circulating blood gases between lungs and chemoreceptor populations may contribute to this blunted response. This may be due to local or systemic alterations in vascular reactivity or cardiac variability. Local variations in astrocyte reactivity, basement membrane restructuring

and fibrosis are potential candidates for disrupted neural vascular communication.

Decreases in respiratory activity may be indirectly altered by stroke. O_2 consumption as a measure of metabolic activity was not altered by ischemic stroke. Taken in consideration with our other findings this suggests the ischemic stroke decreases basal respiratory activity in the presence of either hypoxia or hypercapnia, while also increasing the incidence of apneas. This culminates in a in a cyclic feed forward loop of respiratory dysfunction.

Since >80% of strokes occur in individuals over the age of 65(2), the aging population bears the major brunt of stroke related mortality and disability. (122) It is critical to investigate the mechanisms underlying stroke induced mortality and functional/cognitive deficits. Surprisingly, our lab has found that although aged male mice have less histological injury, they have significantly higher mortality and functional deficits than their young counterparts. (134, 135) We performed a comprehensive assessment of the effects of age on respiratory physiology in stroke and sham mice.

Aged male mice display a higher level of respiratory activity, reflective of an increase in minute ventilation (normalized to body weight), which may be explained by changes in metabolic activity that accompany aging. The SIRD phenotype witnessed in aged males was similar to that of young. They displayed a decrease in respiratory frequency, a blunted minute ventilatory response to both hypercapnia and hypoxia, with no changes to chemosensitivity. Aged males also suffer from an increase in apneas during respiratory assessments conducted during the acute

phase of ischemia. Collectively, the stroke induced respiratory phenotype is similar regardless of age in males. At baseline aged females display an increased minute ventilation under room air conditions compared to males, which is explained by increased metabolic activity. Interestingly, aged females have a less pronounced disordered breathing phenotype despite having similar sized infarcts as aged males. This may partly explain why aged male mice have worse functional outcomes and higher post stroke mortality than females. The hormonal and chromosomal contributions to sex differences in stroke are an area of ongoing investigation. For example, ischemia induced astrocyte reactivity is differentially regulated by age and sex. Increased levels of IL-6, IL-1b and TNF-α were observed in aged male astrocytes compared to astrocytes derived from females. (136, 137) There are likely many mechanisms contributing to the sex based variations in respiratory dysfunction following ischemia. The long-term consequences of apnea may differ greatly based on the age and sex of the animal, and this may contribute to increased mortality and worse outcomes following ischemia.

3.10. Future Directions.

We identified and characterized a stroke induced disordered breathing model in mice characterized by hypoventilation and apneas, resulting in systemic hypoxia. Recapitulating the breathing phenotype observed in the human population suffering from stroke. To further understand how stroke disturbs respiration, cellular electrical properties of major respiratory central chemoreceptor sites such as the NTS and RTN, as well as rate control sites (Botzinger and pre-Botzinger complex) should be examined. Intrinsic characteristics such as resting membrane potential, basal firing

rate and chemosensitivity must be studied to completely understand how stroke induces respiratory dysfunction.

Before we can conclude that disordered breathing is strictly a result of a decrease in basal respiratory activity the other components of loop gain must be evaluated. MCAO may have direct effects on cardiac output and rhythmicity. Cardiac instability could contribute to time delays in circulation between the lungs and chemoreceptors. Implantable telemetry can be employed to monitor changes in blood pressure and EKG variability. To further corroborate these findings measurements of arterial CO_2 and O_2 should be collected from the pulmonary vein and the entrance of the brain to assess time delays between heart/lung and brain tissue. Lastly, the apneic threshold in mice may be perturbed following stroke. Utilizing mechanical ventilation and diaphragmatic electromyography (EMG) as previously described(138); alterations to CO_2 apneic threshold can then be addressed under steady state conditions.

Chapter 4. The Severity of Respiratory Dysfunction Correlates with Progressive Cognitive Decline.

Rationale: Patients suffering from stroke induced respiratory dysfunction display signs of progressive cognitive decline for years following stroke. To determine if MCAO induced respiratory dysfunction produces cognitive decline, we performed longitudinal studies to evaluate the progression of respiratory parameters and cognitive outcomes over a six-week period.

4.1. MCAO results in progressive cognitive decline.

Sham and stroke mice underwent cognitive assessment utilizing the Barnes maze on days 21 and 42 post surgery. On day 21-post surgery stroke mice take longer to find the escape hole than sham (stroke 53.26±8.45 seconds vs. sham 21.04±2.6, $p<0.01$, Fig. 4.1a). On day 42-post surgery stroke mice again perform worse than sham in both escape time (stroke 95.02±26.75 seconds vs. sham 22.83±6.72, $p<0.05$) and total errors made prior to finding escape hole (stroke 50.91±9.5 vs. sham 15.2 ±5.7, $p=0.01$, Fig. 4.1b). More importantly stroke mice performed worse on day 42 than on day 21, taking longer to escape and making more total errors (day 21 25.8± vs. day 42 50.91±9.5 errors, $p=0.01$), suggestive of progressive cognitive decline. Coinciding with these findings stroke mice perform worse on the Novel Object Recognition Test and in Contextual Fear Conditioning. Stroke mice spend dramatically reduced time with the novel object compared to sham on day 28 (2.51±0.7 vs 1.29±0.19 ratio of time (s), $p<0.05$, Fig. 4.1c). On day

42, stroke mice display less freezing behavior compared to sham in fear conditioning arena (65.49$\pm$6.87% vs 48.91$\pm$3.6, $p<0.05$, Fig. 4.1d).

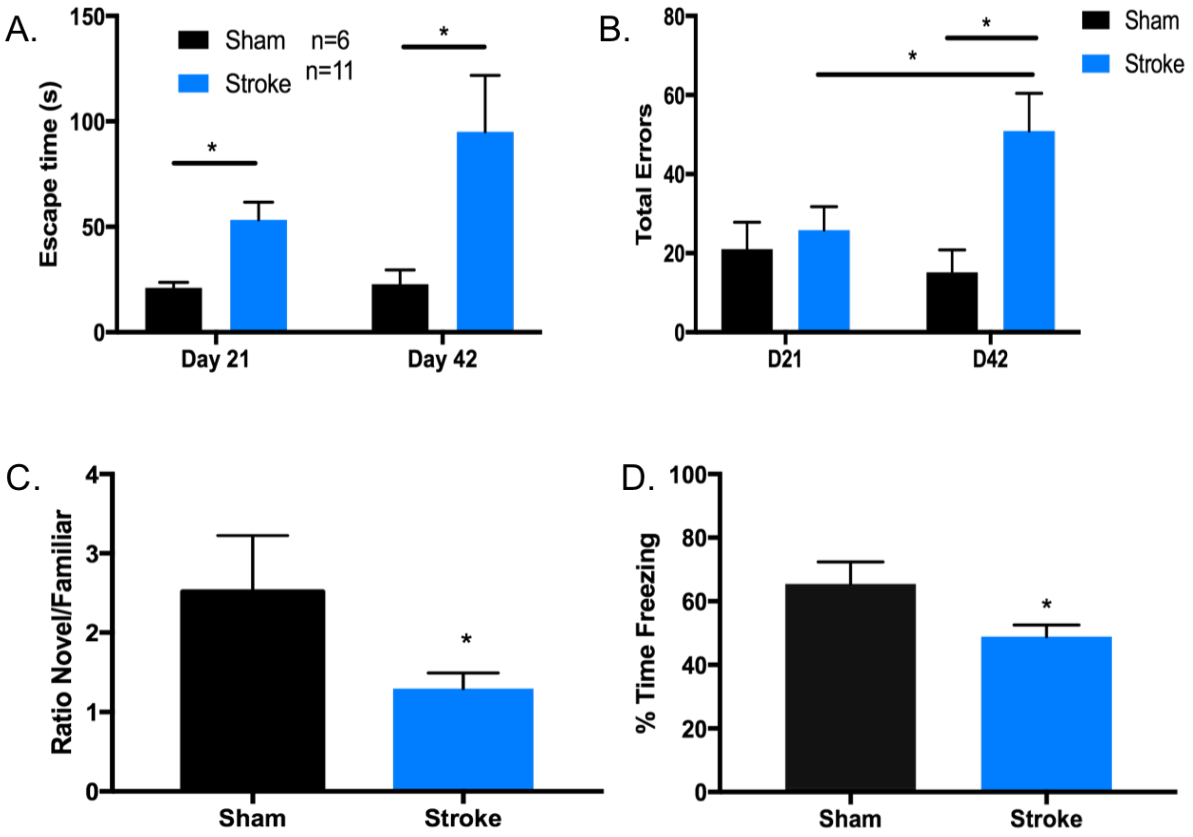

Figure 4.1. MCAO results in cognitive decline. During Barnes maze testing stroke mice take longer to find escape hole on day 21 than sham (stroke 53.26±8.45 seconds vs. sham 21.04±2.6, $p<0.01$) indicative of cognitive impairment, stroke n =11, sham n=6. Barnes maze assessment on day 42 post surgery stroke mice again perform worse than sham, increasing the time to find the escape hole compared to day 21, stroke 95.02 ± 26.75 seconds vs. sham 22.83 ± 6.72, $p<0.05$ (**A**). Interestingly, on day 21 stroke mice make approximately the same number of errors as sham, yet on day 42, stroke mice not only make more errors than sham but more errors than they did on day 21, suggesting progressive cognitive decline (stroke 50.91±9.5 vs. sham 15.2 ±5.7, $p=0.01$) (**B**). Findings of day 28 NORT also are

indicative of cognitive decline, stroke mice spend less time with the novel object in relation to the familiar object when compared to sham, 2.51±0.7 vs 1.29±0.19 ratio of time (s), $p<0.05$ (**C**). Lastly, stroke mice spend less time displaying freezing behavior during contextual fear condition on day 42, 65.49±6.87% vs 48.91±3.6, $p<0.05$, n=11 and n=6 respectively (**D**).

4.2. Evolution of stroke induced respiratory dysfunction.

Following plethysmography assessment on day 42-post surgery, we found that stroke mice can be stratified into two groups based on the number of apneas per minute. The minor group presented with 5 or less apneas a minute, while the severe group had 5 or more apneas a minute, representative plethysmography waveforms shown (Fig. 4.2a). The determination to separate groups based on the number of apneas a minute was adapted from American Academy of Sleep Medicine criteria used in humans. (75) The respiratory pattern of the severe group is indicative of Cheyne-Stokes patterned breathing, marked by waxing and waning of tidal volume followed by periods of apnea, representative waveforms (Fig. 4.2c). Consistent with day 3 findings, we find no indications of alteration in chemosensitivity as measured by the ventilatory response to CO_2, p= 0.51 (Fig. 4.2b).

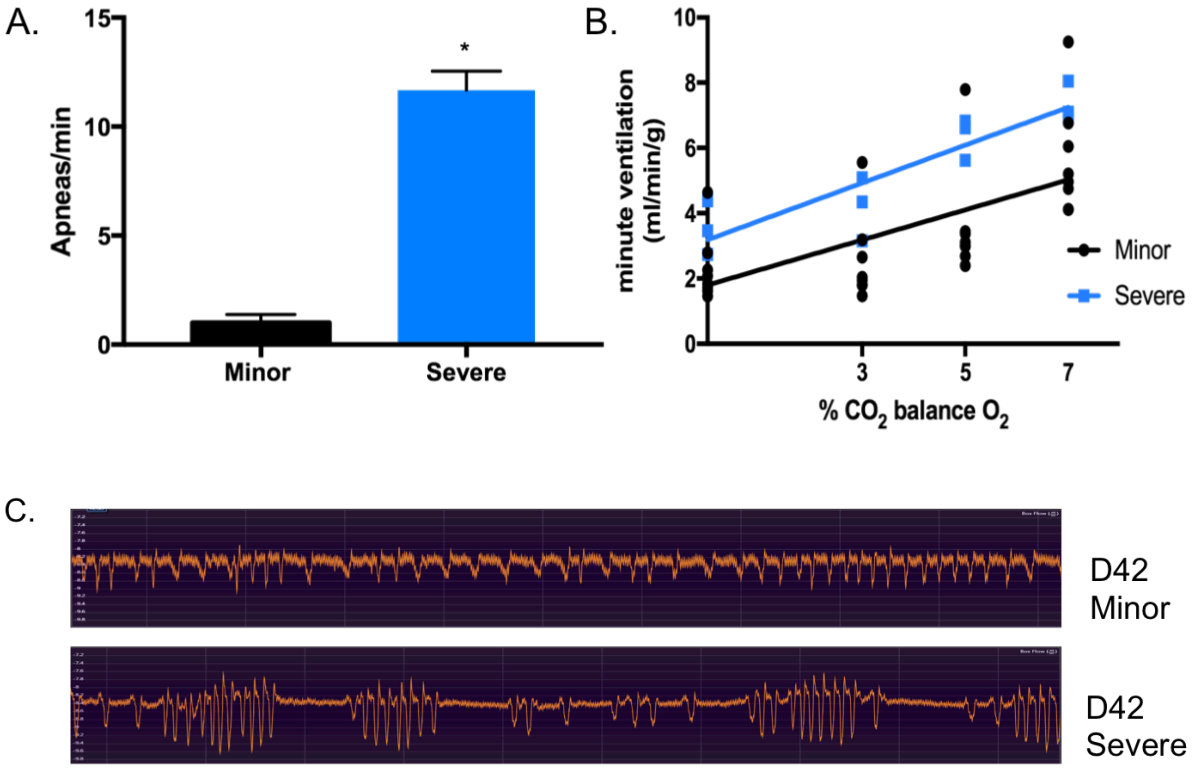

Figure 4.2. Evolution of the SIRD phenotype. On day 42 post surgery, stroke mice can be stratified into 2 groups based on the number of apneas a minute. The minor group experience 5 or less while the severe group suffers 5 or more apneas a minute (**A**). The central chemosensitivity did not differ between the minor or the severe groups, p=0.51 (**B**). Representative waveforms of the minor and severe groups on day 42 post surgery, n=7 respectively (**C**). The waveform of the severe group is indicative of the Cheyne-Stokes respiratory pattern, marked by waxing and waning of tidal volume followed by apnea.

4.3. Progressive cognitive decline correlates with the severity of disordered breathing.

After stratifying stroke mice based on the severity of respiratory dysfunction cognitive functions were reevaluated based on this criteria. Surprisingly, we found that mice that suffer severe form of disordered breathing display signs of progressive cognitive decline while those with minor apneas, do not. Performance on Barnes maze was consistent with progressive cognitive decline (Fig. 4.3). There is an effect of time on total errors made in the stroke group as a whole (D21 vs D42, $p=0.01$, $n=7$ Fig. 4.3a). Interestingly, multiple comparisons analysis revealed that animals with the most severe disordered breathing made more errors on day 42 (D21 28.3 ± 13.1 vs. D42 70 ± 21.6 errors, $p=0.05$, Fig 4.3a). Again, on Barnes maze there was an effect of time to escape hole in the stroke cohort as a whole (D21 vs. D42, $p<0.05$). Multiple comparison analysis exposed the severe group to have increasing escape time (D21 86.96 ± 36.3 seconds vs. D42 217.9 ± 82.1, $p=0.05$, Fig. 4.3b). These findings were consistent during contextual fear conditioning.

Mice with the most severe disordered breathing display less freezing behavior in fear conditioning arena on day 42 post stroke (Minor 47.1 ± 2.1 secs vs. severe 35.8 ± 4.8 secs. $P<0.05$) (Fig. 4.3c.). Linear regression analysis of percent time freezing compared to the number of apneas a minute, found a significant non-zero slope ($p<0.05$), indicating a negative correlation between apneas and freezing behavior. (Fig. 4.3d)

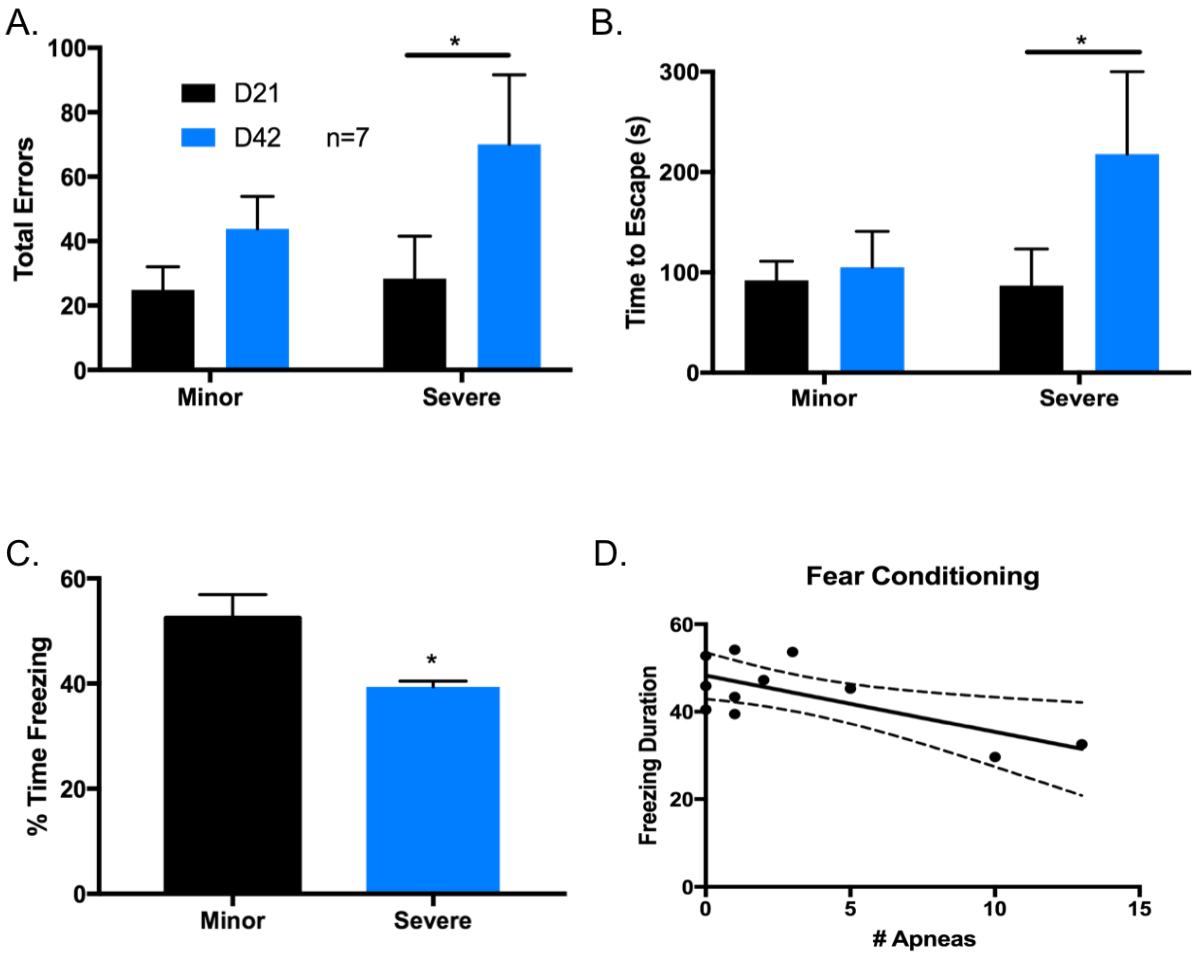

Figure 4.3 Progressive cognitive decline correlates with the severity of SIRD. Barnes maze performance was similar on day 21 between the minor and severe groups on time to escape and number of errors made. On day 42-post stroke, the minor group is consistent in their performances on day 21. The severe group on the other hand not only takes longer to find the escape hole (D21 86.96±36.3 seconds vs. D42 217.9±82.1, p=0.05), but also makes more errors than they did on day 21 (D21 28.3±13.1 vs. D42 70±21.6, p=0.05, n=7), (**A** & **B**). During contextual fear condition testing, the severe group displays less freezing behavior than the minor group suggesting cognitive impairment, (minor 47.1±2.1 secs vs. severe 35.8±4.8

secs. P<0.05) (**C**). Linear regression analysis found a negative correlation between the number of apneas and cognitive performance measured as freezing time during contextual fear conditioning test, p<0.05 (**D**).

4.4. Variations in stroke severity do not define the severity of respiratory dysfunction.

To rule out variation in infarct variability amongst the two groups of disordered breathing we assessed cerebral atrophy and day 3 post stroke assessments. No differences were observed in measurements of cerebral atrophy between the minor and severe groups after sacrifice on day 42, p=0.66. NDS, p=0.19. Corner test, a measurement of sensory motor function were the same for both groups of mice when they were assessed at day 3-post stroke, p=0.75 (Fig. 4.4).

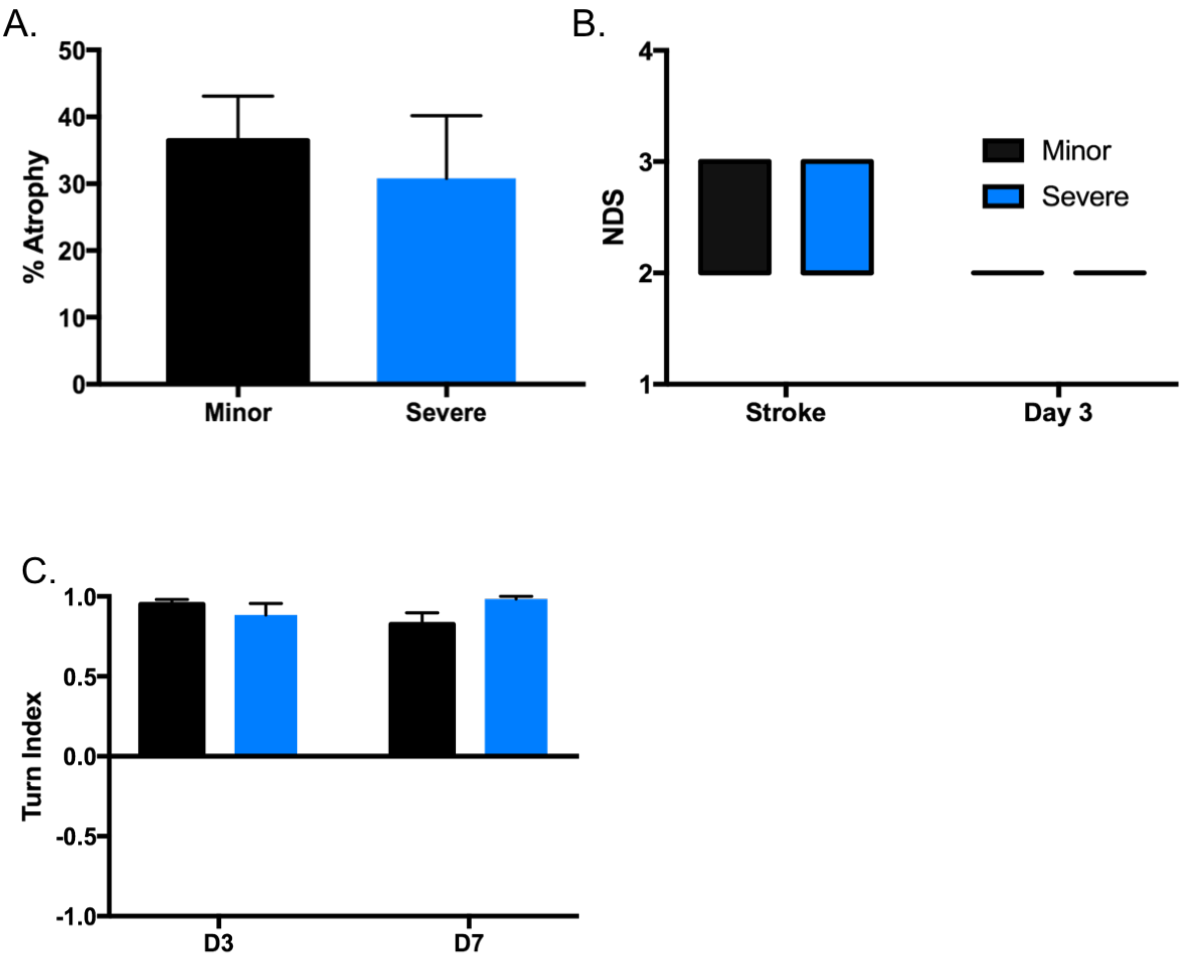

Figure 4.4. Variations in stroke severity do not define the severity of respiratory dysfunction. No differences in volume of cerebral atrophy were found at day 42 post stroke between the minor and severe groups of disordered breathing, p=0.66 (**A**). Neurological deficit scores at 1 hour following ischemia and day 3 post stroke were identical between the two groups, p=0.19, n=7 (**B**). Functional outcomes, measured by the corner test, at day 3 (p=0.75) and 7-post stroke (p=0.23) were similar amongst the groups (**C**).

4.5. Distal MCAO does not produce disordered breathing or cognitive decline.

Distal MCAO was employed to determine if a smaller cortical infarct produces disordered breathing or cognitive decline in a similar manner to MCAO. Plethysmography assessment on days 3, 21 or 42-post surgery found no indications of disordered breathing, hypoventilation, p=0.97, or apneas, p=0.77, day 3 data shown (Fig. 4.5a and 4.5b). Cognitive performance, assessed by Barnes Maze, p=0.7, and NORT, p=0.56, was found to be unremarkable between stroke and sham groups (Fig. 4.5).

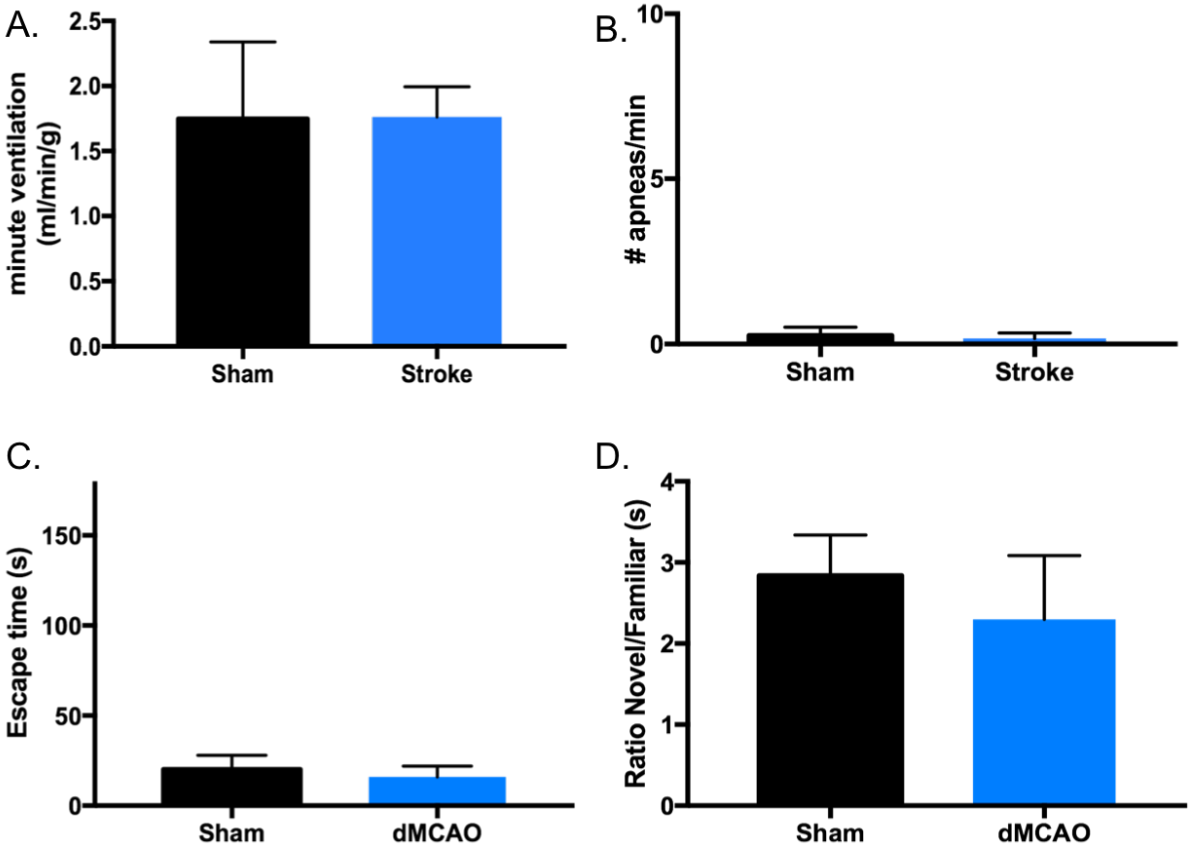

Figure 4.5. Distal MCAO does not result in disordered breathing or cognitive decline. Mice undergoing dMCAO do not develop respiratory dysfunction evident by no change in minute ventilation, p=0.97 (**A**) or absence of apneas, p=0.77 (**B**). Sham and stroke mice had similar escape times on Barnes maze on day 42, p=0.7, n=6 (**C**). Both groups of mice showed a preference for the novel object, indicative of no deterioration in cognitive performance, p=0.56 (**D**).

4.6. Discussion.

Our six-week studies reproduced findings of many studies reporting cognitive deficits following ischemic stroke. (139, 140) Cognitive deficits following MCAO may be detected as early as 3 days following ischemia and persist for months in rodents and for years in humans. (141) Human studies have one additional prominent finding; they report signs of persistent cognitive decline over many years following stroke. Our current study found indications of progressive cognitive decline in spatial learning and memory, a hippocampal dependent task, over a six-week period following MCAO. The hippocampus receives blood supply via the anterior choroidal artery and the posterior communication artery(142), both of which are unaffected by MCAO. This suggests that other factors are contributing to post stroke cognitive decline such as inflammation, disordered breathing and hypoxia.(143)

During the course of six weeks mice underwent weekly plethysmography studies to assess respiratory function post stroke. To our surprise we discovered that mice could be divided into one of two groups based on the number of apneas per minute. This criteria is similar to the Apnea-Hypopnea Index (AHI) used in humans to report the number of apneas an hour during sleep. Mice were stratified as either minor (less than 5 apneas a minute) or severe (10 or more apneas a minute). Respiratory tracings from mice in the severe group represent a Cheyne-Stokes like form of periodic breathing, with a waxing and waning of tidal volume. While the minor group displays a relatively stable respiratory pattern, displaying improvements from day 3 tracings. The slope of the ventilatory response to CO_2 remains unchanged in either group, consistent with our previous findings, suggesting no

change in chemoreception. The variations in tidal volume in the severe group suggest it is the effects of ventilation on blood gases that may be contributing to the development of apneas in mice. Respiratory chemoreceptors contribute to both respiratory rate and tidal volume based on stimulus of CO_2/H^+, the increases in tidal volume on a breath to breath basis eliminate larger volumes of CO_2, decreasing the CO_2 reserve until CO_2 levels drop below apneic threshold resulting in apnea. We can infer that CO_2 levels begin to drop by the decreases in tidal volume observed in the one or two breaths preceding an apnea. Increases in plant gain are predicted to destabilize breathing by decreasing the CO_2 reserve. Breath by breath measurements of tidal volume and exhaled CO_2 will confirm our conclusions that MCAO increases plant gain therefore destabilizing breathing.

Based on our respiratory findings, we performed a post hoc analysis of cognitive function based on our assigned apnea criteria. Surprisingly, only mice with a severe form of disordered breathing suffer from progressive cognitive decline. Both groups had similar outcomes in the number of errors made prior to finding the escape hole, as well as time to find the escape hole on Barnes Maze at a 21-day time point. In contrast, on day 42 the severe group made more errors prior to finding the whole and took longer than the minor group. More importantly, performance on day 42 was worse than day 21 within the severe group, indicative of progressive cognitive decline. The minor group displayed similar performance on both days 21 and 42.

Freezing behavior measured on contextual fear conditioning arena, an amygdala-hippocampal associative learning task, found that the severe group

displayed less freezing behavior than the minor group. We also found a negative correlation between the number of apneas per minute and percent time freezing, indicative of a relationship between the severity of disordered breathing and deteriorating cognitive function.

Although studies in human patients found no association between stroke size or location and the development of disordered breathing, we wanted to assess the effect of stroke size on the development of disordered breathing. Differences in cerebral atrophy volumes between the two groups at day 42 was negligible. We also found no histological indications of posterior hemisphere or brainstem infarction. NDS measured at the time of ischemia and on day 3 were identical between animals in both groups. Corner test, a measure of functional disabilities, again was identical between animals of both groups on day 3 and 7. Taken together, we conclude that variation in stroke severity does not impact the development of disordered breathing.

Lastly, we employed the distal MCAO model to determine if a small stroke limited to the cortex produced disordered breathing or cognitive decline. When followed for a six week time period no detectable differences were noted between stroke and sham groups in any of the respiratory parameters previously assessed. We did not find any evidence of cognitive decline on either Barnes Maze or NORT. These findings are important for two reasons. First the mechanism by which stroke induces disordered breathing is not initiated or sustained in a smaller, cortical stroke. Until we have a better understanding of the mechanism(s) underlying the development of disordered breathing the use of the distal model to rule out stroke as the primary contributor to progressive cognitive decline is limited. Second, a single

cortical stroke does not result in cognitive decline, suggesting that disordered breathing is a factor in contributing to progressive cognitive decline witnessed in MCAO mice.

4.7. Future Directions.

To better understand the role of disordered breathing, namely apneas, in the development of progressive cognitive decline steps must be taken to separate other possible contributions induced by ischemic stroke. Currently, animal models of disordered breathing are not well equipped to answer this question. Models inducing central apneas are not specifically targeted to disrupt only breathing such as whole animal monoamine oxidase-A knock out mouse. (144) Recently, a GPR4 channel was determined to be a major chemosensing mechanism of RTN neurons, and lentiviral knock down of this protein produced hypoventilation and an increase in the incidence of apneas. (46) GPR4 knock out mice are available but come with many downfalls, such as decreased litter size, spontaneous hemorrhage and altered kidney function. The development of an inducible Phox2b Cre floxed GPR4 mouse line would avoid many of these issues. An inducible line would bypass any potential detrimental outcomes in knocking out this protein during development while limiting the knockdown of GPR4 to Phox2b positive neurons such as the RTN and NTS. This KO line would allow for further assessment of apneas role in progressive cognitive decline.

Chapter 5. Brainstem reactive gliosis and the role of TGF-*B*

Rationale: Evidence from our previous studies suggests that hemispheric stroke does not result in direct brainstem neuronal cell death to produce disordered breathing. With this in mind we began to explore other cell types as possible contributors to disordered breathing. As we began our investigation a study was published determining that intracerebroventricular (ICV) injections of streptozotocin not only induced blunted respiratory response but also produced reactive gliosis surrounding many key respiratory control centers such as the NTS and pre-Botzinger complex. (145) This suggests that there is a pathway of communication from the cerebral hemispheres to the brainstem that may be transmitted via CSF and provides evidence that glia cells may be contributing to respiratory dysfunction. TGF-*B* expression increases following ischemic stroke leading to reactive astrogliosis in infarct area. We explore this as a possible mechanism of stroke induced respiratory dysfunction.

5.1. MCAO results in pronounced brainstem astrogliosis.

GFAP staining of young and aged brainstem slices revealed a pronounced astrogliosis in brainstem areas of the NTS and ventral medullary surface (VMS) young shown, a region containing RTN neurons (average # cells/field of view VMS: 47.67$\pm$4.33 vs. 94$\pm$11.15, $p<0.05$, NTS: 13$\pm$3.78 vs. 125.7$\pm$31.6, $p<0.05$, Fig. 5.1). This reactive gliosis is evident as early as day 3-post stroke and remains present on day 21 and day 42.

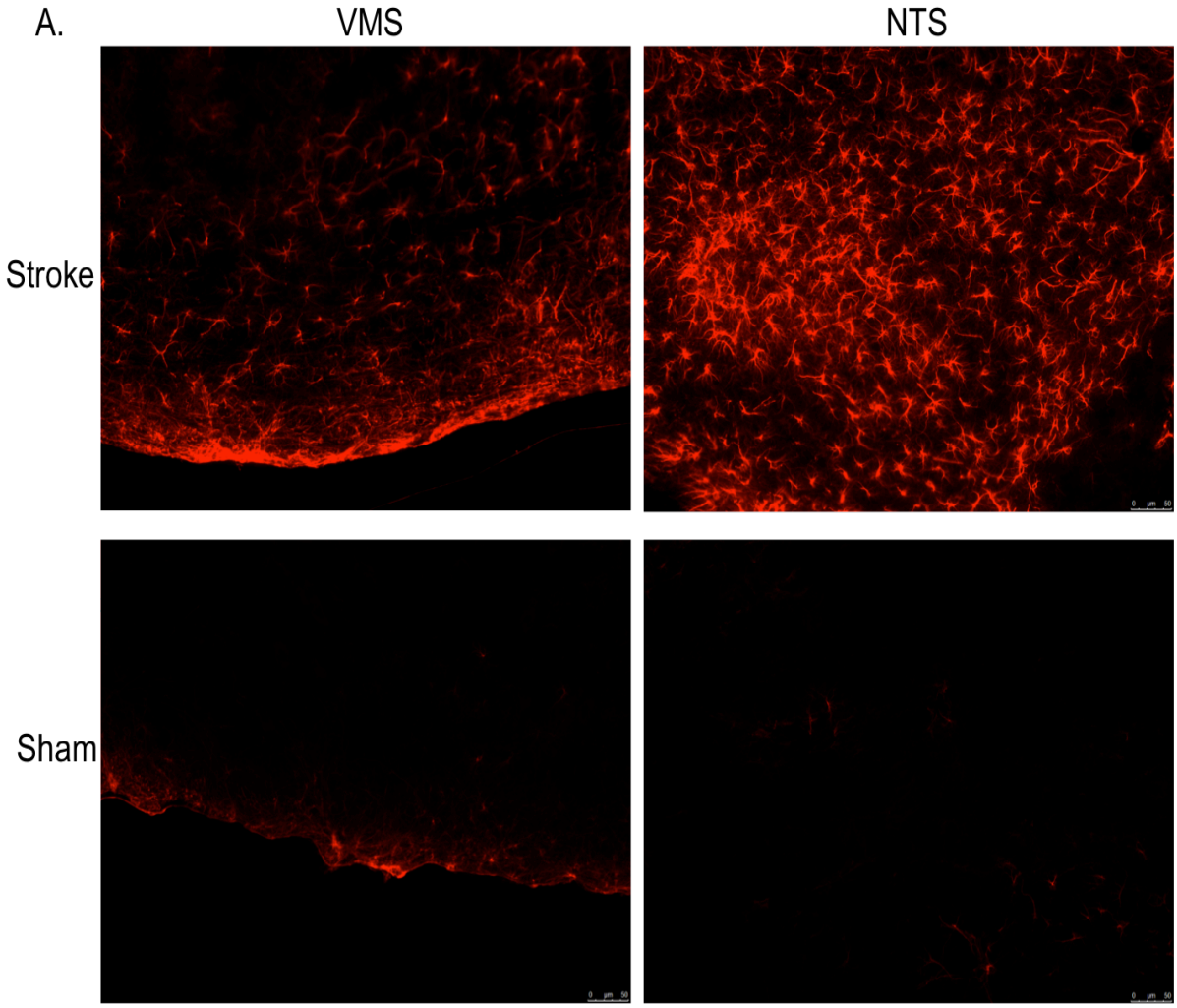
A.
VMS
NTS
Stroke
Sham

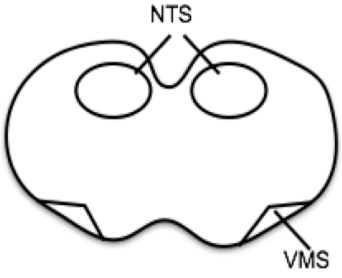
NTS
VMS

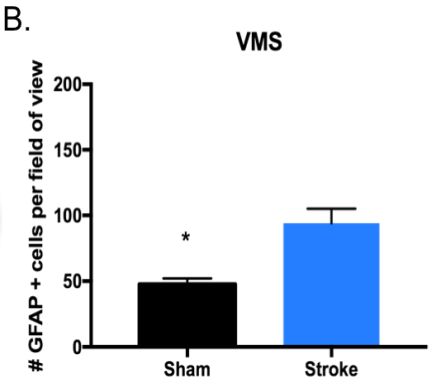
B.
VMS
GFAP + cells per field of view
200
150
100
50
0
*
Sham
Stroke

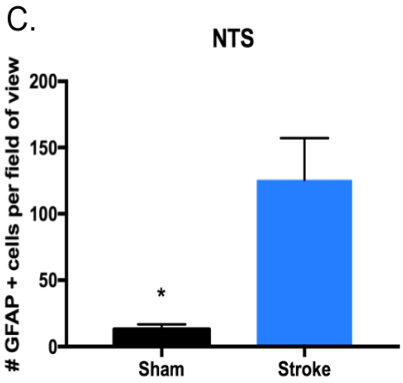
C.
NTS
GFAP + cells per field of view
200
150
100
50
0
*
Sham
Stroke

Figure 5.1. MCAO induces pronounced astrogliosis surrounding key brainstem respiratory neuronal populations. 20x view of GFAP IHC staining of brainstem slices from day-3 post stroke mice revealed a pronounced astrogliosis in the VMS and NTS compared to sham, average # cells/field of view VMS: sham 47.67±4.33 vs. 94±11.15, $p<0.05$, NTS: sham 13±3.78 vs. 125.7±31.6, $p<0.05$ (**A**). Schematic included showing geographical location of these sites. GFAP + cell counts were significant in both regions compared to sham (**B** & **C**).

5.2. ICV injection of TGF-B produces disordered breathing and reactive gliosis in the brainstem.

ICV injections of TGF-*B* into the lateral ventricle of naïve mice produced respiratory dysfunction characterized by hypoventilation (minute ventilation room air 2.076±0.008 vs. 1.157±0.07 ml/g/min, $p<0.001$, Fig. 5.2b) and an increase in apneas compared to saline injected animals (1.3±0.3 vs. 5.6±1.6, not significant $p=0.06$, Fig. 5.2c) on day 1. Brainstem IHC analysis revealed a pronounced astrogliosis compared to vehicle in areas of the NTS and VMS (Fig. 5.2d).

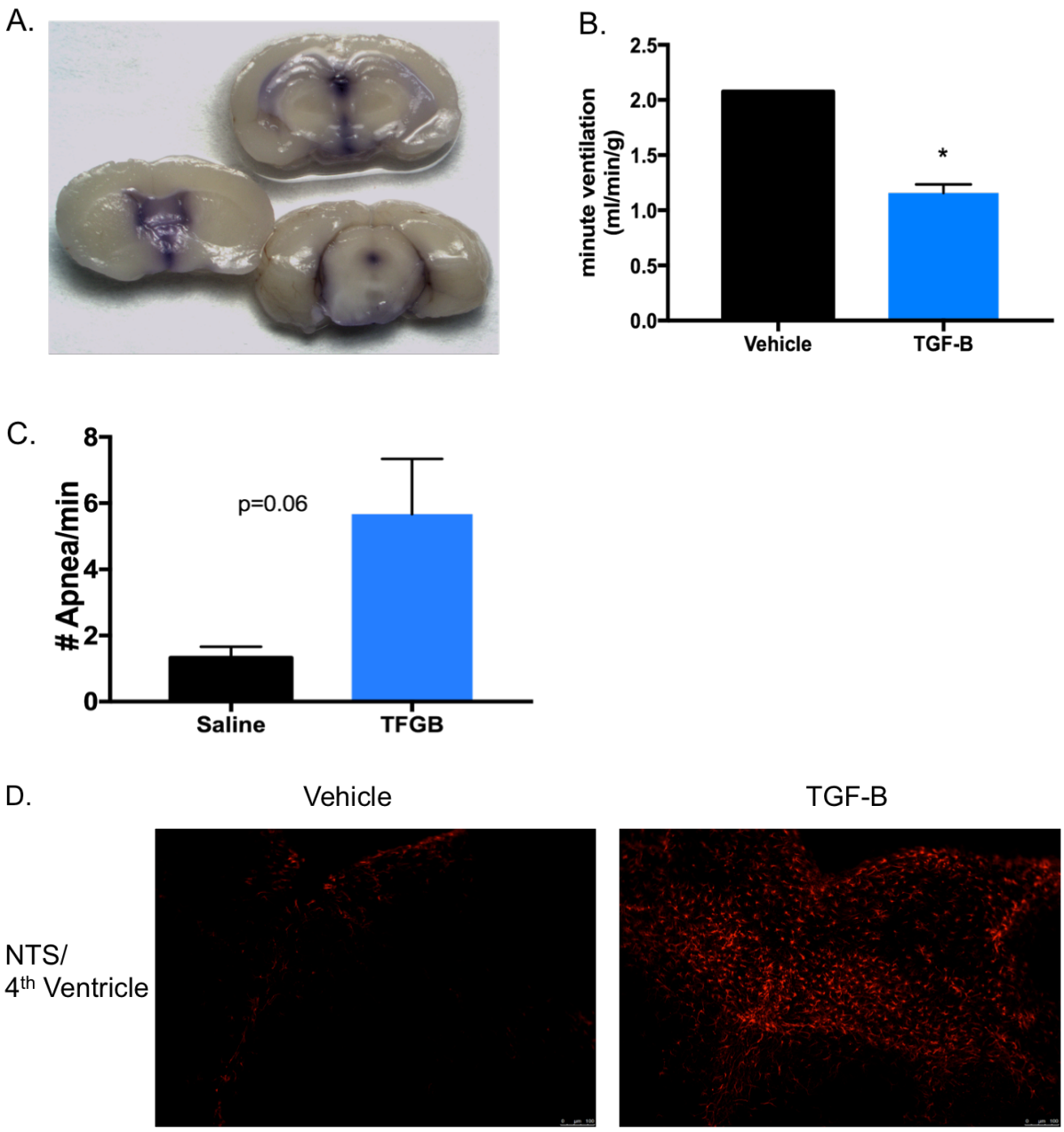

Figure 5.2. ICV TGF-β injections induce altered respiratory activity and brainstem astrogliosis. 2mm brain slices following Evan's Blue ICV injection into cerebrospinal fluid. Lateral ventricle injection diffuses throughout CSF compartments (**A**). On day 1 following injection mice display blunted minute ventilation, 2.076±0.008 vs. 1.157±0.07 ml/g/min, p<0.001, n=3 (**B**) as well as an increase in

the incidence of apneas, 1.3±0.3 vs. 5.6±1.6, not significant p=0.06 (**C**). IHC performed on tissue day 7-post injection revealed pronounced astrogliosis in brainstem regions of respiratory control (**D**).

5.3. TFG-B signaling in brainstem astrocytes increases following MCAO.

Increases in TGF-*B*1 expression following stroke are proposed to be neuroprotective while other isoforms enhance glial reactivity obstructing recovery, but have only been assessed in the peri-infarct region following stroke. (85) We performed IHC using pSmad2, a downstream component of the TFG-*B* signaling cascade, to assess both increases in TGF-*B* signaling as well as evidence of co-localization with reactive astrocytes. On day 3 post surgery increases in GFAP immunoreactivity were observed in stroke mice compared to sham as previously reported. pSmad2/GFAP co-localization was increased in stroke tissue, although it only accounted for a small number of GFAP positive astrocytes (0.33 ± 0.33 vs. 5.4 ± 1.3, $p<0.01$, Fig. 5.3c). Representative images shown of 20x and 63x views (Fig. 5.3a and b). Total pSmad2 signaling in brainstem regions was unaffected by MCAO as measured by IHC, data not shown. N=3 animals per group, 2 slices per animal.

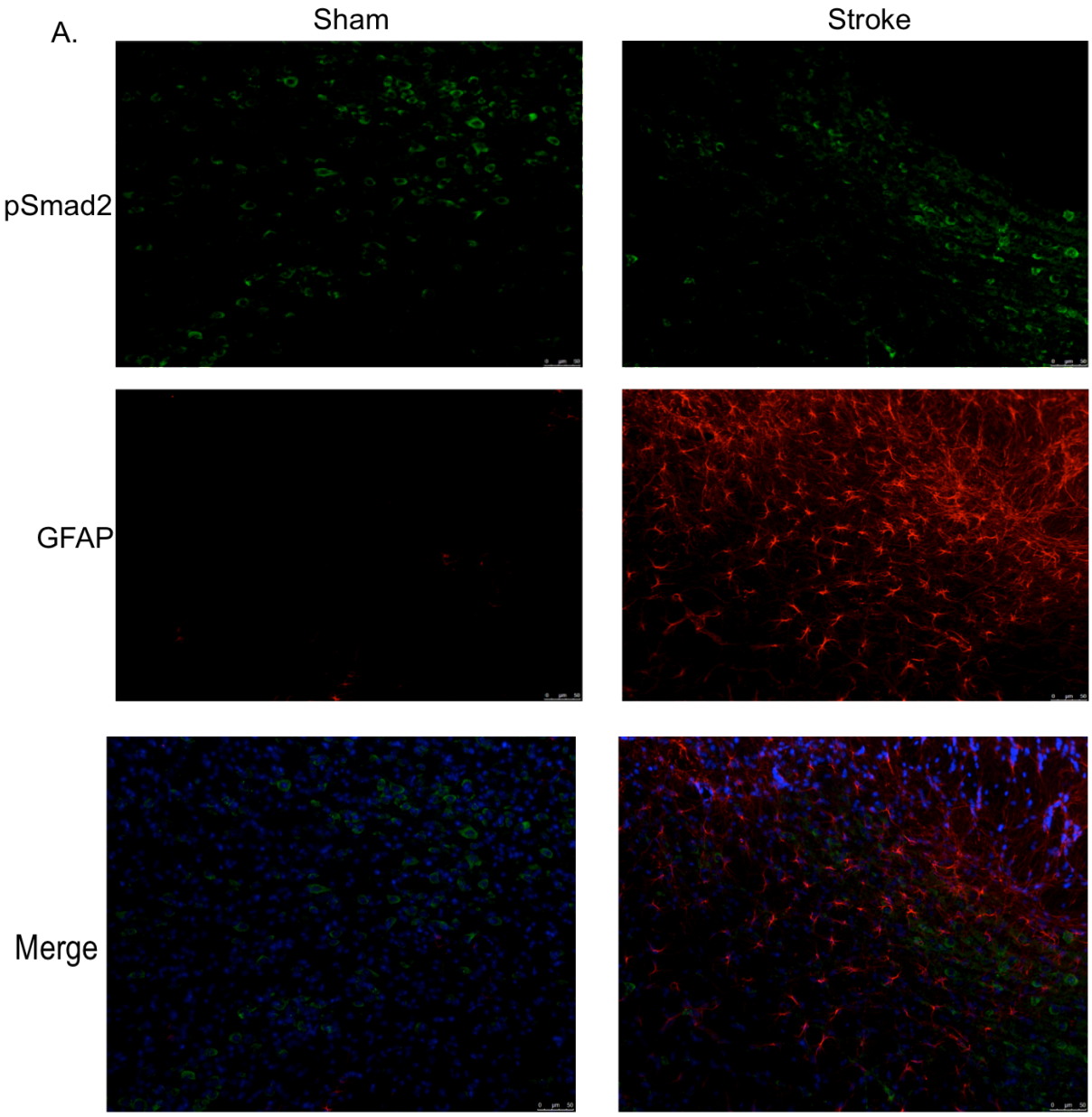
A.
Sham
Stroke
pSmad2
GFAP
Merge

B. Stroke - 63x

pSmad2

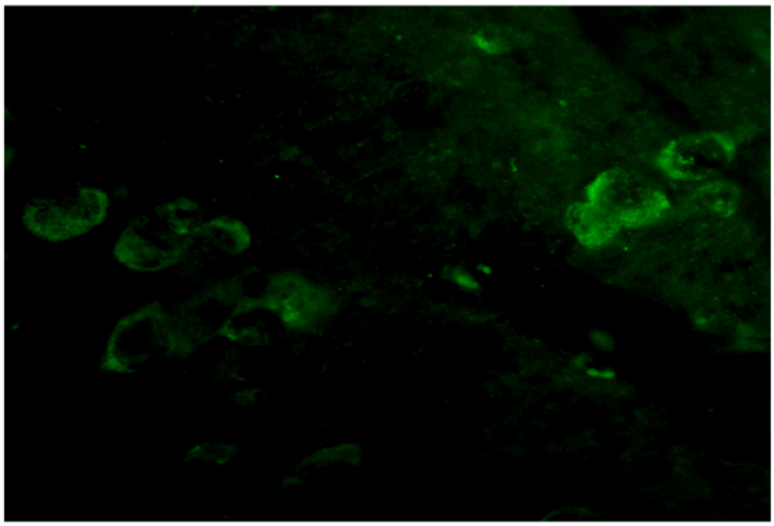

GFAP

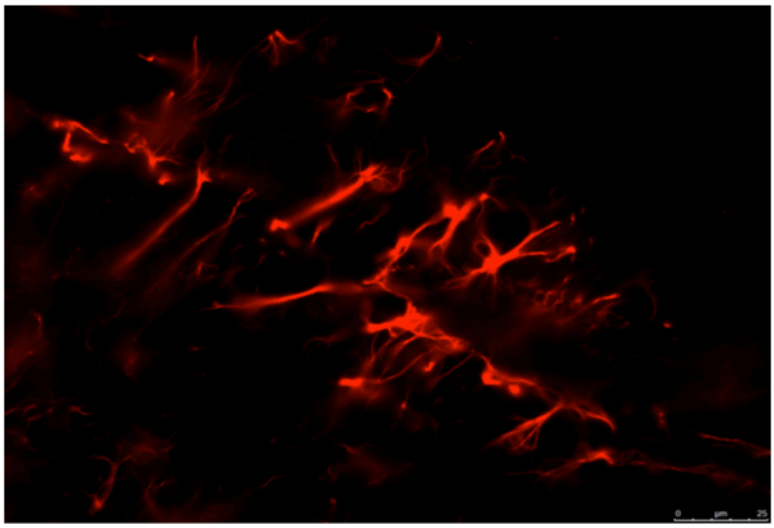

Merge

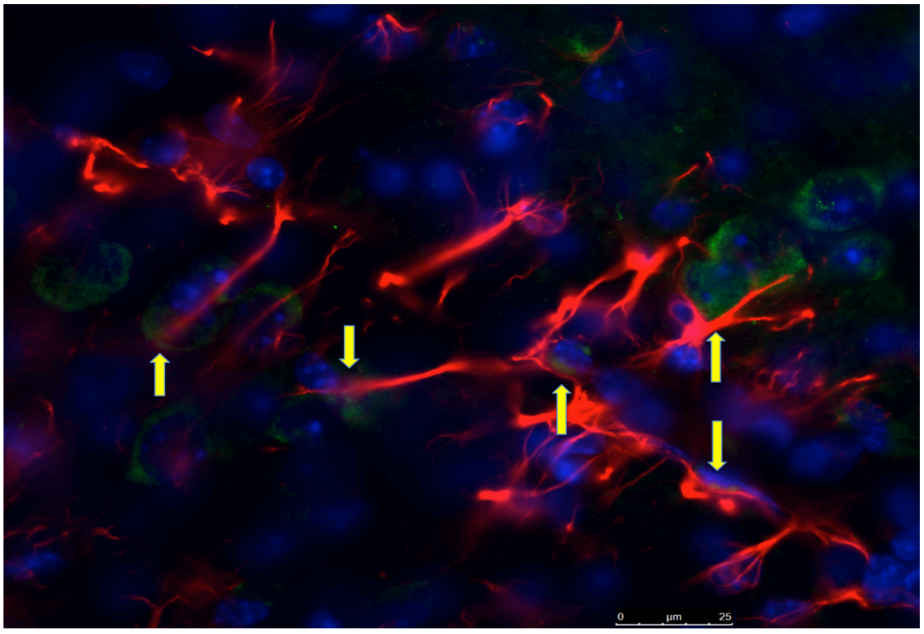

C.

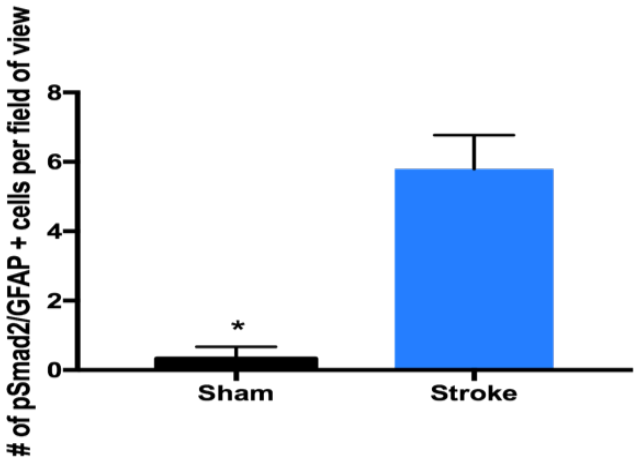

Figure 5.3. TGF-β signaling increases in the brainstem following MCAO. pSmad2 immunoreactivity, indicative of TGF-β signaling, was co-localized with astrocytes on day 3 following MCAO, 20x images shown (**A**), 63x image, arrows indicating colocalization of GFAP and pSmad2. (**B**). Quantification of pSmad2/GFAP co-localization quantified, sham 0.33±0.33 vs. 5.4±1.3, $p<0.01$ (**C**). pSmad2-green, GFAP-red, Dapi-blue.

5.4. Distal MCAO does not result in brainstem astrogliosis.

To understand if brainstem reactive gliosis is unique to MCAO we performed GFAP IHC on brainstem slices of mice that underwent distal MCAO. We found no indications of reactive gliosis as evident by GFAP immunofluorescence in distal MCAO or sham mice, sham 20.67±10.88 vs. 19.33±1.76, p=0.53 (Fig. 5.4).

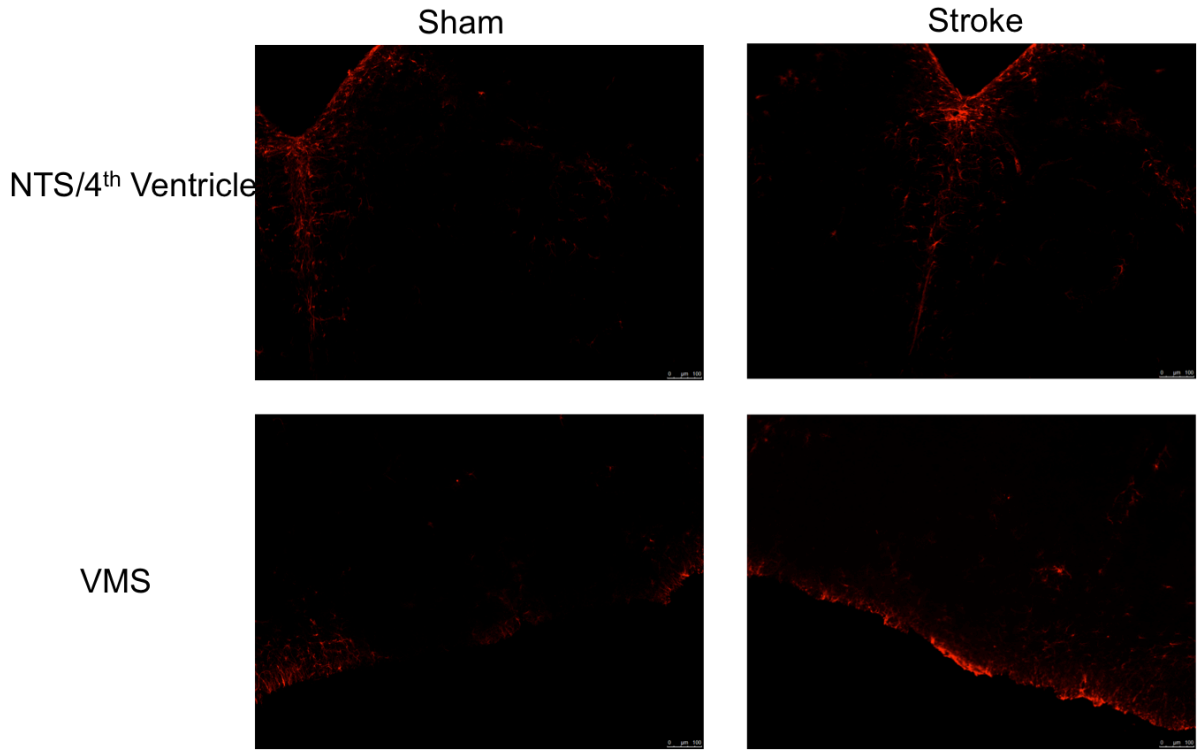

Figure 5.4. dMCAO does not up regulate GFAP expression in the brainstem. No measureable differences in the level of GFAP expression in the regions of NTS or VMS following dMCAO, sham 20.67±10.88 vs. 19.33±1.76, p=0.53. N=3 animals per group, 2 slices per animal.

5.5. Discussion:

MCAO induces a multifaceted, progressive inflammatory response affecting a variety of cells both locally and systemically. Following ischemia, injured or dying neurons, astrocytes, microglia or endothelial cells release components containing damage associated molecular patterns (DAMPs), triggering innate immune activation and production of numerous cytokines including IL-6, IL-1, TNF-α and TGF-β. (85, 146, 147) These cytokines induce systemic responses inducing reactivity in both bone marrow and the spleen. We considered whether MCAO induced an inflammatory response in the brainstem contributing to respiratory dysfunction. IHC analysis of serial slices of brainstem tissue revealed pronounced astrogliosis, markedly in the region of the VMS, 4^{th} ventricle and NTS. This reactive gliosis was evident on day 3 and persisted through day 42-post stroke. It is worth noting that GFAP immunoreactivity is the current hallmark of astrocyte reactivity and that its detection may be extremely limited in quiescent astrocytes. (64) As the contributions of astrocytes to respiratory activity are continuously being investigated, this finding is conceivably an indicator of how stroke disrupts breathing. Brainstem astrogliosis may disrupt breathing via many mechanisms not limited to: basement membrane fibrosis, purinergic control of vascular tone or stimulation to neuronal activity. Alterations in basement membrane fibrosis may inhibit both neuronal and astrocyte detection of CO_2/H^+. The latter two will be discussed in the following chapter.

In the peri-infarct region following stroke, astrocytes play a major role in extracellular matrix remodeling and glial scar formation by secreting numerous

proteins including laminin and fibronectin. (148) The presence of these molecules along with glial scar formation contributes to inhibition of neural regeneration and communication into the injury site. Numerous factors including context dependent signaling and distance from lesion influence the degree of astrocyte reactivity and alterations in gene profile. It is not possible to equate GFAP reactivity with a single unique astrocyte profile. (149)

A number of cytokines are up regulated following stroke that can induce astrocyte reactivity such as TGF-β. Increases in astrocyte TGF-β signaling following stroke have been recently demonstrated. (85) As others have shown ICV injections of other compounds, such as Streptozatocin, induces respiratory dysfunction and brainstem astrogliosis. (145) To explore this signaling mechanism TGF-β ICV injections were performed in naïve mice. To our surprise, respiratory parameters were blunted by TFG-β injection on day 1 and persisted for a week in a similar fashion following MCAO. GFAP staining of these tissues additionally demonstrated a pronounced reactive astrogliosis in the brainstem. This indicates that CSF-perfused TGF-β induces astrocyte reactivity in the brainstem as well as producing respiratory dysfunction. Total levels of brainstem pSMAD2, indicative of TGF-β signaling, were not increased following MCAO at day 3 or 21 in the brainstem. Only accounting for a small percentage of reactive astrocytes, co-labeling of pSmad2/GFAP was increased in stroke animals on day 3. Albeit a small one, this suggests that TGF-β/Smad2 signaling plays a role in astrocyte activation. While phosphorylation of Smad2 has been accepted as marker of TGF-B signaling in astrocytes, most likely as a neuroprotective signal, it fails to account for any contribution of Smad3

signaling. Ablation of Smad3 signaling reduces inflammation, gliosis, and fibronectin deposition in the weeks following injury. (150, 151) Numerous inflammatory cytokines, many of which are up regulated following ischemic stroke, can induce astrocyte reactivity and should be explored to further understand post stroke brainstem gliosis. Neuroinflammation activates the Jak2-Stat3 signaling pathway prior to the up regulation of GFAP. (152) Conditional astrocyte Stat3 knockout mice attenuated astrogliosis in a model of MPTP neurotoxicity(153) and could be utilized to understand if astrogliosis induces respiratory dysfunction following MCAO.

Previously, we have shown that dMCAO produces neither disordered breathing nor cognitive decline. IHC analysis of brainstem tissue revealed no differences in GFAP immunoreactivity between dMCAO stroke and sham mice, further supporting a strong a contribution of astrogliosis to disordered breathing.

5.6. Future Directions.

Our experimental findings demonstrate a pronounced astrogliosis in major sites of brainstem respiratory control, as evident by increased GFAP expression. Although understood to be a marker of reactive astrocytes, GFAP expression is not indicative of a beneficial or detrimental role of astrocytes. At this time we are unaware if this reactivity disrupts normal astrocytic functions in respect to respiratory control. A cytokine profile of CSF and brainstem tissue may provide insight to what molecules are potentially activating brainstem astrocytes. Yet, those findings may denote numerous molecules are contributing to a reactive phenotype. Many pro-inflammatory cytokines converge on the same signaling pathway, providing a more

strategic target. The p38 MAPK pathway is activated by numerous pro-inflammatory cytokines(154) and plays an important role in ischemic stroke induced gliosis. Inhibition of this pathway reduced glial scar formation without affecting infarct volumes or functional outcomes when measured 4 days after stroke. (152) It would be interesting if overexpression of p38 MAPK or Jak2-Stat3 in astrocytes induces respiratory dysfunction. Furthermore, inhibition of these pathways following MCAO should be explored as potential therapeutic targets to prevent SIRD.

Further experimentation must be performed to understand the relationship between TGF- β induced astrogliosis and disordered breathing. We our currently in the process of crossing a floxed TGF- β receptor to an inducible GFAP cre line resulting in an astrocyte specific TGF- β receptor knockout mouse. The inducible feature of this animal model allows for temporal control of TGF-β knockout.
Assessments of gliosis and disordered breathing will be obtained following the ICV administration of TGF- β. We anticipate that this animal model will further our understanding of the role of gliosis in the development of disordered breathing.

Chapter 6. Pharmacological stabilization of respiratory activity to improve cognitive outcomes.

Rational: Clinical evidence suggests respiratory dysfunction slows recovery and contributes to increased mortality. For example, although CPAP is not recommended for treatment of central apneas and is poorly tolerated by elderly patients, it has been shown to enhance neurological recovery in some stroke patients thus underscoring the importance of normal respiratory function in stroke, and suggesting treatments targeting respiratory dysfunction can improve post-stroke recovery. Consistent with these clinical observations, preliminary evidence in male mice show that stroke results in a respiratory phenotype in conjunction with other behavioral deficits including functional disabilities, cognitive decline and a high mortality rate. These results suggest ventilatory problems contribute to stroke-induced functional deficits and high mortality. To test this, we will evaluate the efficacy of treatments designed to improve respiratory function on motor and cognitive outcomes.

6.1. Administration of KCNQ agonist Retigabine destabilizes breathing.

In an effort to stabilize post stroke respiratory dysfunction we utilize the KCNQ channel agonist Retigabine, to target RTN KCNQ channels. On day 3-post surgery mice underwent plethysmography, followed by Retigabine (10mg/kg) or DMSO vehicle SQ with subsequent plethysmography testing. Retigabine decreased both respiratory frequency and minute ventilation in stroke and sham mice (data not

shown). This was a result of increasing the interbreath interval as observed (Fig.6.1). For 90% of the breaths taken in stroke mice, the time between breaths is 368ms or less. Retigabine increases that interval to 468ms. Following these observations, we hypothesized that XE991, a KCNQ channel antagonist previously shown to increase basal activity of RTN neurons in vitro, would stimulate respiratory activity following MCAO. XE991 (2mg/kg) or vehicle was administered to mice day 3-post surgery with no detectable effect on any respiratory parameter, data not shown.

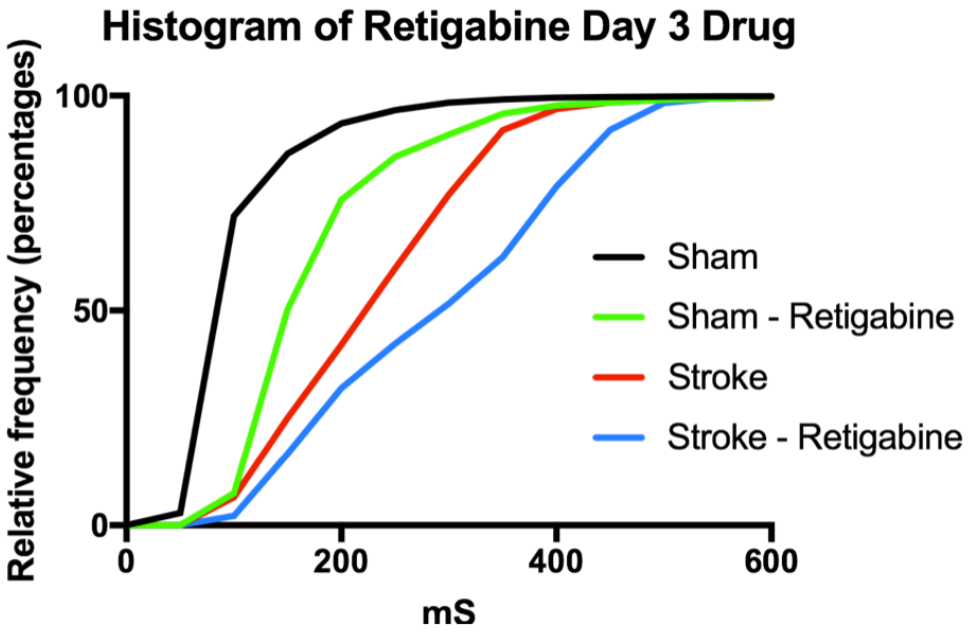

Figure 6.1. Retigabine increases the interbreath interval further destabilizing breathing. Retigabine (10mg/kg) administered on day 3-post surgery results in a right shift of the histogram indicating increase in time between all breaths, expected to further destabilize respiratory activity.

6.2. Acetazolamide administration eliminates apneas.

Acetazolamide is known to enhance basal breathing by inducing metabolic acidosis, commonly used to treat acute altitude sickness. Acetazolamide (40mg/kg) or saline vehicle was administered SQ to mice on day 3 following surgery. Acetazolamide increased respiratory frequency in stroke mice compared to vehicle (152.6$\pm$6.49 vs. 318.4$\pm$61.95 bpm, $p<0.05$, Fig.6.2a) (Sham respiratory frequency 286.7±13.97). While concurrently decreasing the incidence of apneas (6$\pm$1.15 vs 0$\pm$0, $p<0.01$, Fig.6.2b). Representative respiratory tracings shown (Fig.6.2c).

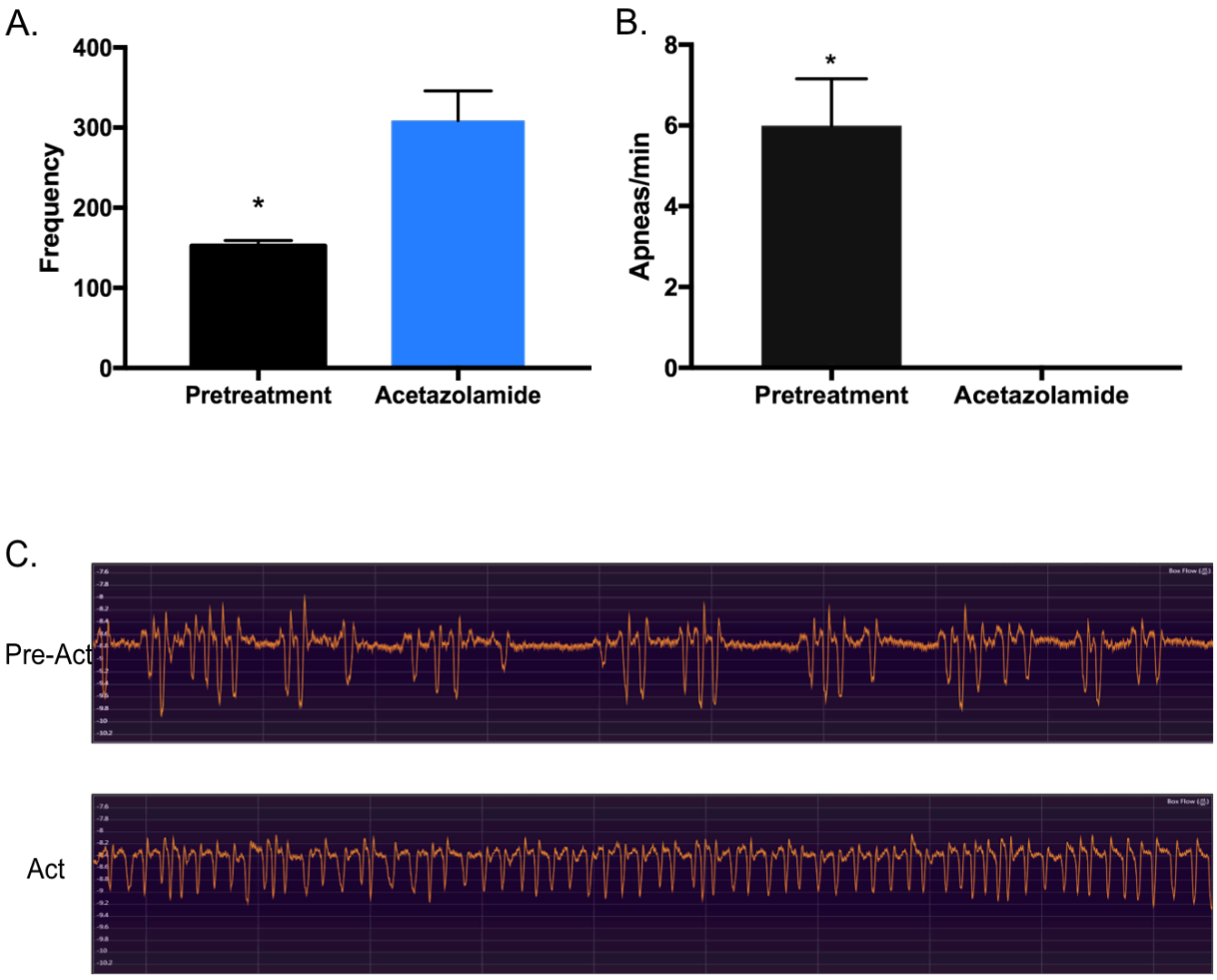

Figure 6.2. Acetazolamide increases respiratory frequency and eliminates apneas. Acetazolamide increases the respiratory frequency of stroke mice, 152.6±6.49 vs. 318.4±61.95 bpm, $p<0.05$ (**A**), while also eliminating apneas under room air conditions, 6±1.15 vs 0±0, $p<0.01$, n=3 (**B**). Representative waveform tracings shown (**C**).

6.3. Long-term administration of acetazolamide improves cognitive outcomes following MCAO.

Acetazolamide (40mg/kg) or saline vehicle was administered over a four week period beginning on day 14 following surgery via osmotically driven SQ implanted Alzet pumps. Cognitive assessments performed on day 21 following surgery detected no differences between the treatment groups, as a group stroke mice perform worse on Barnes maze than sham, (Mantel-Cox test, $p<0.001$, Fig.6.3a). On day 42 stroke mice treated with Acetazolamide had significantly improved cognitive performance compared to sham ($p=0.0005$, n=6 per sham group, n=11 per stroke group Fig. 6.3b). Upon sacrifice histological assessment of hemisphere atrophy was conducted. There were no differences in cerebral hemisphere atrophy between acetazolamide and saline vehicle administered stroke groups, (sham 34.53 ± 3.45 vs. 29.94 ± 6.47, $p=0.5$, Fig. 6.3c).

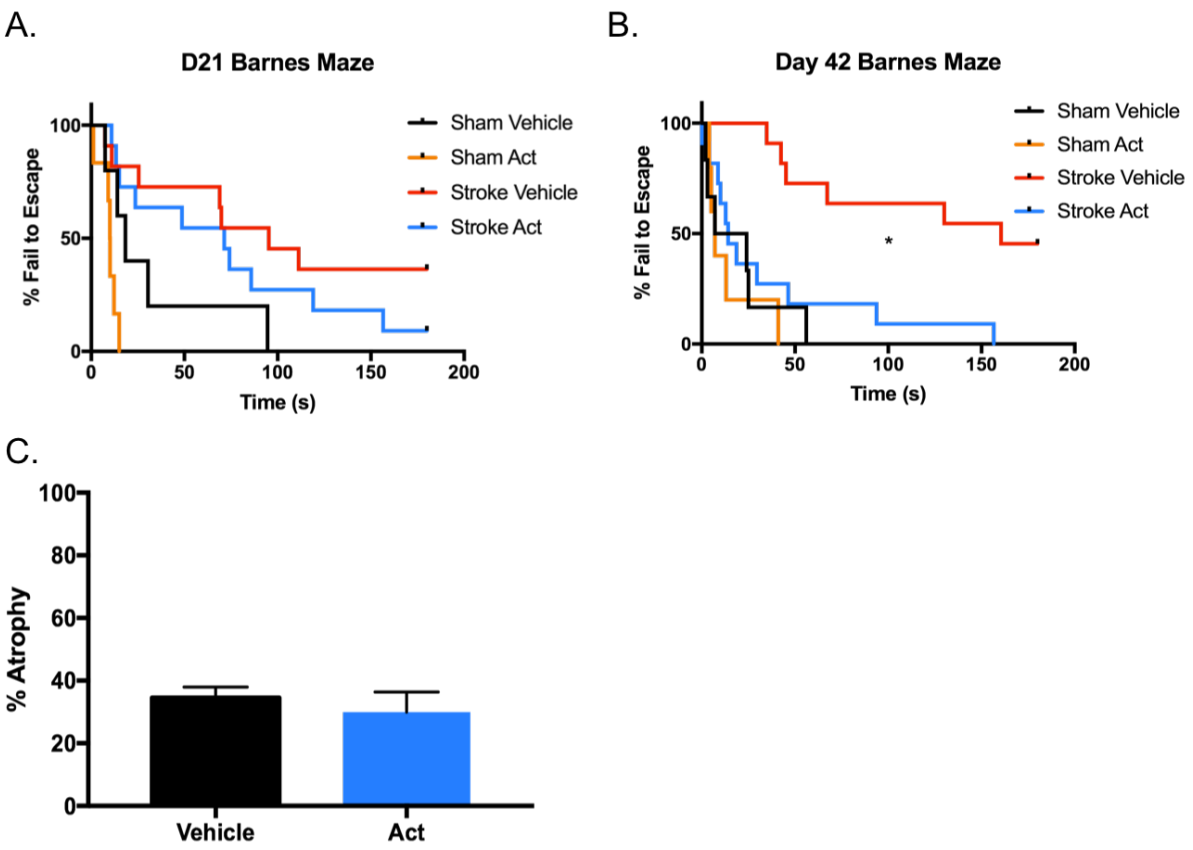

Figure 6.3. Continuous administration of Acetazolamide improves long term cognitive outcomes following MCAO. Mice underwent spatial learning and memory testing using the Barnes maze on day 21 and day 42-post surgery. On day 21 stroke mice as a group perform worse than sham, taking longer to locate the escape hole, Mantel-Cox test, $p<0.001$ (**A**). On day 42 testing, acetazolamide administered stroke mice show a marked improvement in their ability to locate the escape hole when compared to vehicle-administered shams, $p=0.0005$ (**B**). No variations in the severity of infarct between the two groups when hemispheric atrophy was measured, sham 34.53 ± 3.45 vs. 29.94 ± 6.47, $p=0.5$ (**C**).

6.4. Acetazolamide dilates cortical arteries while constricting brainstem arteries in slice recordings.

Slices of brain tissue from naïve mice were collected to measure arteriole vessel diameter in the cortices and brainstem under physiological conditions (5% CO_2 balanced air) and after application of Acetazolamide (500 um plus 5% CO_2 balanced air). We reconfirmed that application of Acetazolamide dilated cortical arteries (mean of differences 0.5584 ± 0.1303 µm, p=0.002, Fig. 6.4c and e). Surprisingly, this effect was reversed in RTN arterioles, were we observed constriction (-0.6089 ± 0.1942 µm, p=0.0095, Fig. 6.4a and e).

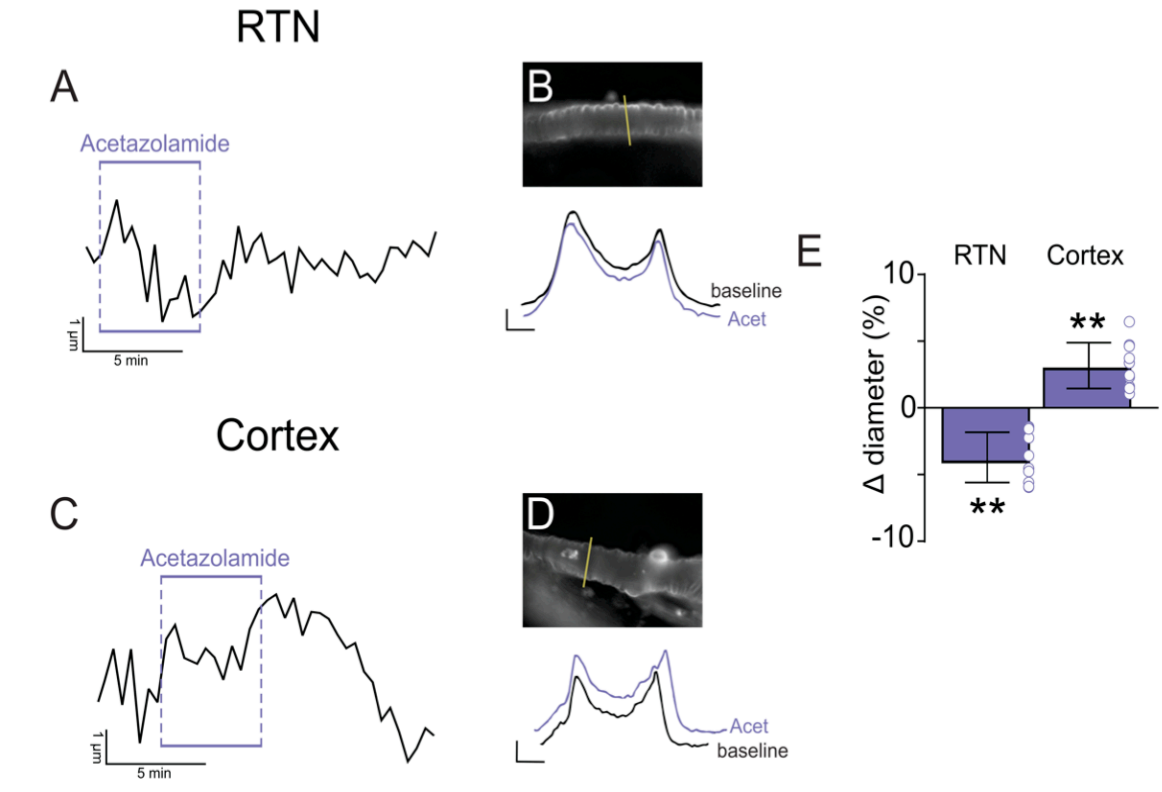

Figure 6.4. RTN and cortical arterioles differentially react in *in vitro* arteriole slice recordings. (A) Diameter trace of an example RTN arteriole constricting in response to bath application of 500 µm Acetazolamide. **(B)** An example RTN vessel image profile plot with application of Acetazolamide, -0.6089±0.1942 µm, p=0.0095. Profile plot scale bars: 2000 a.u., 10 µm. **(C)** Diameter trace of an example cortical arteriole dilating in response to application of 500 µm Acetazolamide, mean of differences 0.5584±0.1303 µm, p=0.002. **(D)** An example cortical vessel image profile plot with application of Acetazolamide. Profile plot scale bars: 2000 a.u., 10 µm **(E)** Summary data shows differential reactivity of Acetazolamide; a vasoconstriction is seen in the RTN (N = 10 vessels) while a vasodilation is seen in the cortex (N = 10 vessels)**, difference in µm from baseline (p<0.01).

6.5. Discussion and Future Directions.

Our earlier experimental results indicate that MCAO produces disordered breathing in mice and that the severity of disordered breathing correlates with worsening cognitive decline. With an understanding of brainstem respiratory physiology we employed Retigabine in effort to improve respiratory instability while eliminating apneas. Retigabine, a high affinity voltage gated potassium channel (KCNQ) agonist, decreases membrane potential altering the firing rate of RTN neurons in vitro. Referencing Figure 4.2c, we originally believed the burst of respiratory activity (segments of waxing and waning of tidal volume) to be problematic and by reducing the activity of RTN neurons (responsibility for both respiratory frequency and tidal volume) would stabilize breathing and eliminate apneas.

Retigabine had a depressive effect on respiratory activity in both stroke and sham mice, while also increasing mortality in the stroke coort. By enhancing potassium channel activity, Retigabine increased the breath-to-breath time interval, reduced tidal volume while overall decreasing minute ventilation. Based on these experimental outcomes, we hypothesized that XE991 (a KCNQ antagonist) would have opposite effects by increasing respiratory activity. When administered systemically we observed no effect on respiratory activity in either stroke or sham mice. To rule out low dosage as the cause, 3mg/kg was administered, which induced seizure like activity in sham mice. This finding does not come as a surprise due to the KCNQ channel's regulation of neuronal excitability. In summary, systemic activation of KCNQ channels decreases respiratory activity.

In subsequent experiments we demonstrate that the administration of Acetazolamide to MCAO mice enhances respiratory activity while suppressing the apneas. Continuous administration of Acetazolamide greatly improves long-term cognitive outcomes. Lastly, in contrast with the observed and expected vasodilation of cortical arterioles, we show that *in vitro* application of Acetazolamide to brainstem slices from young male animals constricts arterioles of the RTN. This may provide insight into the mechanism of how Acetazolamide enhances respiratory activity, and how MCAO disturbs brainstem respiratory function. To address the later, similar experiments must be performed in brainstem slices of MCAO and sham mice to examine vascular responsiveness to changes in CO_2. The concept of differential regulation of vascular tone is not new to mammalian physiology. Unlike systemic arterioles, which dilate in response to low levels of O_2, pulmonary arterioles constrict in a process referred to as hypoxic pulmonary vasoconstriction or pulmonary shunting. (155) Although the precise mechanism underlying this phenomenon is still be resolved, there is increasing evidence that suggests hypoxia stimulates a rise of intracellular calcium in pulmonary artery smooth muscle culminating in vascular constriction. (156) This concept must be considered when studying the physiology of brainstem arterioles as well as the mechanisms in which stroke disrupts brainstem processes producing disordered breathing.

It has been hypothesized that the Acetazolamide mediated increase in respiratory activity following acute altitude sickness is in response to increase in H^+ concentration. This increase in H^+ can have a two-fold effect on respiratory activity. First, an increase in H^+/CO_2 concentration would intensify central chemoreceptor

stimulation, increasing respiratory activity, while concurrently expanding the CO_2 reserve, stabilizing breathing. Second, acetazolamide decreases arteriole diameter in the region of the RTN in a similar manner as increased H^+/CO_2, effectively decreasing regional blood flow.

Alternatively, it is understood that vascular tone in the region of the RTN is mediated in part by purinergic signaling. Previous evidence indicates RTN astrocytes release ATP in response to increases in CO_2/H^+. Pharmacological activation of RTN astrocytes reconfirmed this finding, while also demonstrating a subsequent purinergic mediated arteriole constriction. To further confirm our findings of acetazolamide-induced vasoconstriction, these experiments should be performed with acetazolamide in combination of purinergic blockade. These outcomes could further support our findings of reactive astrogliosis in the brainstem as pathological.

Consistent with our earlier data, we find that elimination of apneas prevents further cognitive decline, suggesting a correlation between apneas and cognitive outcomes. We must acknowledge the possibility that acetazolamide enhanced respiratory activity while independently improving cognitive function by a different and distinct mechanism. Intralateral ventricular administration of carbonic anhydrase inhibitors enhanced synaptic efficacy and improved spatial learning/memory in rats. (157) At the moment this model does not allow for the delineation of the two. The inducible RTN specific GPR4 knockout model described previously could be of use to further our understanding of this matter. The GPR4 knockout model presents with a greatly diminished CO_2/H^+ sensing capacity of RTN neurons, therefore Acetazolamide mediated increase of H^+ should not induce a large alteration in

respiratory activity. If this model of disordered breathing results in cognitive decline, Acetazolamide therapy could also be initiated to understand the direct effects of the drug on cognitive performance. Models of intermittent hypoxia would fail to answer this question as Acetazolamide therapy stimulates respiratory activity in an attempt to improve oxygenation, adverting hippocampal cell stress/loss.

Collectively, our findings indicate that 1.) MCAO induces respiratory dysfunction possibly by disrupting astrocyte control of vascular tone in key brainstem regions. 2.) The severity of respiratory instability, namely apneas, correlates with progressive cognitive decline following MCAO. 3.) Improving respiratory activity by suppressing apneas, as seen with Acetazolamide administration, prevents further post stroke cognitive decline.

Chapter 7. Conclusion.

The first report of stroke disrupting respiratory function originated in the early 1960s from the studies of Brown and Plum. (158) Since then numerous studies have described a high prevalence of sleep disordered breathing following stroke. Disordered breathing that accompanies stroke is associated with higher one-year mortality and worse functional outcomes at the time of discharge, 3 months and 12 months following stroke. (17, 18) Importantly, a decrease in cognitive performance was closely associated with the severity of respiratory disturbance, and an increase in daytime sleepiness after stroke was a strong predictor of cognitive decline. (19)

Numerous experimental studies have been undertaken to comprehend the effects of obstructive sleep apnea and/or intermittent hypoxia on the maladaptive consequences of hypertension, heart failure and cognitive impairment. Our review of the literature discovered only one experimental report of stroke altering ventilatory patterns. Koo et al. reported that following transient 60-minute left middle cerebral artery occlusion, A/J mice displayed an increase in the coefficients of variation for respiratory frequency, tidal volume and minute ventilation 24 hours after stroke. They concluded that ischemic stroke could develop a characteristic-breathing pattern similar to Cheyne-Stokes respiration. (159) Albeit a significant finding, this work did not fully characterize the respiratory phenotype induced by MCAO and lacked any discussion of apnea, the fundamental feature of stroke disordered breathing and a major contributor to hypoxia and cognitive decline. Advanced chronological age is the most important non-modifiable risk factor for stroke and is

an independent predictor of poor outcome after stroke. To date no studies have been undertaken to investigate either age or sex as a biological variable in the study of stroke induced respiratory dysfunction.

A large body of evidence exists suggesting that obstructive sleep apnea increases the risk of declining neurological function, cardiovascular disease, cancer and death. A majority of these studies employ intermittent hypoxia as a model to mimic the episodes of apnea observed in sleep apnea. Potential mechanisms contribute to cognitive decline include neuro-inflammation, mitochondrial dysfunction, oxidative stress and neuronal apoptosis. (160) In the models of intermittent hypoxia, investigators subjected animals to severe hypoxic conditions resulting in arterial oxygen levels that plummeted to levels between 40-48 mmHg. (161) These levels of PaO_2 are extreme and far from measureable levels in human studies of OSA (88.14$\pm$17.83 mmHg). (162) Our studies found mice suffering from SIRD present with PaO_2 levels of 79.3 and SpO_2 desaturations to 90%, consistent with human reports.

On the other end of the spectrum many studies report a neuroprotective effect of intermittent hypoxia. Several animal models of neurological disease or injury, including Alzheimer's, brain and spinal cord injury have shown benefits of hypoxic conditioning on enhancing neuroplasticity, cerebral vascular function and preventing further cognitive decline. (163-165) Furthermore, the concept of rapid and delayed post-conditioning induced neuroprotection, is proposed to minimize reperfusion injury following a cerebral ischemic event by engaging the brain's own endogenous

responses. (166) This raises a critical question of whether stroke induced alterations in respiratory activity serve as a compensatory response to improve outcomes, a question that this study answers.

This study reports similar findings of Koo *et al.* in that 60 minutes of MCAO produces alterations of respiratory activity in a separate mouse strain, C57B6. Koo *et al.* reported alterations in respiratory frequency and minute ventilation 24 hours after ischemia. Our findings indicate that these respiratory parameters are continuously perturbed 3 and 7 days following ischemia. A key finding of this work was that apneas are the underlying cause of respiratory instability. These episodes of apnea not only decrease breaths per minute and subsequently minute ventilation, but also result in periods of oxygen desaturation and systemic hypoxia. After fully characterizing the respiratory phenotype resulting from following stroke, we sought to understand if apneas are a consequence or compensatory response to ischemia. We found that the number of apneic events an animal suffered per a minute correlated with worse cognitive outcomes over a 42 day period. Consistent with evidence from human stroke patients, a higher apnea-hypopnea index (AHI) directly correlates with a decline in cognitive function.

Continuous positive airway pressure (CPAP) is a well-established therapy for the treatment of obstructive sleep apnea and is currently the only treatment for stroke disordered breathing despite its poor efficacy in these patients. Utilizing knowledge of the molecular mechanisms contributing to neuronal respiratory activity, we utilized the carbonic anhydrase inhibitor, Acetazolamide, to stimulate respiration.

Which resulted in the elimination of apneas and ultimately improved long-term cognitive outcomes following stroke. This study also demonstrates that Acetazolamide differentially modifies vascular reactivity in the brainstem, offering an alternative mechanism of stabilizing post stroke respiratory activity. The next line of experiments conducted should aim to further clarify the mechanism(s) of Acetazolamide stabilizing respiratory activity.

Lastly, this work provided insight into how stroke may disrupt respiratory activity resulting in apneas. We discovered a pronounced astrogliosis surrounding two key brainstem respiratory neuronal populations; the NTS and RTN. Intracerebrovascular administration of TGF-β induced brainstem astrogliosis as well as respiratory dysfunction and apneas. Suggesting a possible causative role of TGF-β mediated astrogliosis disrupting respiration. Further studies using astrocyte specific TGF-β receptor knockout mice will further our understanding of respiratory dysfunction stemming form TGF- β mediated astrogliosis and may help in the design of efficacious therapies to prevent the development of SIRD.

This work was the first to fully characterize stroke induced respiratory dysfunction and show that it is a maladaptive response resulting in progressive cognitive decline. Although this work highlights the correlation between apnea induced hypoxia and cognitive decline, further work is necessary. As previously discussed in Chapter 4, the use of inducible RTN specific GPR4 knockout model can further confirm a causal role of apneas leading to cognitive decline, while also providing a model to study the underlying mechanism(s). This proposed work would

have significant relevance beyond the field of stroke. Recently the Alzheimer's Association released a statement summarizing the findings of 3 separate studies concluding that sleep disordered breathing is associated with an increase in amyloid deposition, suggesting that SDB is an independent risk factor for Alzheimer's. This raises the possibility that interventions targeted to improving respiratory activity may reduce the risk of Alzheimer's. Interestingly, overproduction of TGF- β, astrogliosis and basement membrane thickening enhanced Alzheimer's disease and cerebrovascular abnormalities. (167) Furthermore, increased levels of TGF-B lead to a decline in cerebrovascular dilatory ability and perturbed resting vessel tone in the same animal model. (168)

This work recapitulated the findings of numerous studies reporting a negative correlation between the incidence of apnea and cognitive function. Further emphasizing this point, we found that elimination of apneas following Acetazolamide therapy prevents further cognitive decline, strengthening the correlation between apneas and cognitive outcomes. This work has established a murine model of stroke induced respiratory dysfunction. Laying the groundwork for further investigations into the mechanisms of disordered breathing and the development of therapies to prevent respiratory dysfunction and ultimately cognitive decline. Ameliorating respiratory instability and sequelae is of high relevance to several disciplines in preventing cardiovascular disease, stroke, cancer and death, improving overall patient health and wellbeing.

Bibliography:

1. Centers for Disease Control and Prevention (CDC). 2009. Prevalence and most common causes of disability among adults--United States, 2005. *MMWR Morb. Mortal. Wkly. Rep.* 58: 421-426.

2. Ovbiagele, B., L. B. Goldstein, R. T. Higashida, V. J. Howard, S. C. Johnston, O. A. Khavjou, D. T. Lackland, J. H. Lichtman, S. Mohl, R. L. Sacco, J. L. Saver, J. G. Trogdon, and American Heart Association Advocacy Coordinating Committee and Stroke Council. 2013. Forecasting the future of stroke in the United States: a policy statement from the American Heart Association and American Stroke Association. *Stroke* 44: 2361-2375.

3. Feigin, V. L., M. H. Forouzanfar, R. Krishnamurthi, G. A. Mensah, M. Connor, D. A. Bennett, A. E. Moran, R. L. Sacco, L. Anderson, T. Truelsen, M. O'Donnell, N. Venketasubramanian, S. Barker-Collo, C. M. Lawes, W. Wang, Y. Shinohara, E. Witt, M. Ezzati, M. Naghavi, C. Murray, and Global Burden of Diseases, Injuries, and Risk Factors Study 2010 (GBD 2010) and the GBD Stroke Experts Group. 2014. Global and regional burden of stroke during 1990-2010: findings from the Global Burden of Disease Study 2010. *Lancet* 383: 245-254.

4. Go, A. S., D. Mozaffarian, V. L. Roger, E. J. Benjamin, J. D. Berry, W. B. Borden, D. M. Bravata, S. Dai, E. S. Ford, C. S. Fox, S. Franco, H. J. Fullerton, C. Gillespie, S. M. Hailpern, J. A. Heit, V. J. Howard, M. D. Huffman, B. M. Kissela, S. J. Kittner, D. T. Lackland, J. H. Lichtman, L. D. Lisabeth, D. Magid, G. M. Marcus, A. Marelli, D. B. Matchar, D. K. McGuire, E. R. Mohler, C. S. Moy, M. E. Mussolino, G. Nichol, N. P. Paynter, P. J. Schreiner, P. D. Sorlie, J. Stein, T. N. Turan, S. S. Virani, N. D. Wong, D. Woo, M. B. Turner, and American Heart Association Statistics Committee and Stroke Statistics Subcommittee. 2013. Executive summary: heart disease and stroke statistics--2013 update: a report from the American Heart Association. *Circulation* 127: 143-152.

5. Demaerschalk, B. M. 2016. Alteplase Treatment in Acute Stroke: Incorporating Food and Drug Administration Prescribing Information into Existing Acute Stroke Management Guide. *Curr. Atheroscler. Rep.* 18: 53-016-0602-5.

6. Sacco, R. L., E. J. Benjamin, J. P. Broderick, M. Dyken, J. D. Easton, W. M. Feinberg, L. B. Goldstein, P. B. Gorelick, G. Howard, S. J. Kittner, T. A. Manolio, J. P. Whisnant, and P. A. Wolf. 1997. American Heart Association Prevention Conference. IV. Prevention and Rehabilitation of Stroke. Risk factors. *Stroke* 28: 1507-1517.

7. Forti, P., F. Maioli, G. Procaccianti, V. Nativio, M. V. Lega, M. Coveri, M. Zoli, and T. Sacquegna. 2013. Independent predictors of ischemic stroke in the elderly: prospective data from a stroke unit. *Neurology* 80: 29-38.

8. Mozaffarian, D., E. J. Benjamin, A. S. Go, D. K. Arnett, M. J. Blaha, M. Cushman, S. de Ferranti, J. P. Despres, H. J. Fullerton, V. J. Howard, M. D. Huffman, S. E. Judd, B. M. Kissela, D. T. Lackland, J. H. Lichtman, L. D. Lisabeth, S. Liu, R. H. Mackey, D. B. Matchar, D. K. McGuire, E. R. Mohler 3rd, C. S. Moy, P. Muntner, M. E. Mussolino, K. Nasir, R. W. Neumar, G. Nichol, L. Palaniappan, D. K. Pandey, M. J. Reeves, C. J. Rodriguez, P. D. Sorlie, J. Stein, A. Towfighi, T. N. Turan, S. S. Virani, J. Z. Willey, D. Woo, R. W. Yeh, M. B. Turner, and American Heart Association Statistics Committee and Stroke Statistics Subcommittee. 2015. Heart disease and stroke statistics--2015 update: a report from the American Heart Association. *Circulation* 131: e29-322.

9. Rochester, C. L. and V. Mohsenin. 2002. Respiratory complications of stroke. *Semin. Respir. Crit. Care. Med.* 23: 248-260.

10. Bassetti, C., M. S. Aldrich, and D. Quint. 1997. Sleep-disordered breathing in patients with acute supra- and infratentorial strokes. A prospective study of 39 patients. *Stroke* 28: 1765-1772.

11. Good, D. C., J. Q. Henkle, D. Gelber, J. Welsh, and S. Verhulst. 1996. Sleep-disordered breathing and poor functional outcome after stroke. *Stroke* 27: 252-259.

12. Hudgel, D. W., P. Devadatta, M. Quadri, E. R. Sioson, and H. Hamilton. 1993. Mechanism of sleep-induced periodic breathing in convalescing stroke patients and healthy elderly subjects. *Chest* 104: 1503-1510.

13. Rowat, A. M., M. S. Dennis, and J. M. Wardlaw. 2006. Central periodic breathing observed on hospital admission is associated with an adverse prognosis in conscious acute stroke patients. *Cerebrovasc. Dis.* 21: 340-347.

14. Cadilhac, D. A., R. D. Thorpe, D. C. Pearce, M. Barnes, P. D. Rochford, N. Tarquinio, S. M. Davis, G. A. Donnan, R. J. Pierce, and SCOPES II Study Group. 2005. Sleep disordered breathing in chronic stroke survivors. A study of the long term follow-up of the SCOPES cohort using home based polysomnography. *J. Clin. Neurosci.* 12: 632-637.

15. Morrell, M. J., P. Heywood, S. H. Moosavi, A. Guz, and J. Stevens. 1999. Unilateral focal lesions in the rostrolateral medulla influence chemosensitivity and breathing measured during wakefulness, sleep, and exercise. *J. Neurol. Neurosurg. Psychiatry.* 67: 637-645.

16. Devereaux, M. W., J. R. Keane, and R. L. Davis. 1973. Automatic respiratory failure associated with infarction of the medulla. Report of two cases with pathologic study of one. *Arch. Neurol.* 29: 46-52.

17. Good, D. C., J. Q. Henkle, D. Gelber, J. Welsh, and S. Verhulst. 1996. Sleep-disordered breathing and poor functional outcome after stroke. *Stroke* 27: 252-259.

18. Kumar, R., J. C. Suri, and R. Manocha. 2017. Study of association of severity of sleep disordered breathing and functional outcome in stroke patients. *Sleep Med.* 34: 50-56.

19. Cohen-Zion, M., C. Stepnowsky, Marler, T. Shochat, D. F. Kripke, and S. Ancoli-Israel. 2001. Changes in cognitive function associated with sleep disordered breathing in older people. *J. Am. Geriatr. Soc.* 49: 1622-1627.

20. Bravata, D. M., J. Concato, T. Fried, N. Ranjbar, T. Sadarangani, V. McClain, F. Struve, L. Zygmunt, H. J. Knight, A. Lo, G. B. Richerson, M. Gorman, L. S. Williams, L. M. Brass, J. Agostini, V. Mohsenin, F. Roux, and H. K. Yaggi. 2011. Continuous positive airway pressure: evaluation of a novel therapy for patients with acute ischemic stroke. *Sleep* 34: 1271-1277.

21. Hsu, C. Y., M. Vennelle, H. Y. Li, H. M. Engleman, M. S. Dennis, and N. J. Douglas. 2006. Sleep-disordered breathing after stroke: a randomised controlled trial of continuous positive airway pressure. *J. Neurol. Neurosurg. Psychiatry.* 77: 1143-1149.

22. Good, D. C., J. Q. Henkle, D. Gelber, J. Welsh, and S. Verhulst. 1996. Sleep-disordered breathing and poor functional outcome after stroke. *Stroke* 27: 252-259.

23. Yadav, S. K., R. Kumar, P. M. Macey, H. L. Richardson, D. J. Wang, M. A. Woo, and R. M. Harper. 2013. Regional cerebral blood flow alterations in obstructive sleep apnea. *Neurosci. Lett.* 555: 159-164.

24. Capone, C., G. Faraco, C. Coleman, C. N. Young, V. M. Pickel, J. Anrather, R. L. Davisson, and C. Iadecola. 2012. Endothelin 1-dependent neurovascular dysfunction in chronic intermittent hypoxia. *Hypertension* 60: 106-113.

25. Buterbaugh, J., C. Wynstra, N. Provencio, D. Combs, M. Gilbert, and S. Parthasarathy. 2015. Cerebrovascular reactivity in young subjects with sleep apnea. *Sleep* 38: 241-250.

26. Tekgol Uzuner, G. and N. Uzuner. 2016. Cerebrovascular reactivity and neurovascular coupling in patients with obstructive sleep apnea. *Int. J. Neurosci.* 1-6.

27. Zhu, Y., P. Fenik, G. Zhan, E. Mazza, M. Kelz, G. Aston-Jones, and S. C. Veasey. 2007. Selective loss of catecholaminergic wake active neurons in a murine sleep apnea model. *J. Neurosci.* 27: 10060-10071.

28. Tonon, C., R. Vetrugno, R. Lodi, R. Gallassi, F. Provini, S. Iotti, G. Plazzi, P. Montagna, E. Lugaresi, and B. Barbiroli. 2007. Proton magnetic resonance spectroscopy study of brain metabolism in obstructive sleep apnoea syndrome before and after continuous positive airway pressure treatment. *Sleep* 30: 305-311.

29. Kim, L. J., D. Martinez, C. Z. Fiori, D. Baronio, N. A. Kretzmann, and H. M. Barros. 2015. Hypomyelination, memory impairment, and blood-brain barrier permeability in a model of sleep apnea. *Brain Res.* 1597: 28-36.

30. Hoch, C. C., C. F. Reynolds 3rd, D. J. Kupfer, P. R. Houck, S. R. Berman, and J. A. Stack. 1986. Sleep-disordered breathing in normal and pathologic aging. *J. Clin. Psychiatry* 47: 499-503.

31. Zhu, B., Y. Dong, Z. Xu, H. S. Gompf, S. A. Ward, Z. Xue, C. Miao, Y. Zhang, N. L. Chamberlin, and Z. Xie. 2012. Sleep disturbance induces neuroinflammation and impairment of learning and memory. *Neurobiol. Dis.* 48: 348-355.

32. Daulatzai, M. A. 2015. Evidence of neurodegeneration in obstructive sleep apnea: Relationship between obstructive sleep apnea and cognitive dysfunction in the elderly. *J. Neurosci. Res.*

33. Ju, G., I. Y. Yoon, S. D. Lee, T. H. Kim, J. Y. Choe, and K. W. Kim. 2012. Effects of sleep apnea syndrome on delayed memory and executive function in elderly adults. *J. Am. Geriatr. Soc.* 60: 1099-1103.

34. Yaffe, K., A. M. Laffan, S. L. Harrison, S. Redline, A. P. Spira, K. E. Ensrud, S. Ancoli-Israel, and K. L. Stone. 2011. Sleep-disordered breathing, hypoxia, and risk of mild cognitive impairment and dementia in older women. *JAMA* 306: 613-619.

35. Levine, D. A., A. T. Galecki, K. M. Langa, F. W. Unverzagt, M. U. Kabeto, B. Giordani, and V. G. Wadley. 2015. Trajectory of Cognitive Decline After Incident Stroke. *JAMA* 314: 41-51.

36. Mellon, L., L. Brewer, P. Hall, F. Horgan, D. Williams, A. Hickey, and ASPIRE-S study group. 2015. Cognitive impairment six months after ischaemic stroke: a profile from the ASPIRE-S study. *BMC Neurol*. 15: 31-015-0288-2.

37. Perez, L. M., M. Inzitari, M. Roque, E. Duarte, E. Valles, M. Rodo, and M. Gallofre. 2015. Change in cognitive performance is associated with functional recovery during post-acute stroke rehabilitation: a multi-centric study from intermediate care geriatric rehabilitation units of Catalonia. *Neurol. Sci*.

38. Khoo, M. C. 2000. Determinants of ventilatory instability and variability. *Respir. Physiol*. 122: 167-182.

39. Dempsey, J. A., C. A. Smith, T. Przybylowski, B. Chenuel, A. Xie, H. Nakayama, and J. B. Skatrud. 2004. The ventilatory responsiveness to CO(2) below eupnoea as a determinant of ventilatory stability in sleep. *J. Physiol*. 560: 1-11.

40. Mitchell, R. A. 1980. Neural regulation of respiration. *Clin. Chest Med*. 1: 3-12.

41. Guyenet, P. G., R. L. Stornetta, D. A. Bayliss, and D. K. Mulkey. 2005. Retrotrapezoid nucleus: a litmus test for the identification of central chemoreceptors. *Exp. Physiol*. 90: 247-53; discussion 253-7.

42. Ott, M. M., S. C. Nuding, L. S. Segers, B. G. Lindsey, and K. F. Morris. 2011. Ventrolateral medullary functional connectivity and the respiratory and central chemoreceptor-evoked modulation of retrotrapezoid-parafacial neurons. *J. Neurophysiol*. 105: 2960-2975.

43. Lazarenko, R. M., T. A. Milner, S. D. Depuy, R. L. Stornetta, G. H. West, J. A. Kievits, D. A. Bayliss, and P. G. Guyenet. 2009. Acid sensitivity and ultrastructure of the retrotrapezoid nucleus in Phox2b-EGFP transgenic mice. *J. Comp. Neurol*. 517: 69-86.

44. Abbott, S. B., R. L. Stornetta, M. B. Coates, and P. G. Guyenet. 2011. Phox2b-expressing neurons of the parafacial region regulate breathing rate, inspiration, and expiration in conscious rats. *J. Neurosci*. 31: 16410-16422.

45. Kanbar, R., R. L. Stornetta, D. R. Cash, S. J. Lewis, and P. G. Guyenet. 2010. Photostimulation of Phox2b medullary neurons activates cardiorespiratory function in conscious rats. *Am. J. Respir. Crit. Care Med*. 182: 1184-1194.

46. Kumar, N. N., A. Velic, J. Soliz, Y. Shi, K. Li, S. Wang, J. L. Weaver, J. Sen, S. B. Abbott, R. M. Lazarenko, M. G. Ludwig, E. Perez-Reyes, N. Mohebbi, C. Bettoni, M. Gassmann, T. Suply, K. Seuwen, P. G. Guyenet, C. A. Wagner, and D. A. Bayliss. 2015. PHYSIOLOGY. Regulation of breathing by CO(2) requires the proton-activated receptor GPR4 in retrotrapezoid nucleus neurons. *Science* 348: 1255-1260.

47. Smith, P. A., H. Chen, D. E. Kurenny, A. A. Selyanko, and J. A. Zidichouski. 1992. Regulation of the M current: transduction mechanism and role in ganglionic transmission. *Can. J. Physiol. Pharmacol.* 70 Suppl: S12-8.

48. Marrion, N. V. 1997. Control of M-current. *Annu. Rev. Physiol.* 59: 483-504.

49. Devinsky, O. 2011. Sudden, unexpected death in epilepsy. *N. Engl. J. Med.* 365: 1801-1811.

50. Faingold, C. L., S. P. Kommajosyula, X. Long, K. Plath, and M. Randall. 2014. Serotonin and sudden death: differential effects of serotonergic drugs on seizure-induced respiratory arrest in DBA/1 mice. *Epilepsy Behav.* 37: 198-203.

51. Massey, C. A., L. P. Sowers, B. J. Dlouhy, and G. B. Richerson. 2014. Mechanisms of sudden unexpected death in epilepsy: the pathway to prevention. *Nat. Rev. Neurol.* 10: 271-282.

52. Weckhuysen, S., V. Ivanovic, R. Hendrickx, R. Van Coster, H. Hjalgrim, R. S. Moller, S. Gronborg, A. S. Schoonjans, B. Ceulemans, S. B. Heavin, C. Eltze, R. Horvath, G. Casara, T. Pisano, L. Giordano, K. Rostasy, E. Haberlandt, B. Albrecht, A. Bevot, I. Benkel, S. Syrbe, B. Sheidley, R. Guerrini, A. Poduri, J. R. Lemke, S. Mandelstam, I. Scheffer, M. Angriman, P. Striano, C. Marini, A. Suls, P. De Jonghe, and KCNQ2 Study Group. 2013. Extending the KCNQ2 encephalopathy spectrum: clinical and neuroimaging findings in 17 patients. *Neurology* 81: 1697-1703.

53. Watanabe, H., E. Nagata, A. Kosakai, M. Nakamura, M. Yokoyama, K. Tanaka, and H. Sasai. 2000. Disruption of the epilepsy KCNQ2 gene results in neural hyperexcitability. *J. Neurochem.* 75: 28-33.

54. Hawryluk, J. M., T. S. Moreira, A. C. Takakura, I. C. Wenker, A. V. Tzingounis, and D. K. Mulkey. 2012. KCNQ channels determine serotonergic modulation of ventral surface chemoreceptors and respiratory drive. *J. Neurosci.* 32: 16943-16952.

55. Mifflin, S. W. 1992. Arterial chemoreceptor input to nucleus tractus solitarius. *Am. J. Physiol.* 263: R368-75.

56. Chitravanshi, V. C. and H. N. Sapru. 1995. Chemoreceptor-sensitive neurons in commissural subnucleus of nucleus tractus solitarius of the rat. *Am. J. Physiol.* 268: R851-8.

57. Pascual, O., M. P. Morin-Surun, B. Barna, M. Denavit-Saubie, J. M. Pequignot, and J. Champagnat. 2002. Progesterone reverses the neuronal responses to hypoxia in rat nucleus tractus solitarius in vitro. *J. Physiol.* 544: 511-520.

58. Zoccal, D. B., W. I. Furuya, M. Bassi, D. S. Colombari, and E. Colombari. 2014. The nucleus of the solitary tract and the coordination of respiratory and sympathetic activities. *Front. Physiol.* 5: 238.

59. Kaur, C., S. Viswanathan, and E. A. Ling. 2011. Hypoxia-induced cellular and vascular changes in the nucleus tractus solitarius and ventrolateral medulla. *J. Neuropathol. Exp. Neurol.* 70: 201-217.

60. Braccialli, A. L., L. G. Bonagamba, and B. H. Machado. 2008. Glutamatergic and purinergic mechanisms on respiratory modulation in the caudal NTS of awake rats. *Respir. Physiol. Neurobiol.* 161: 246-252.

61. Braga, V. A., R. N. Soriano, A. L. Braccialli, P. M. de Paula, L. G. Bonagamba, J. F. Paton, and B. H. Machado. 2007. Involvement of L-glutamate and ATP in the neurotransmission of the sympathoexcitatory component of the chemoreflex in the commissural nucleus tractus solitarii of awake rats and in the working heart-brainstem preparation. *J. Physiol*. 581: 1129-1145.

62. Dauger, S., A. Pattyn, F. Lofaso, C. Gaultier, C. Goridis, J. Gallego, and J. F. Brunet. 2003. Phox2b controls the development of peripheral chemoreceptors and afferent visceral pathways. *Development* 130: 6635-6642.

63. Sobrinho, C. R., I. C. Wenker, E. M. Poss, A. C. Takakura, T. S. Moreira, and D. K. Mulkey. 2014. Purinergic signalling contributes to chemoreception in the retrotrapezoid nucleus but not the nucleus of the solitary tract or medullary raphe. *J. Physiol*. 592: 1309-1323.

64. Sofroniew, M. V. and H. V. Vinters. 2010. Astrocytes: biology and pathology. *Acta Neuropathol*. 119: 7-35.

65. Sofroniew, M. V. 2009. Molecular dissection of reactive astrogliosis and glial scar formation. *Trends Neurosci*. 32: 638-647.

66. Li, Y., X. L. Xu, D. Zhao, L. N. Pan, C. W. Huang, L. J. Guo, Q. Lu, and J. Wang. 2015. TLR3 ligand Poly IC Attenuates Reactive Astrogliosis and Improves Recovery of Rats after Focal Cerebral Ischemia. *CNS Neurosci. Ther*. 21: 905-913.

67. Mulkey, D. K., A. M. Mistry, P. G. Guyenet, and D. A. Bayliss. 2006. Purinergic P2 receptors modulate excitability but do not mediate pH sensitivity of RTN respiratory chemoreceptors. *J. Neurosci*. 26: 7230-7233.

68. Kasymov, V., O. Larina, C. Castaldo, N. Marina, M. Patrushev, S. Kasparov, and A. V. Gourine. 2013. Differential sensitivity of brainstem versus cortical astrocytes to changes in pH reveals functional regional specialization of astroglia. *J. Neurosci*. 33: 435-441.

69. Gourine, A. V., V. Kasymov, N. Marina, F. Tang, M. F. Figueiredo, S. Lane, A. G. Teschemacher, K. M. Spyer, K. Deisseroth, and S. Kasparov. 2010. Astrocytes control breathing through pH-dependent release of ATP. *Science* 329: 571-575.

70. Huda, R., D. R. McCrimmon, and M. Martina. 2013. pH modulation of glial glutamate transporters regulates synaptic transmission in the nucleus of the solitary tract. *J. Neurophysiol*. 110: 368-377.

71. Rajani, V., Y. Zhang, V. Jalubula, V. Rancic, S. SheikhBahaei, J. D. Zwicker, S. Pagliardini, C. T. Dickson, K. Ballanyi, S. Kasparov, A. V. Gourine, and G. D. Funk. 2017. Release of ATP by pre-Botzinger complex astrocytes contributes to the hypoxic ventilatory response via a Ca2+ -dependent P2Y1 receptor mechanism. *J. Physiol*.

72. Takano, T., G. F. Tian, W. Peng, N. Lou, W. Libionka, X. Han, and M. Nedergaard. 2006. Astrocyte-mediated control of cerebral blood flow. *Nat. Neurosci*. 9: 260-267.

73. Hawkins, V. E., A. C. Takakura, A. Trinh, M. R. Malheiros-Lima, C. M. Cleary, I. C. Wenker, T. Dubreuil, E. M. Rodriguez, M. T. Nelson, T. S. Moreira, and D. K. Mulkey. 2017. Purinergic

regulation of vascular tone in the retrotrapezoid nucleus is specialized to support the drive to breathe. *Elife* 6: 10.7554/eLife.25232.

74. Lipford, M. C., J. G. Park, and K. Ramar. 2014. Sleep-disordered breathing and stroke: therapeutic approaches. *Curr. Neurol. Neurosci. Rep.* 14: 431-013-0431-7.

75. Kapur, V. K., D. H. Auckley, S. Chowdhuri, D. C. Kuhlmann, R. Mehra, K. Ramar, and C. G. Harrod. 2017. Clinical Practice Guideline for Diagnostic Testing for Adult Obstructive Sleep Apnea: An American Academy of Sleep Medicine Clinical Practice Guideline. *J. Clin. Sleep Med.* 13: 479-504.

76. Fowler, A. C. and G. P. Kalamangalam. 2000. The role of the central chemoreceptor in causing periodic breathing. *IMA J. Math. Appl. Med. Biol.* 17: 147-167.

77. Nemati, S., B. A. Edwards, S. A. Sands, P. J. Berger, A. Wellman, G. C. Verghese, A. Malhotra, and J. P. Butler. 2011. Model-based characterization of ventilatory stability using spontaneous breathing. *J. Appl. Physiol. (1985)* 111: 55-67.

78. Murphy, D. J. 2016. Apneic events - A proposed new target for respiratory safety pharmacology. *Regul. Toxicol. Pharmacol.* 81: 194-200.

79. Massague, J. 2012. TGFbeta signalling in context. *Nat. Rev. Mol. Cell Biol.* 13: 616-630.

80. Khalil, N. 1999. TGF-beta: from latent to active. *Microbes Infect.* 1: 1255-1263.

81. Derynck, R., Y. Zhang, and X. H. Feng. 1998. Smads: transcriptional activators of TGF-beta responses. *Cell* 95: 737-740.

82. Unsicker, K., K. C. Flanders, D. S. Cissel, R. Lafyatis, and M. B. Sporn. 1991. Transforming growth factor beta isoforms in the adult rat central and peripheral nervous system. *Neuroscience* 44: 613-625.

83. Yamashita, K., U. Gerken, P. Vogel, K. Hossmann, and C. Wiessner. 1999. Biphasic expression of TGF-beta1 mRNA in the rat brain following permanent occlusion of the middle cerebral artery. *Brain Res.* 836: 139-145.

84. Ruocco, A., O. Nicole, F. Docagne, C. Ali, L. Chazalviel, S. Komesli, F. Yablonsky, S. Roussel, E. T. MacKenzie, D. Vivien, and A. Buisson. 1999. A transforming growth factor-beta antagonist unmasks the neuroprotective role of this endogenous cytokine in excitotoxic and ischemic brain injury. *J. Cereb. Blood Flow Metab.* 19: 1345-1353.

85. Doyle, K. P., E. Cekanaviciute, L. E. Mamer, and M. S. Buckwalter. 2010. TGFbeta signaling in the brain increases with aging and signals to astrocytes and innate immune cells in the weeks after stroke. *J. Neuroinflammation* 7: 62-2094-7-62.

86. Wang, Y., H. Moges, Y. Bharucha, and A. Symes. 2007. Smad3 null mice display more rapid wound closure and reduced scar formation after a stab wound to the cerebral cortex. *Exp. Neurol.* 203: 168-184.

87. Liu, B. P., W. B. Cafferty, S. O. Budel, and S. M. Strittmatter. 2006. Extracellular regulators of axonal growth in the adult central nervous system. *Philos. Trans. R. Soc. Lond. B. Biol. Sci*. 361: 1593-1610.

88. Badan, I., B. Buchhold, A. Hamm, M. Gratz, L. C. Walker, D. Platt, C. Kessler, and A. Popa-Wagner. 2003. Accelerated glial reactivity to stroke in aged rats correlates with reduced functional recovery. *J. Cereb. Blood Flow Metab*. 23: 845-854.

89. Popa-Wagner, A., S. T. Carmichael, Z. Kokaia, C. Kessler, and L. C. Walker. 2007. The response of the aged brain to stroke: too much, too soon? *Curr. Neurovasc Res*. 4: 216-227.

90. von Bernhardi, R., L. Eugenin-von Bernhardi, and J. Eugenin. 2015. Microglial cell dysregulation in brain aging and neurodegeneration. *Front. Aging Neurosci*. 7: 124.

91. Norden, D. M., A. M. Fenn, A. Dugan, and J. P. Godbout. 2014. TGFbeta produced by IL-10 redirected astrocytes attenuates microglial activation. *Glia* 62: 881-895.

92. Norden, D. M., P. J. Trojanowski, F. R. Walker, and J. P. Godbout. 2016. Insensitivity of astrocytes to interleukin 10 signaling following peripheral immune challenge results in prolonged microglial activation in the aged brain. *Neurobiol. Aging* 44: 22-41.

93. Lindskog, S. 1997. Structure and mechanism of carbonic anhydrase. *Pharmacol. Ther*. 74: 1-20.

94. Edwards, B. A., J. G. Connolly, L. M. Campana, S. A. Sands, J. A. Trinder, D. P. White, A. Wellman, and A. Malhotra. 2013. Acetazolamide attenuates the ventilatory response to arousal in patients with obstructive sleep apnea. *Sleep* 36: 281-285.

95. Ritchie, N. D., A. V. Baggott, and W. T. Andrew Todd. 2012. Acetazolamide for the prevention of acute mountain sickness--a systematic review and meta-analysis. *J. Travel Med*. 19: 298-307.

96. Supuran, C. T. 2015. Acetazolamide for the treatment of idiopathic intracranial hypertension. *Expert Rev. Neurother* 15: 851-856.

97. Igarashi, H., M. Tsujita, I. L. Kwee, and T. Nakada. 2014. Water influx into cerebrospinal fluid is primarily controlled by aquaporin-4, not by aquaporin-1: 17O JJVCPE MRI study in knockout mice. *Neuroreport* 25: 39-43.

98. Haj-Yasein, N. N., V. Jensen, I. Ostby, S. W. Omholt, J. Voipio, K. Kaila, O. P. Ottersen, O. Hvalby, and E. A. Nagelhus. 2012. Aquaporin-4 regulates extracellular space volume dynamics during high-frequency synaptic stimulation: a gene deletion study in mouse hippocampus. *Glia* 60: 867-874.

99. Magnotta, V. A., H. Y. Heo, B. J. Dlouhy, N. S. Dahdaleh, R. L. Follmer, D. R. Thedens, M. J. Welsh, and J. A. Wemmie. 2012. Detecting activity-evoked pH changes in human brain. *Proc. Natl. Acad. Sci. U. S. A*. 109: 8270-8273.

100. Vorstrup, S., L. Henriksen, and O. B. Paulson. 1984. Effect of acetazolamide on cerebral blood flow and cerebral metabolic rate for oxygen. *J. Clin. Invest*. 74: 1634-1639.

101. Tzeng, Y. C. and P. N. Ainslie. 2014. Blood pressure regulation IX: cerebral autoregulation under blood pressure challenges. *Eur. J. Appl. Physiol.* 114: 545-559.

102. Kety, S. S. and C. F. Schmidt. 1946. The Effects of Active and Passive Hyperventilation on Cerebral Blood Flow, Cerebral Oxygen Consumption, Cardiac Output, and Blood Pressure of Normal Young Men. *J. Clin. Invest.* 25: 107-119.

103. Meng, L., A. W. Gelb, B. S. Alexander, A. E. Cerussi, B. J. Tromberg, Z. Yu, and W. W. Mantulin. 2012. Impact of phenylephrine administration on cerebral tissue oxygen saturation and blood volume is modulated by carbon dioxide in anaesthetized patients. *Br. J. Anaesth.* 108: 815-822.

104. Ainslie, P. N. and J. Duffin. 2009. Integration of cerebrovascular CO2 reactivity and chemoreflex control of breathing: mechanisms of regulation, measurement, and interpretation. *Am. J. Physiol. Regul. Integr. Comp. Physiol.* 296: R1473-95.

105. Xie, A., J. B. Skatrud, B. Morgan, B. Chenuel, R. Khayat, K. Reichmuth, J. Lin, and J. A. Dempsey. 2006. Influence of cerebrovascular function on the hypercapnic ventilatory response in healthy humans. *J. Physiol.* 577: 319-329.

106. Longa, E. Z., P. R. Weinstein, S. Carlson, and R. Cummins. 1989. Reversible middle cerebral artery occlusion without craniectomy in rats. *Stroke* 20: 84-91.

107. Li, J., S. E. Benashski, V. R. Venna, and L. D. McCullough. 2010. Effects of metformin in experimental stroke. *Stroke* 41: 2645-2652.

108. O'Keefe, L. M., S. J. Doran, L. Mwilambwe-Tshilobo, L. H. Conti, V. R. Venna, and L. D. McCullough. 2014. Social isolation after stroke leads to depressive-like behavior and decreased BDNF levels in mice. *Behav. Brain Res.* 260: 162-170.

109. Perez-de-Puig, I., F. Miro-Mur, M. Ferrer-Ferrer, E. Gelpi, J. Pedragosa, C. Justicia, X. Urra, A. Chamorro, and A. M. Planas. 2015. Neutrophil recruitment to the brain in mouse and human ischemic stroke. *Acta Neuropathol.* 129: 239-257.

110. DRORBAUGH, J. E. and W. O. FENN. 1955. A barometric method for measuring ventilation in newborn infants. *Pediatrics* 16: 81-87.

111. Tankersley, C. G., R. S. Fitzgerald, and S. R. Kleeberger. 1994. Differential control of ventilation among inbred strains of mice. *Am. J. Physiol.* 267: R1371-7.

112. Speakman, J. R. 2013. Measuring energy metabolism in the mouse - theoretical, practical, and analytical considerations. *Front. Physiol.* 4: 34.

113. Liu, F., S. E. Benashski, Y. Xu, M. Siegel, and L. D. McCullough. 2012. Effects of chronic and acute oestrogen replacement therapy in aged animals after experimental stroke. *J. Neuroendocrinol.* 24: 319-330.

114. Venna, V. R., G. Weston, S. E. Benashski, S. Tarabishy, F. Liu, J. Li, L. H. Conti, and L. D. McCullough. 2012. NF-kappaB contributes to the detrimental effects of social isolation after experimental stroke. *Acta Neuropathol.* 124: 425-438.

115. Hall, E. D., Y. D. Bryant, W. Cho, and P. G. Sullivan. 2008. Evolution of post-traumatic neurodegeneration after controlled cortical impact traumatic brain injury in mice and rats as assessed by the de Olmos silver and fluorojade staining methods. *J. Neurotrauma* 25: 235-247.

116. Li, J., J. Lang, Z. Zeng, and L. D. McCullough. 2008. Akt1 gene deletion and stroke. *J. Neurol. Sci*. 269: 105-112.

117. Patil, S. S., B. Sunyer, H. Hoger, and G. Lubec. 2009. Evaluation of spatial memory of C57BL/6J and CD1 mice in the Barnes maze, the Multiple T-maze and in the Morris water maze. *Behav. Brain Res*. 198: 58-68.

118. Uliana, D. L., S. C. Hott, S. F. Lisboa, and L. B. Resstel. 2016. Dorsolateral periaqueductal gray matter CB1 and TRPV1 receptors exert opposite modulation on expression of contextual fear conditioning. *Neuropharmacology* 103: 257-269.

119. Li, X., K. K. Blizzard, Z. Zeng, A. C. DeVries, P. D. Hurn, and L. D. McCullough. 2004. Chronic behavioral testing after focal ischemia in the mouse: functional recovery and the effects of gender. *Exp. Neurol*. 187: 94-104.

120. Wenker, I. C., C. R. Sobrinho, A. C. Takakura, T. S. Moreira, and D. K. Mulkey. 2012. Regulation of ventral surface CO2/H+-sensitive neurons by purinergic signalling. *J. Physiol*. 590: 2137-2150.

121. Tschop, M. H., J. R. Speakman, J. R. Arch, J. Auwerx, J. C. Bruning, L. Chan, R. H. Eckel, R. V. Farese Jr, J. E. Galgani, C. Hambly, M. A. Herman, T. L. Horvath, B. B. Kahn, S. C. Kozma, E. Maratos-Flier, T. D. Muller, H. Munzberg, P. T. Pfluger, L. Plum, M. L. Reitman, K. Rahmouni, G. I. Shulman, G. Thomas, C. R. Kahn, and E. Ravussin. 2011. A guide to analysis of mouse energy metabolism. *Nat. Methods* 9: 57-63.

122. Liu, F., R. Yuan, S. E. Benashski, and L. D. McCullough. 2009. Changes in experimental stroke outcome across the life span. *J. Cereb. Blood Flow Metab*. 29: 792-802.

123. Petrea, R. E., A. S. Beiser, S. Seshadri, M. Kelly-Hayes, C. S. Kase, and P. A. Wolf. 2009. Gender differences in stroke incidence and poststroke disability in the Framingham heart study. *Stroke* 40: 1032-1037.

124. Seshadri, S., A. Beiser, M. Kelly-Hayes, C. S. Kase, R. Au, W. B. Kannel, and P. A. Wolf. 2006. The lifetime risk of stroke: estimates from the Framingham Study. *Stroke* 37: 345-350.

125. Gall, S. L., P. L. Tran, K. Martin, L. Blizzard, and V. Srikanth. 2012. Sex differences in long-term outcomes after stroke: functional outcomes, handicap, and quality of life. *Stroke* 43: 1982-1987.

126. Brischetto, M. J., R. P. Millman, D. D. Peterson, D. A. Silage, and A. I. Pack. 1984. Effect of aging on ventilatory response to exercise and CO2. *J. Appl. Physiol. Respir. Environ. Exerc. Physiol*. 56: 1143-1150.

127. Kronenberg, R. S. and C. W. Drage. 1973. Attenuation of the ventilatory and heart rate responses to hypoxia and hypercapnia with aging in normal men. *J. Clin. Invest*. 52: 1812-1819.

128. Holley, H. S., M. Behan, and J. M. Wenninger. 2012. Age and sex differences in the ventilatory response to hypoxia and hypercapnia in awake neonatal, pre-pubertal and young adult rats. *Respir. Physiol. Neurobiol.* 180: 79-87.

129. Wenninger, J. M., E. B. Olson Jr, C. J. Cotter, C. F. Thomas, and M. Behan. 2009. Hypoxic and hypercapnic ventilatory responses in aging male vs. aging female rats. *J. Appl. Physiol. (1985)* 106: 1522-1528.

130. Hader, C., A. Schroeder, M. Hinz, G. H. Micklefield, and K. Rasche. 2005. Sleep disordered breathing in the elderly: comparison of women and men. *J. Physiol. Pharmacol.* 56 Suppl 4: 85-91.

131. Yaffe, K., A. M. Laffan, S. L. Harrison, S. Redline, A. P. Spira, K. E. Ensrud, S. Ancoli-Israel, and K. L. Stone. 2011. Sleep-disordered breathing, hypoxia, and risk of mild cognitive impairment and dementia in older women. *JAMA* 306: 613-619.

132. Iturriaga, R., M. P. Oyarce, and A. C. R. Dias. 2017. Role of Carotid Body in Intermittent Hypoxia-Related Hypertension. *Curr. Hypertens. Rep.* 19: 38-017-0735-0.

133. Faulk, K. E., T. P. Nedungadi, and J. T. Cunningham. 2017. Angiotensin converting enzyme 1 in the median preoptic nucleus contributes to chronic intermittent hypoxia hypertension. *Physiol. Rep.* 5: 10.14814/phy2.13277.

134. Suenaga, J., X. Hu, H. Pu, Y. Shi, S. H. Hassan, M. Xu, R. K. Leak, R. A. Stetler, Y. Gao, and J. Chen. 2015. White matter injury and microglia/macrophage polarization are strongly linked with age-related long-term deficits in neurological function after stroke. *Exp. Neurol.* 272: 109-119.

135. Manwani, B., F. Liu, V. Scranton, M. D. Hammond, L. H. Sansing, and L. D. McCullough. 2013. Differential effects of aging and sex on stroke induced inflammation across the lifespan. *Exp. Neurol.* 249: 120-131.

136. Loram, L. C., P. W. Sholar, F. R. Taylor, J. L. Wiesler, J. A. Babb, K. A. Strand, D. Berkelhammer, H. E. Day, S. F. Maier, and L. R. Watkins. 2012. Sex and estradiol influence glial pro-inflammatory responses to lipopolysaccharide in rats. *Psychoneuroendocrinology* 37: 1688-1699.

137. Santos-Galindo, M., E. Acaz-Fonseca, M. J. Bellini, and L. M. Garcia-Segura. 2011. Sex differences in the inflammatory response of primary astrocytes to lipopolysaccharide. *Biol. Sex. Differ.* 2: 7-6410-2-7.

138. Boden, A. G., M. C. Harris, and M. J. Parkes. 1998. Apneic threshold for CO2 in the anesthetized rat: fundamental properties under steady-state conditions. *J. Appl. Physiol. (1985)* 85: 898-907.

139. Chin, Y., M. Kishi, M. Sekino, F. Nakajo, Y. Abe, Y. Terazono, O. Hiroyuki, F. Kato, S. Koizumi, C. Gachet, and T. Hisatsune. 2013. Involvement of glial P2Y(1) receptors in cognitive deficit after focal cerebral stroke in a rodent model. *J. Neuroinflammation* 10: 95-2094-10-95.

140. Li, W., R. Huang, R. A. Shetty, N. Thangthaeng, R. Liu, Z. Chen, N. Sumien, M. Rutledge, G. H. Dillon, F. Yuan, M. J. Forster, J. W. Simpkins, and S. H. Yang. 2013. Transient focal cerebral

ischemia induces long-term cognitive function deficit in an experimental ischemic stroke model. *Neurobiol. Dis*. 59: 18-25.

141. Levine, D. A., A. T. Galecki, K. M. Langa, F. W. Unverzagt, M. U. Kabeto, B. Giordani, and V. G. Wadley. 2015. Trajectory of Cognitive Decline After Incident Stroke. *JAMA* 314: 41-51.

142. Erdem, A., G. Yasargil, and P. Roth. 1993. Microsurgical anatomy of the hippocampal arteries. *J. Neurosurg*. 79: 256-265.

143. Zimmerman, M. E. and M. S. Aloia. 2012. Sleep-disordered breathing and cognition in older adults. *Curr. Neurol. Neurosci. Rep*. 12: 537-546.

144. Davis, E. M. and C. P. O'Donnell. 2013. Rodent models of sleep apnea. *Respir. Physiol. Neurobiol*. 188: 355-361.

145. Ebel, D. L., C. G. Torkilsen, and T. D. Ostrowski. 2017. Blunted Respiratory Responses in the Streptozotocin-Induced Alzheimer's Disease Rat Model. *J. Alzheimers Dis*. 56: 1197-1211.

146. Famakin, B. M. 2014. The Immune Response to Acute Focal Cerebral Ischemia and Associated Post-stroke Immunodepression: A Focused Review. *Aging Dis*. 5: 307-326.

147. Lambertsen, K. L., K. Biber, and B. Finsen. 2012. Inflammatory cytokines in experimental and human stroke. *J. Cereb. Blood Flow Metab*. 32: 1677-1698.

148. Jones, L. L., R. U. Margolis, and M. H. Tuszynski. 2003. The chondroitin sulfate proteoglycans neurocan, brevican, phosphacan, and versican are differentially regulated following spinal cord injury. *Exp. Neurol*. 182: 399-411.

149. Anderson, M. A., Y. Ao, and M. V. Sofroniew. 2014. Heterogeneity of reactive astrocytes. *Neurosci. Lett*. 565: 23-29.

150. McKillop, W. M., M. Dragan, A. Schedl, and A. Brown. 2013. Conditional Sox9 ablation reduces chondroitin sulfate proteoglycan levels and improves motor function following spinal cord injury. *Glia* 61: 164-177.

151. Filous, A. R. and J. Silver. 2016. "Targeting astrocytes in CNS injury and disease: A translational research approach". *Prog. Neurobiol*. 144: 173-187.

152. Roy Choudhury, G., M. G. Ryou, E. Poteet, Y. Wen, R. He, F. Sun, F. Yuan, K. Jin, and S. H. Yang. 2014. Involvement of p38 MAPK in reactive astrogliosis induced by ischemic stroke. *Brain Res*. 1551: 45-58.

153. O'Callaghan, J. P., K. A. Kelly, R. L. VanGilder, M. V. Sofroniew, and D. B. Miller. 2014. Early activation of STAT3 regulates reactive astrogliosis induced by diverse forms of neurotoxicity. *PLoS One* 9: e102003.

154. Cuadrado, A. and A. R. Nebreda. 2010. Mechanisms and functions of p38 MAPK signalling. *Biochem. J*. 429: 403-417.

155. Evans, A. M., D. G. Hardie, C. Peers, and A. Mahmoud. 2011. Hypoxic pulmonary vasoconstriction: mechanisms of oxygen-sensing. *Curr. Opin. Anaesthesiol.* 24: 13-20.

156. Aaronson, P. I., T. P. Robertson, G. A. Knock, S. Becker, T. H. Lewis, V. Snetkov, and J. P. Ward. 2006. Hypoxic pulmonary vasoconstriction: mechanisms and controversies. *J. Physiol.* 570: 53-58.

157. Sun, M. K. and D. L. Alkon. 2001. Pharmacological enhancement of synaptic efficacy, spatial learning, and memory through carbonic anhydrase activation in rats. *J. Pharmacol. Exp. Ther.* 297: 961-967.

158. Brown, H. and F. Plum. 1961. The neurologic basis of Cheyne-Stokes respiration. *American Journal of Medicine* 30: 849.

159. Koo, B. B., K. P. Strohl, C. B. Gillombardo, and F. J. Jacono. 2010. Ventilatory patterning in a mouse model of stroke. *Respir. Physiol. Neurobiol.* 172: 129-135.

160. Gildeh, N., P. Drakatos, S. Higgins, I. Rosenzweig, and B. D. Kent. 2016. Emerging co-morbidities of obstructive sleep apnea: cognition, kidney disease, and cancer. *J. Thorac. Dis.* 8: E901-E917.

161. Kheirandish, L., D. Gozal, J. M. Pequignot, J. Pequignot, and B. W. Row. 2005. Intermittent hypoxia during development induces long-term alterations in spatial working memory, monoamines, and dendritic branching in rat frontal cortex. *Pediatr. Res.* 58: 594-599.

162. Lin, T., J. F. Huang, Q. C. Lin, G. P. Chen, B. Y. Wang, J. M. Zhao, and J. C. Qi. 2017. The effect of CPAP treatment on venous lactate and arterial blood gas among obstructive sleep apnea syndrome patients. *Sleep Breath* 21: 303-309.

163. Baillieul, S., S. Chacaroun, S. Doutreleau, O. Detante, J. L. Pepin, and S. Verges. 2017. Hypoxic conditioning and the central nervous system: A new therapeutic opportunity for brain and spinal cord injuries? *Exp. Biol. Med. (Maywood)* 242: 1198-1206.

164. Manukhina, E. B., H. F. Downey, X. Shi, and R. T. Mallet. 2016. Intermittent hypoxia training protects cerebrovascular function in Alzheimer's disease. *Exp. Biol. Med. (Maywood)* 241: 1351-1363.

165. Bouslama, M., H. Adla-Biassette, N. Ramanantsoa, T. Bourgeois, B. Bollen, O. Brissaud, B. Matrot, P. Gressens, and J. Gallego. 2015. Protective effects of intermittent hypoxia on brain and memory in a mouse model of apnea of prematurity. *Front. Physiol.* 6: 313.

166. Fan, Y. Y., W. W. Hu, F. Nan, and Z. Chen. 2017. Postconditioning-induced neuroprotection, mechanisms and applications in cerebral ischemia. *Neurochem. Int.* 107: 43-56.

167. Wyss-Coray, T., C. Lin, D. A. Sanan, L. Mucke, and E. Masliah. 2000. Chronic overproduction of transforming growth factor-beta1 by astrocytes promotes Alzheimer's disease-like microvascular degeneration in transgenic mice. *Am. J. Pathol.* 156: 139-150.

168. Ongali, B., N. Nicolakakis, C. Lecrux, T. Aboulkassim, P. Rosa-Neto, P. Papadopoulos, X. K. Tong, and E. Hamel. 2010. Transgenic mice overexpressing APP and transforming growth factor-beta1 feature cognitive and vascular hallmarks of Alzheimer's disease. *Am. J. Pathol.* 177: 3071-3080.

Vita

Anthony Nicholas Patrizz III was born in Manchester, Connecticut on July 31, 1984, the son of Janice Patrizz and Anthony Patrizz Jr. After completing his work at Rockville High School, Vernon, Ct, in 2002, he began working as a Paramedic for a number of years before entering the University of Connecticut receiving his Bachelor of Arts in Political Science in 2009. He continued working as a Paramedic before taking a position as a research technician in the Department of Neuroscience at the University of Connecticut. In 2013 he entered the University of Connecticut Graduate School. In 2015, the lab of his PI, Dr. Louise McCullough, transferred to The University of Texas MD Anderson Cancer Center UTHealth Graduate School of Biomedical Science.